VISUAL ASPECTS OF IMAGE INTENSIFICATION

PROEFSCHRIFT

TER VERKRIJGING VAN DE GRAAD VAN DOCTOR IN DE WISKUNDE
EN NATUURWETENSCHAPPEN AAN DE RIJKSUNIVERSITEIT TE UTRECHT,
OP GEZAG VAN DE RECTOR MAGNIFICUS PROF. DR. SJ. GROENMAN,
VOLGENS BESLUIT VAN HET COLLEGE VAN DEKANEN IN HET OPENBAAR
TE VERDEDIGEN OP MAANDAG 24 SEPTEMBER 1973
DES NAMIDDAGS TE 4.00 UUR PRECIES

DOOR

AART VAN MEETEREN

GEBOREN OP 29 APRIL 1937 TE MAURIK

1973
BRONDER-OFFSET B.V. - ROTTERDAM

PROMOTOR: PROF. DR. M.A. BOUMAN

This thesis is also published as a report of the
Institute for Perception TNO, Soesterberg
The Netherlands.

Aan mijn ouders
Aan Hanneke

VOORWOORD

Bij de voltooiing van dit proefschrift is het een vreugde dank te betuigen aan allen, die mij deelgenoot maakten van hun kennis en inzicht. Ik denk daarbij aan de docenten van het Stedelijk Gymnasium te Tiel, aan de docenten van de afdeling Technische Physica van de Technische Hogeschool te Delft, en aan hen, die mij bijstonden in het hier beschreven onderzoek.

Hooggeleerde Bouman, hooggeachte promotor, U dank ik voor de vrijheid die U mij liet inzake de vorm en de inhoud van dit proefschrift, voor de intensieve wijze waarop U er zich in heeft willen verdiepen, en voor de vele goede raad die U mij gaf. U leerde mij in het bijzonder de samenhang tussen zorgvuldig formuleren en zorgvuldig denken.

Zeergeleerde Vos, zonder twijfel heeft U de grootste invloed op mijn werk gehad. Met name kwam ook dit proefschrift mede onder Uw leiding tot stand. U heeft mij in het vak ingewijd, waarbij U mij tegelijkertijd toch mijn eigen weg liet vinden. Ik zou het tot een eer rekenen indien zich iets van Uw pragmatische wetenschapsbeoefening in mijn werk mocht weerspiegelen.

Zeergeleerde Walraven, aan Uw opvattingen over de evenwichtige verhouding van toegepast en fundamenteel natuurwetenschappelijk onderzoek heb ik zowel de gelegenheid als de aanmoediging tot het bewerken van een proefschrift te danken. De Rijksverdedidingsorganisatie TNO dank ik voor de mogelijkheid om voor haar verricht onderzoek als proefschrift te publiceren.

Waarde Boogaard, ik beschouw het experimentele gedeelte van het onderzoek als ons beider werk, niet alleen om ons afwisselend optreden als proefleider en proefpersoon, maar ook om Uw oplossing van talrijke experimentele problemen, en om de diepgaande diskussies over het onderwerp zelf.

Alle medewerkers van het Instituut voor Zintuigfysiologie, die bij de voorbereiding en de uitvoering van het onderzoek betrokken waren en die bijdroegen tot de vormgeving van dit proefschrift, zeg ik van harte dank, in het bijzonder voor de vriendschappelijke wijze waarop dat gebeurde.

Te veel hulp om op te noemen heb ik van andere personen en instellingen binnen en buiten TNO gehad in de vorm van apparatuur, advies en diskussie. Hen allen ben ik zeer erkentelijk.

CONTENTS

CHAPTER 1

INTRODUCTION

§1.1. THE SUBJECT

Object size, luminance and contrast are the main parameters of vision and the corresponding visual aids are angular magnification, image intensification and contrast enhancement. Angular magnification and contrast enhancement have been realized by optical instruments such as telescopes, microscopes and phase-contrast microscopes. Image intensification on the other hand cannot be realized by optical aids alone, and had to wait for the development of photography and electro-optics. With that a new visual problem arose: the effect of graininess or speckle-noise upon visual performance. In this thesis vision through photo-electronic image intensification is studied in particular and compared with unaided vision.

§1.2. CONTRAST SENSITIVITY FUNCTIONS

The most important aspects of visual performance are resolving power and contrast sensitivity, *i.e.*, the abilities to distinguish small details and to detect small luminance differences. Neither of them can be characterized by a single number, however, since the resolving power is a function of contrast and contrast sensitivity is a function of object size. Indeed the quality of optical instruments was expressed for a time in the resolving power for high contrast only, but high contrast seldomly occurs, especially in the open air. Arnulf (1937) therefore measured the resolution of bar patterns observed through telescopes as a function of contrast.

Now it is preferable to measure contrast sensitivity for sine wave gratings (Fig. 1) as a function of spatial frequency. The resulting contrast sensitivity functions link up with the modulation transfer functions (MTF's), which are currently used to describe the imaging quality of optical instruments (Baker, 1971). In addition to the transfer of contrast they also reflect the sensitivity of the detection process including the possible effect of noise.

It is not claimed here that vision is unequivocally characterized by sine wave responses. One may reasonably assume, however, that contrast sensitivity functions comprise sufficient information to predict the performance of realistic visual tasks. Classical test objects, such as circular disks and Landolt-rings may be equally representative as sine wave gratings, and in some special cases they may be even more representative. Contrast sensitivity functions for sine wave gratings, however, have the additional advantage that they can be easily analyzed in and synthesized from their components.

§1.3. OUTLINE

Unaided vision

In chapter 2 the measurements of contrast sensitivity functions for unaided vision are described. These contrast sensitivity functions are primarily used in the later comparison of aided and unaided vision. Naturally the De Vries (1943) and Rose (1948) hypothesis, that vision is limited by photon noise at low luminances is discussed. The Poisson-fluctuations in a signal of $\bar{N}$ photons amount to $\sqrt{\bar{N}}$. Thus the signal to noise ratio is $\bar{N}/\sqrt{\bar{N}} = \sqrt{\bar{N}}$, and indeed contrast sensitivity is found to be proportional to the square root of luminance in appropriate conditions. This behaviour is complicated by changes in spatial summation. At low luminances larger summation areas favour contrast sensitivity at the cost of resolution. At higher luminances smaller summation areas improve resolution at the cost of contrast sensitivity. Considering this the integral I of contrast sensitivity over spatial frequency is proposed as an index for visual performance:

$$I = \int(w).dw \qquad (1.1)$$

It will be shown that I obeys the square root law of the fluctuation theory over a large range of luminances.

From photon-noise to speck-noise

Fundamental questions concerning vision with image intensification are investigated experimentally in chapter 3. Electronic amplification can not compensate fully for the absence of light in object space. Although each photon that is detected by a photocathode can be displayed as a more or less bright speck on a phosphor screen, the speck-density will reflect the Poisson-fluctuations. The user's eye views a speck-image as illustrated in Fig. 2 instead of the normal "photon-image". It is generally assumed in literature (§3.2), that vision is limited by speck-noise in exactly the same way as it is by photon-noise in unaided vision at low luminances. From this point of view the specks must be sufficiently bright to be detected by the retina, and any further intensification is useless, because it amplifies the noise as much as the signal.

This simple signal-to-noise theory is not self-evident with respect to the visual system. It is conceivable, that the visual system processes speck-noise differently. Undoubtedly speck-noise will limit contrast sensitivity. The question is, however, whether this is the same limit that photon-noise places on unaided vision. Apart from that an important practical question concerns the minimum required speck-intensity to insure that the specks are detected by the observer's retina. Are the available threshold data for single flashes applicable to the different situation of specks in a speck-image?

To answer these questions contrast sensitivity is measured for vision at speck-images, generated by a special experimental set up. Speck density and speck-intensity both are parameters in these experiments. By varying the intensity of the specks from low to high the gradual transition from photon-noise-limited vision to speck-noise-limited vision can be followed.

Quantum efficiency

The basic advantage of image intensifying devices is that they collect more photons than the unaided human eye. Their entrance pupil is usually larger and the sensitivity of their photocathode may be higher than the sensitivity of the retina. The literature on the quantum efficiency of the retina (briefly reviewed in §4.2) reports values between 0,5% and 10% for the dark-adapted peripheral retina at the optimum wavelength. This gives rise to different opinions on the relative effectiveness of image intensifiers, of which the maximum quantum efficiency can be about 10%. In chapter 4 a new method to determine the quantum efficiency of the retina is introduced. This method is based upon the speck-image experiments of chapter 3. If photon-noise and speck-noise affect contrast sensitivity equally, then the quantum efficiency can be found as the ratio of the photon-density and the speck-density that are required to obtain a certain contrast sensitivity in both cases.

Vision through intensifier telescopes

In chapter 5 vision through telescopes equipped with image intensifier tubes is evaluated and compared with unaided vision and vision through night-glasses. Speck-density and speck-intensity in image space follow from the relevant properties of telescope and intensifier tube. Imperfect imaging, expressed in the modulation transfer function of the device, can be accounted for as well as the possible contrast rendition by straylight. Thus the final speck-image observed by the user of an image intensifier telescope can be specified, and contrast sensitivity can be predicted from the speck-image experiments of chapter 3. This procedure is verified for vision with some actual image intensifier telescopes.

Optical modulation transfer of the human eye

The contrast sensitivity functions mentioned represent the visual system as a whole and as such they are directly useful. For insight in the underlying visual processes, however, they should be analyzed into their optical and neural components. One might question for instance whether the high-frequency decay is of optical origin only?

The optical quality of the eye is discussed in chapter 6. Experimental data on the various geometrical aberrations are available in literature. Modulation transfer functions can be calculated from these data. Considering that the chromatic difference of focus is the predominating aberration in whitish light and that this aberration is not different in individual eyes, the results of such calculations may be generally representative.

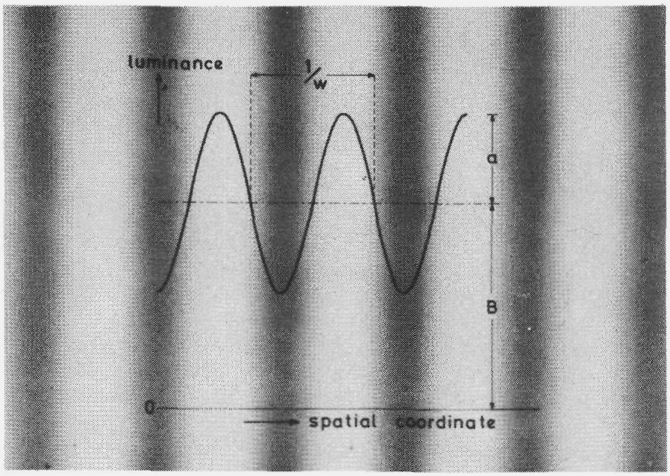

Fig. 1. Spatial sine wave pattern. The luminance is sinusoidally modulated as a function of spatial coördinate. The contrast is defined as a/B. The spatial frequency w is the number of periods per unit of angle.

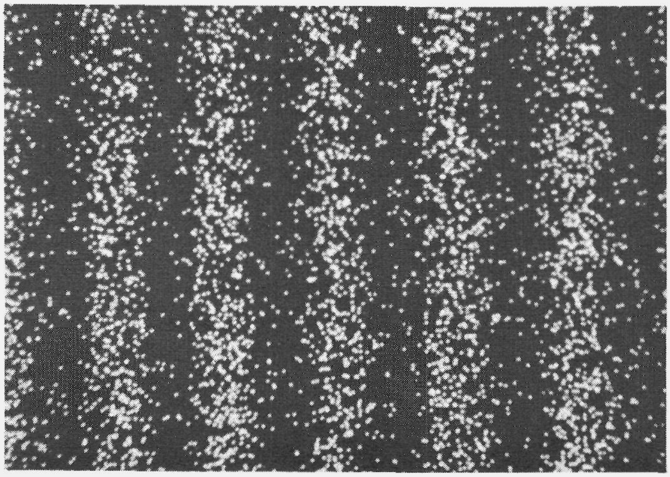

Fig. 2. Speck-image of a sine wave grating. Speck-density is modulated sinusoidally as a function of spatial coördinate. The contrast of the sine wave gratings is defined as the ratio of amplitude and mean speck-density.

Modulation transfer functions have also been measured, by Campbell and Gubish (1966) among others. They managed to reconstruct MTF's from the weak image of a narrow slit, that is reflected by the *fundus* of the eye. The interpretation of these fundus reflection measurements is not completely clear. Nature and origin of the fundus reflection are uncertain and at least some contrast reduction by retinal scattering is included. Thus the present calculations may complement these measurements. They further reveal the connection of modulation transfer and aberrations and can be extended to the special conditions of vision at low luminances.

Spatial interactions in the retina-brain system

The ratios of the contrast sensitivity functions of the visual system as a whole and the MTF's of the optics of the eye can be interpreted as contrast sensitivity functions of the retina-brain system. The form of these contrast sensitivity functions may be related to the spatial interactions in the retina-brain system. Various models on spatial interactions have been proposed, all more or less succesful in explaining one type of experiments. Rose (1948) assumed, that the visual system summates the retinal photon-flux over the whole test object regardless of its size and compared the result with the photon-flux in an equal area of the background. Most of the literature on vision through image intensification (§3.2) adheres to this idea, even though it is unfeasible. Rose's model is contrary to the experimental evidence of so-called Ricco-areas with fixed size. Bouman and Van der Velden (1947) differentiated two kinds of spatial interactions in their two-quanta explanation of threshold vision: direct summation of the photon flux within Ricco-areas, followed by summation of detection probability when a test object is larger than Ricco's area. Which model is supported by the contrast sensitivity functions of the retina-brain system?

§1.4. RESTRICTIONS

In this thesis vision with and without image intensification is studied in terms of modulation transfer and contrast sensitivity for sine wave gratings. Some important restrictions may be mentioned. First, aids to vision are used for realistic visual tasks like the detection and recognition of relevant objects. The gap between such realistic tasks and the present elementary sine wave responses has still to be bridged and is subject to further study (Van Meeteren and Zonneveld, 1972). Second, not all aspects of optical instruments, the eye included, may be expressed in terms of contrast sensitivity functions or MTF's. This especially applies to the function of the field of view in visual search. Third, temporal and spatio-temporal aspects of moving objects remain untouched.

CHAPTER 2

CONTRAST SENSITIVITY FUNCTIONS FOR UNAIDED VISION

§2.1. LITERATURE

In this chapter natural unaided vision at low luminances will be described briefly on the basis of contrast sensitivity functions for spatial sine wave gratings. A rather extensive literature on contrast sensitivity functions has been published since their introduction by Selwyn (1948). Westheimer (1965), Ronchi and Van Nes (1966), and Van Meeteren (1966) present literature surveys. Contrast sensitivity functions depend in absolute value and in form upon luminance, field size, retinal position, orientation, presentation time and pupil size, but not upon colour. In natural vision these factors operate simultaneously. Their separate effects may be surveyed here in bird's-eye view.

The independency of colour was established by Van Nes and Bouman (1967), who measured contrast sensitivity functions for monochromatic blue, green and red lights and found no difference in photopic conditions. This does not imply necessarily, that the three receptor systems have the same contrast sensitivity functions when isolated (Green, 1968; Kelly, 1973), but possible differences do not come out in practical vision.

Luminance was varied by Schade (1956), Rosenbruch (1959), Robson and Campbell (1964), Patel (1966), Van Nes and Bouman (1967), Daitch and Green (1969), and Van Meeteren, Vos and Boogaard (1971). Just like for other test objects, contrast sensitivity for sine wave gratings first increases roughly with the square root of luminance and finally levels off to the Weber-fraction when luminance is raised. The visual system is a bandpass filter for spatial frequencies: contrast sensitivity is not only subject to high-frequency decay but is also suppressed at low spatial frequencies. This bandpass filter shifts to higher spatial frequencies at higher luminances. The high-frequency decay may be caused by optical blurring and neural sampling. The low-frequency suppression must be exclusively of neural origin.

Contrast sensitivity depends markedly on the size of the sine wave fields. The larger the sine wave field the higher the contrast sensitivity, but the improvement is only marginal when the field contains more than 7 periods of the pattern (Rosenbruch, 1959; Coltman and Anderson, 1960; Findlay, 1969) and when the length of the bars exceeds 1^{o} (Schober and Hilz, 1965). Thus sine wave fields should extend over some degrees of visual angle and the lowest spatial frequencies should be excluded from the measurements in order to avoid field size complications. We will return to this in chapter 7.

Contrast sensitivity functions are different in fovea and periphery (Patel, 1966; Daitch and Green, 1969). Contrast sensitivity is higher in the periphery, whereas spatial bandwidth is larger in the fovea.

Contrast sensitivity is about two times higher for gratings in the vertical and the horizontal orientation as compared with the oblique orientation (Campbell, Kulikowski and Levinson, 1966). The difference is at least partly of neural origin and seems to be somewhat larger at high spatial frequencies.

Presentation time is a determinant factor also. According to Schober and Hilz (1965) contrast sensitivity is improved by more than a factor 10 when the presentation time is raised from 15 to 1000 msec. Unfortunately it is not made clear whether a further improvement might be expected from longer presentation times. The relative suppression of low spatial frequencies is not found for short presentation times and apparently takes some time to develop. This also fits with experiments of Van Nes, Koenderink and Bouman (1967)on spatio-temporal contrast sensitivity for moving and flickering sine wave gratings.

Finally the effect of pupil size is twofold. First, pupil size controls retinal illuminance and as such its effect is equal to that of varying luminance. Second, the quality of the retinal image depends upom pupil size as will be amply discussed in chapter 6. The effect of pupil size was controlled as a rule in the experiments cited, by the use of artificial pupils.

The more recent literature on experiments with sine wave gratings concentrates predominantly on the possible existence of sine-wave-channels, mediating Fourier-analysis in vision (Campbell, 1969). We will return to this question in chapter 7. To avoid possible misunderstandings it should be noted, that the use of contrast sensitivity functions measured with sine wave gratings does not stand or fall with the existence of Fourier-analytical processing in the visual system.

The above literature survey is far from complete and deals with those factors only that might be related to the present problem. The measurements on natural vision at low luminances described in this chapter are comparable to the measurements of Schade (1956). Schade, however, presented normalized contrast sensitivity functions and did not mention absolute values of contrast sensitivity. Moreover, new measurements were required to characterize the unaided visual performance of the same observers, that participated in the experiments on aided vision.

§2.2. THE MEASUREMENTS

A set of sine wave gratings with different spatial frequencies was produced photographically in the form of slides by making blurred contact prints of bar patterns. These slides could be illuminated from behind and observed directly, when only small sine wave fields were needed, as in the experiments of §3.6, §4.3, §5.5 (it-1) and §6.2. Large sine wave fields, as used in the experiments of §2.3, §5.2 and §5.5 (it-2), were realized by projection. The special use of the sine wave slides in the speck-image experiments of chapter 3 will be illustrated on the spot.

The contrast a/B of the sine wave gratings (see Fig. 1) is varied by superposition of a uniform veiling field. To reduce the contrast, for instance, the average luminance of the sine wave grating itself is decreased, whereas the luminance of the veiling field is increased by the same amount. Thus the total mean luminance B is kept constant. Luminance calibrations were made with a Weston Viscor photocell.

The procedure of the measurements was as follows. In fact two contrast sensitivity functions were measured simultaneously by presenting the sine wave gratings in vertical and horizontal orientation. The experimenter presented a number of contrast settings near threshold in random order and in steps of a factor 1.3 (1.2 in the latter experiments of chapters 3, 4, 5 and 7). The observer's task was to detect the orientation of the grating. He was asked to respond with "vertical", "horizontal" or "no choice". The responses were registered as follows:

contrast	0.10	0.12	0.14	0.17	0.20	0.24	0.28	0.33
horizontal		0	0	0 /	+	+		+
vertical	0	0	0 /	+	+	+		

where 0 stands for "no choice" and + for correct "horizontal" or "vertical" responses. The threshold was defined as indicated by the slash and is 0.185 for the horizontal grating and 0.155 for the vertical grating in the above example. About 5 per cent of the "horizontal" and "vertical" responses were incorrect. Incorrect responses were considered as a sign of guessing and neighbouring correct and incorrect responses were interpreted as neutralizing each other to "no choice" responses. Admittedly, this method is a coarse one, relying upon the stability of the observer's criterion. It must be realized that rigid measurements of frequency of seeing curves require 150-200 presentations and are impractical when the interest is mainly in mutual comparison of contrast sensitivity functions. In practice the reproducability, especially of complete contrast sensitivity functions, is satisfactorily. Repeated measurements of the same threshold contrast show a standard deviation of 20%. As followed from a pilot experiment thresholds determined in this simplified way correspond roughly to a detection probability of 70 per cent with 30 per cent false alarms.

Most of the experiments were made by two observers, JB and AvM, in order to verify the results of one at least by one other one. The visual acuity defined as the reciprocal of the just resolvable Landolt-ring gap in min of arc, was 2 for both subjects when they wore their normal correction glasses. The latter were built in to the apparatus, when artificial pupils were used, as well as in the measurements with night-glasses and intensifier telescopes in order to avoid discomfort.

For the sake of brevity and clarity the average results of both observers and both pattern orientations will be presented, if not mentioned otherwise. Only small differences between observers and orientations have been found, which in general may remain undiscussed in this study.

§2.3. CONTRAST SENSITIVITY AND RESOLVING POWER

To characterize natural unaided vision a set of contrast sensitivity functions was measured in the luminance range of 10^{-4} to 10 cd/m^2 with large sine wave fields of $17^0 \times 11^0$ projected on a white screen. The sine wave gratings were observed from a distance of 4 m in free fixation with both eyes, unlimited presentation time and natural pupil. The size of the natural pupil was measured in the experimental conditions and changed from about 5 mm at 10 cd/m^2 to about 7 mm at 10^{-4} cd/m^2 for both observers. The measured contrast sensitivity functions are plotted in Fig. 3 and show the general properties known from literature.

Starting at low light levels, contrast sensitivity first rises pro-

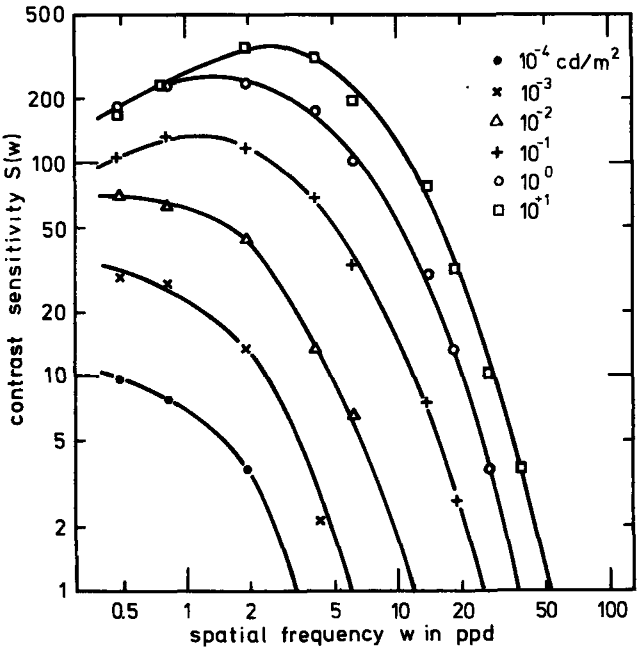

Fig. 3. Contrast sensitivity functions. Spatial frequency is plotted in periods per degree. These measurements refer to normal free vision to a field of $17^0 \times 11^0$. The natural pupil was 5-7 mm in the luminance range concerned.

portional to the square root of luminance in agreement with the De Vries-Rose law, and finally levels off submitting to Weber's law. Naturally contrast sensitivity is cut off at higher spatial frequencies. The high-frequency decay reflects the total fusion caused by the optics of the eye and by the retina-brain system. It appears that the contrast sensitivity functions for the various luminances cannot be brought to coincide by vertical shifts alone. They are also shifted horizontally towards higher spatial frequencies at higher luminances, mainly because of shrinking neural fusion, as will be shown. Remarkably, contrast sensitivity is suppressed also at low spatial frequencies when the light level is sufficiently high. This "differentiator" effect is exclusively of neural origin and associated with lateral inhibition (Ratliff, 1965). In short, contrast sensitivity as a function of luminance obeys to well-known visual laws, and contrast sensitivity as a function of spatial frequency is controlled by spatial imaging and neural processing. The quality of the eye optics is dealed with in chapter 6. Some models of neural processing are discussed in chapter 7. The fluctuation theory underlying the De Vries-Rose law is explained in §2.4.

The curves of Fig. 3 are intentionally plotted to read contrast sensitivity as a function of spatial frequency. One may read also from the same curves resolving power as a function of contrast, when resolving power is defined here as the highest spatial frequency that can be resolved at a certain contrast. Thus the curves clearly reflect two important aspects of vision: contrast sensitivity in their height and resolving power in their width. The maximum resolving power - akin to the visual acuity for optotypes - is obtained in particular for unitary contrast and can be read from the intersections of the contrast sensitivity functions with the abscissa. Maximum contrast sensitivity and maximum resolving power as derived from Fig. 3 are replotted *vs.* luminance in Fig. 4. The square root law for contrast sensitivity is approximated indeed, though not over a large luminance range. The maximum resolving power also improves with rising luminance but at a lower rate, which is in agreement with visual acuity measurements (König, 1897). The amelioration of the maximum resolving power is partly implied by the rising contrast sensitivity, as will be evident from inspection of Fig. 3. This has been pointed out before by Denier van der Gon (1959) in his fluctuation theoretical treatment of visual acuity. The improvement of visual

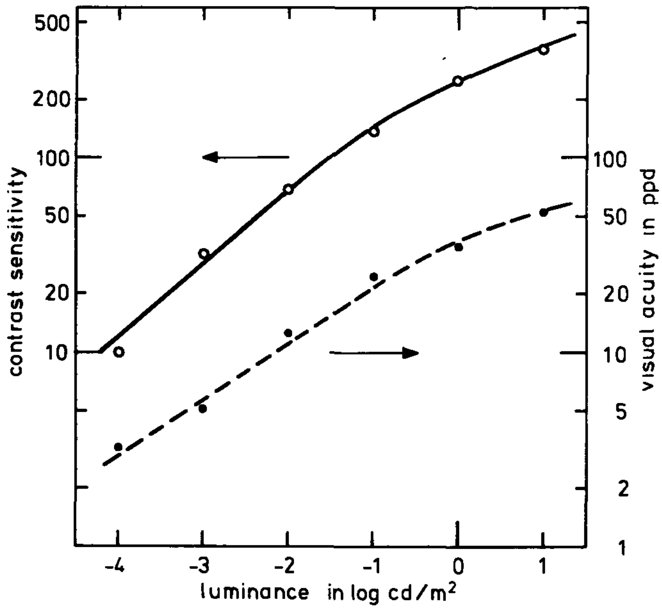

Fig. 4. Contrast sensitivity and visual acuity for sine wave gratings as a function of luminance. Data derived from Fig. 3.

acuity is yet smaller than would follow from the square root law, due to the convex form of the contrast sensitivity functions. Apart from this the resolving power is further improved at higher luminances by the changes in image quality and neural processing mentioned above.

§2.4. FLUCTUATION THEORY

According to the fluctuation theory of De Vries (1943) and Rose (1948) vision is limited at low luminances by the Poisson-fluctuations in the collected photon flux. Let the photon flux that enters the eye be ϕ_p photons per sec per min^2 of arc upon the retina. To get measurable signals the retina collects ϕ_p over some area α^2 and some time τ. The number $\bar{N}_c$ of collected photons in such a sample is:

$$\bar{N}_c = \tau\alpha^2\eta\phi_p, \tag{2.1}$$

where η is the quantum efficienct and α^2 and τ are expressed in min^2 of arc and sec respectively. $\bar{N}_c$ is the average number of collected photons in the sample. Repeated countings will show a standard deviation $\sqrt{\bar{N}_c}$, due to Poisson-fluctuations. Possible differences $\Delta\bar{N}_c$ in different coutings can be detected at best with a certain probability P(k) if:

$$\Delta\bar{N}_c = k \cdot \sqrt{\bar{N}_c}$$

Thus the threshold contrast $\Delta\bar{N}_c/\bar{N}_c$ that must be exceeded to detect the difference $\Delta\bar{N}_c$ with a probability $\geqq$ P(k) is:

$$C_{th} = k \cdot \frac{\sqrt{\bar{N}_c}}{\bar{N}_c}$$

and the corresponding contrast sensitivity S becomes:

$$S = \frac{1}{k} \cdot \frac{\bar{N}_c}{\sqrt{\bar{N}_c}} = \frac{1}{k}\sqrt{\tau\alpha^2\eta\phi_p} \tag{2.2}$$

Eq. (2.2) puts an upper limit to contrast sensitivity inherent to the quantum nature of light. Contrast sensitivity can at best be proportional to the signal to noise ratio $\bar{N}_c/\sqrt{\bar{N}_c}$ in the collected photon flux.

The most important inference of Eq. (2.2) is that contrast sensitivity is expected to be proportional to the square root of the photon flux that enters the eye. This De Vries-Rose law is roughly in agreement with the well known experimental data of Blackwell (1946) among others, as Rose (1948) demonstrated. This may indicate indeed, that the visual system follows the photon-noise limit close on. How closely the photon-noise limit is approximated has to be judged by a quantitative evaluation of Eq. (2.2), which unfortunately is problematic because of uncertainty on the quantum efficiency η (see chapter 4).

Rose (1948) further attempted to predict contrast sensitivity for circular disks as a function of their size. He assumed that the visual system summates the incoming photon-flux over the area of the test object and compares the result with a sample of equal size taken from the background. In other words the integration area would adapt to the test object and Rose substituted the size of the testobject for α^2 in Eq. (2.2). This model, which has been borrowed as a rule in the theoretical evaluations of vision with image intensifiers, leads to a simple description of spatial vision.

Rose's assumption is unlikely all the same. The forthcoming description of spatial vision is too simple in fact and holds at best for a small range of medium object sizes, as Rose (1948) demonstrated himself. It is more likely that the visual system summates the incoming photon-flux over constant summation areas, which do not specifically adapt to the size of the test object; as will be discussed in chapter 7. A complication of the De Vries-Rose law is, that the size of these summation areas depends upon the light level. At lower luminances the visual system summates over larger Ricco-areas, in favour of contrast sensitivity as will be evident from Eq. (2.2). Morgan (1965) recognized this and substituted the reciprocals of the spatial and temporal "noise equivalent bandwidths" for α and τ. Deriving "noise equivalent bandwidths" from contrast sensitivity functions measured by Schade (1956) and Kelly (1961), he found contrast sensitivity data of DePalma and Lowry (1962), Blackwell (1946) and Sturm and Morgan (1949) in good agreement with Eq. (2.2).

The use of the "noise-equivalent bandwidth" is debatable here, however. It presumes that each point of the retina is the center of a summation area in a continuously overlapping array. The retina in fact contains a mosaic of only partly overlapping receptive fields. Considering this, one should substitute the effective size α_e of the receptive fields in Eq. (2.2). This size α_e can nevertheless be derived from the form of the contrast sensitivity functions for sine wave gratings as will be argued in §7.4. The contrast sensitivity functions S(w) can be written as the product S·T(w) of contrast sensitivity S and modulation transfer T(w). It can be shown then that:

$$\alpha_e = \frac{1}{2\int T(w)dw} = \frac{S}{2\int S(w)dw} \tag{2.3}$$

Combining this with Eq. (2.2) it follows that:

$$I = \int_0^\infty S(w)dw \therefore \sqrt{\phi_p} \tag{2.4}$$

In other words the integral I of contrast sensitivity over spatial frequency should be proportional to the square root of the detected photon flux. This prediction is confirmed by the integrated contrast sensitivities derived from the data of Fig. 3 and plotted vs. luminance in Fig. 5: integrated contrast sensitivity is proportional to the square root of lu-

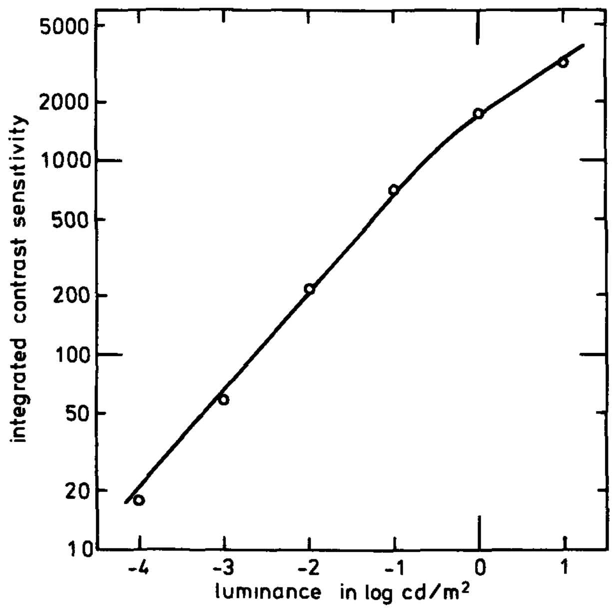

Fig. 5. Integrated contrast sensitivity according to Eq. (2.4) plotted *vs.* log luminance. Note the square root slope. Data derived from Fig. 3.

minance over almost five decades. At higher luminances the integrated contrast sensitivity remains behind the square root relation, partly because of shorter summation time and smaller pupils, partly as an onset of the Weber regime.

It may be remarked finally that the fluctuation theory has developed to a general principle explaining chromaticity discrimination as well as contrast sensitivity (Walraven, 1962; Vos and Walraven, 1972). The fluctuation theory describes the photon-noise limitation of vision without specifying any threshold mechanism. Bouman and his coworkers investigated possible mechanistic models (Bouman and Koenderink, 1972).

§2.5. THE INTEGRATED CONTRAST SENSITIVITY

The integrated contrast sensitivity I is proposed here as a summary measure for visual performance. It characterizes the total amount of information that is assimilated, irrespective of the form of the contrast sensitivity functions. The absolute height of the contrast sensitivity functions represents the amount of metric information, whereas the spatial bandwidth represents the amount of structural information (Van Soest, (1952). The total amount of information carried by a photon flux is proportional to the square root of that photon flux. This is reflected in the integrated contrast sensitivity of the unaided eye. At low luminances the visual system summates over large Ricco-areas in favour of contrast sensitivity at the cost of resolution. This results in a relatively high contrast sensitivity function over a relatively small range of spatial frequencies. At higher luminances smaller Ricco-areas favour resolution while contrast sensitivity levels off. This finds expression in relatively low contrast sensitivity functions over a large range of spatial frequencies. Irrespective of this change in strategy the integrated contrast sensitivity is a good summary measure of the total amount of information that is assimilated.

As will be discussed in chapter 5 the total gain in visual performance provided by intensifier telescopes can be distributed more or less at choice over angular magnification or concentration of the detected photon flux. By angular magnification the contrast sensitivity functions are shifted towards higher spatial frequency. The contrast sensitivity functions are shifted upwards on the other hand by concentration of the detected photon flux, *i.e.*, by intensification of the effective luminance. Whatever choice is preferred the total gain in integrated contrast sensitivity is governed by the photon-catch of entrance pupil and photocathode.

It may be expected that the performance of realistic visual tasks like the detection and recognition of relevant objects correlates well with the integrated contrast sensitivity I. A high correlation was found at least between the akin MTFA and the interpretability of photographs (Snyder, 1973). This MTFA integrates the *difference* of the modulation transfer function $T(w)$ of the photographs and the threshold contrast $C_{th}(w)$:

$$MTFA = \int\{T(w) - C_{th}(w)\}dw$$

The integrated contrast sensitivity I in this case would integrate the *ratio* of $T(w)$ and $C_{th}(w)$:

$$I = \int T(w) \cdot S(w) dw = \int \frac{T(w)}{C_{th}(w)} dw$$

The MTFA proved to be a good measure for the interpretability of photographs with different modulation transfer functions T(w). In the case of aided and unaided vision, however, the integrated contrast sensitivity I is preferable as a performance measure for its simple relation to the detected photon flux and since it reflects contrast sensitivity uniformely over its whole range. The MTFA hardly appreciates the difference between threshold contrasts of 0.01 and 0.10, for instance.

It should be realized that summary measures to characterize visual performance in one dimension are of limited use. The integrated contrast sensitivity I, for instance, attaches the same weight to contrast sensitivity and resolving power. In practice, however, one may be more important than the other, depending on circumstances.

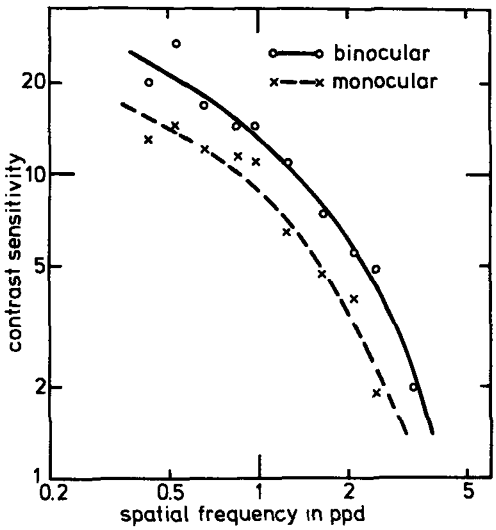

Fig. 6. Comparison of binocular and monocular vision.

§2.6. BINOCULAR AND MONOCULAR VISION

In normal vision both eyes are used and from the beginning on great value has been set on the binocular make-up of telescopes (De Waard, 1906). And indeed, leaving the greater comfort aside, two eyes see more than one. This has to be taken into account in the comparison of vision through monocular instruments with natural unaided vision. The mechanisms of binocular interaction will not be discussed here. Suffice it to illustrate and quantify the effect. In Fig. 6 contrast sensitivity functions, measured with a large sine wave field of 15^{0} in diameter at a luminance of 3.5×10^{-4} cd/m^2, are presented for binocular and monocular vision. Contrast sensitivity is about a factor $\sqrt{2}$ higher for binocular vision in agreement with measurements of Campbell and Green (1965b).

§2.7. RECAPITULATION

Natural unaided vision at low luminances was discussed briefly with the aid of contrast sensitivity functions. The integral I of contrast sensitivity over spatial frequency was proposed as a summary measure for visual performance. In agreement with the fluctuation theory this integrated contrast sensitivity is proportional to the square root of luminance over almost five decades. At higher luminances the integrated contrast sensitivity levels off, according to the Weber-Fechner law. The spatial bandwidth of the contrast sensitivity functions is smaller at low luminances, which can be related to summation over larger Ricco-areas in favour of contrast sensitivity. The contrast sensitivity functions represent the visual system as a whole: a further analysis into the optical and the neural components is required.

CHAPTER 3

FROM PHOTON-NOISE TO SPECK-NOISE

§3.1. INTRODUCTION

Once detected by the photocathode of electro-optical instruments, photons can be made visible as bright specks on an image screen by electronic amplification. When the detected photon flux is sufficiently high these specks combine in space and time to form a normal, smooth image. At lower light levels in object space, however, the detected photon flux can be so small, that the corresponding specks are visible as such, especially when the amplification is high. Fig. 2 illustrates such a speck-image of a sine wave grating.

The speck-density reflects the Poisson-fluctuations of the underlying photon flux. Where unaided vision is already limited by photon-noise, vision at speck-images will be the more so by the corresponding speck-noise. As far as we know, all theoretical evaluations of vision with image intensification, accordingly are variations of the fluctuation theory, discussed in §2.4. One simply replaces photon flux by speck-density in the formulations. Contrast sensitivity for vision at speck-images thus should be proportional to the square root of speck-density, and this prediction was confirmed experimentally by Coltman (1954) and others. After several experimental determinations of the factor k in Eq. (2.2), which will be surveyed in §3.2, the evaluation of vision with image intensification thus seems to be complete.

On reflection, however, some important questions remain to be answered. In its basic form the fluctuation theory states, that contrast sensitivity is governed unambiguously by the retinal signal-to-noise ratio. From this point of view there is no difference between photon-noise and speck-noise. It is conceivable, however, that the visual system processes speck-noise differently. Taking for granted that photon-noise and speck-noise put a limit to unaided and aided vision respectively, the question is whether this is exactly the same limit, as was assumed more or less tacitly in the literature. As long as each speck results in not more than one photon detected by the retina the assumption is acceptable. What happens, however, when the intensity of the specks is higher so that the speck-noise becomes visible as such? It notably is conceivable, that speck-images as illustrated in Fig. 2, would be processed at a central stage of the visual system in a more sophisticated way, resulting in higher contrast sensitivity. It is further conceivable that spatial and temporal processing are different at such a central stage of the visual system. This would result in a different form of the contrast sensitivity functions. It is possible also that the visibility of the speck-noise disturbs the detection proces at a central level and reduces contrast sensitivity henceforward.

It will be evident that the specks must be sufficiently bright to ensure that each of them is detected by the retina of the observer's eye. A practical question, then, first of all is: what is the minimum required speck-intensity to make sure that all specks are detected? In the fovea a single speck must contain about 450-900 "corneal" photons (see the literature survey in §4.2.2). "Corneal" here and in the following means: measured at the cornea and over the entrance pupil. In the periphery about 50-110 corneal photons are required to see a single speck (§4.2.2). It is questionable, however, whether these data apply to the different situation of specks in a speck-image. In the latter case it is only required that the specks are detected by the retina, not that they are seen by the observer.

Vision at speck-images is investigated in this chapter with these doubts in mind. Are the effects of speck-noise and photon-noise the same? And what is the minimum required speck-intensity? To answer these questions contrast sensitivity functions were measured with speck-density and speck-intensity as parameters.

§3.2. LITERATURE

3.2.1. Direct experiments with speck images

In the following literature survey we will connect to Eq. (2.2), re-written as:

$$S = \frac{1}{k}(\tau\alpha^2\phi_s)^{\frac{1}{2}} \qquad (3.1)$$

where ϕ_s is the retinal speck-density expressed in the number of specks per sec per min^2 of arc.

Rose (1948) simulated speck-images of a test-chart with circular black disks on a kinescope-screen. To determine the value of k he made photographs of the image on the kinescope-screen and counted the number of specks N_s within an area equal to the area of the just detectable black disk. Assuming that the visual system summates the signal over the whole test object indeed, Rose thus found k to be about 5.0. Returning to the kinescope screen he concluded that the integration time τ was about 0.2 seconds.

Sturm and Morgan (1949) and Tol (1953) measured contrast thresholds for circular holes in a Burger-phantom observed through a fluorescopic screen intensification system. Their results are roughly described by Eq. (3.1) for medium sized objects. They found k-values between 3 and 5 when the summation time was taken as 0.2 sec.

Coltman (1954) simulated speck-images of a bar pattern of about 5 ppd on a kinescope-screen and measured contrast sensitivity as a function of speck-density. The square root relation of Eq. (3.1) was roughly confirmed. What about spatial integration with respect to bar patterns? Coltman assumed that the visual system summates over the light bars and the dark bars separately and then compares the difference with the noise in an equal area. Taking the values of Rose (1948) for τ and k Coltman concluded that the aforesaid integration area extended over "1/4 of the test pattern" in the experiment concerned. This is a rather loose interpretation, and there is no indication how to extrapolate the data to other spatial frequencies than the one that was investigated.

Schagen (1963) presented experimental data on the resolution of Landolt-rings observed through an actual intensifier telescope as a function of the luminance in object space. He found Eq. 3.1 confirmed and derived a value of 1.9 for k when the integration time was taken as 0.2 sec. According to Schagen this k-value is in agreement with the theoretical value for "a detection probability" of 75 per cent in a four-channel forced choice situation".

Some experimenters added white beam current noise to video signals. The resulting display noise differs from the speck-noise mentioned sofar in its analog character compared with the digital character of speck-noise. This difference may be visible at extreme low signal to noise ratios. However, when the display noise is really white, it can be argued that Eq. (3.1) applies here also if $\sqrt{\phi_s}$ is replaced by an appropriate expression for the beam current signal to noise ratio.

Coltman and Anderson (1960) added white noise to bar patterns on a television display and found the just resolvable number of line pairs per picture to be proportional to the current signal to noise ratio. However, they urged the observers to optimize the viewing distance in order to obtain the highest resolution. As the authors point out themselves, the best strategy then is, to change the viewing distance inversely proportional to the current signal to noise ratio, and to keep the retinal signal to noise ratio constant in this way. Considering this the experiment only confirmed that the performance of the eye is the same when the retinal image is the same.

Rosell (1971) studied the probability of detecting rectangular targets on a television display with additive white noise. The target was presented in one of four quadrants. The possible target positions were located on the corners of a square of 8^o x8^o. It should be remarked that this is a search task rather than a detection task. The experimental probability of detection curve, measured as a function of the display signal-to-noise ratio, fitted satisfactorily to the theoretical curve and spatial integration proved to be complete within squares up to 1 degree^2 and rectangulars of 0.13 x 6.2 degree^2. This large spatial integration may be typical for search tasks. According to Rosell the theoretical and experimental value of k is 3.7 for "a detection probability of 75 per cent in a four-channel forced choice situation".

The experiments mentioned sofar regarded vision with image intensification directly. In general they confirm the fluctuation theory. In presenting k-values for various types of test objects and threshold criteria they make Eq. (3.1) fit for use. The value of k seems to be in agreement with its detection theoretical value. The higher k-values of Rose (1948) and Tol (1953) may indicate that in their case the threshold criterion corresponded to a high probability of detection. How contrast sensitivity depends upon target size or spatial frequency in vision with image intensification has not been settled by these experiments. All authors assume, as Rose (1948) did, that the retina summates over the whole area of the test object and compares the result with the noise in an equal area of the background. They consequently substitute the size of the test object for α^2 in Eq. (3.1). This may be correct for medium sized objects. Spatial summation, however, may not be complete over larger test objects, whereas the detection of small test objects is complicated by spatial blur and neural fusion. It finally is not clear how to extent this relation to sine wave gratings.

3.2.2. Comparison with unaided vision

Vision with image intensification has also been evaluated indirectly by comparison with the naked eye. It is postulated, then, that the visual system processes speck-noise and photon-noise equally. Dirksen and Van Schie (1963) in this way transfered Blackwell's (1946) contrast threshold data for unaided vision to the object space of intensifier telescopes. And Morgan (1965) predicted contrast sensitivity functions for vision with image intensification from contrast sensitivity functions for unaided vision. If correct, this approach is attractive. All data on unaided vision would be available at once for the detailed evaluation of vision with image intensification. Two objections stand in its way. First the quantum efficiency of the unaided eye must be known. Dirksen and Van Schie adopted a value of 6%, whereas Morgan took 12%, and Schagen about 1%. We will return to the quantum efficiency of the retina in chapter 4. Second, the starting point of the method is not selfevident as will be discussed in the next section.

3.2.3. The effect of speck-intensity

Are there experimental indications that the visual system processes speck-noise and photon-noise equally? This question is identical to another one: what is the effect of varying speck-intensity? At low speck-intensities (10 corneal photons per speck for instance) the speck-images cannot be distinguished from "photon-images". When the speck-intensity is raised to a high level (500 corneal photons per speck for instance) the speck-noise becomes visible as such and one might speak of speck-images indeed. The effect of speck-intensity is hardly touched by the authors cited sofar. They simply assumed that the specks were sufficiently bright in their case, in other words, that there is no effect of speck-intensity above a certain critical level.

This level is not explicitly specified by most authors and has not been experimentally verified in the literature known to us. Refering to a retinal quantum efficiency of 10% (Pirenne, 1956), Schagen (1963) argued that 10 corneal photons per speck are sufficient in scotopic vision and that this can be realized with single stage intensifier tubes. Dirksen and Van Schie (1963) refered to a retinal quantum efficiency of 6% which implies a critical speck-intensity of about 17 corneal photons. On the other hand one could also have referred to absolute threshold data for single specks (§4.2.2). The problem really is that neither the quantum efficiency nor the single-speck-threshold need to be representative for the critical intensity of specks in a speck-image, so that an experimental determination will be worthwhile.

A curious reasoning is held by Balaskovic (1965). His starting point is that the contrast sensitivity of the eye levels off anyhow to the Weber-fraction at about 60 lux. Next, he calculates the minimum speck-density to obtain the Weber contrast sensitivity on the basis of the fluctuation theory. The required speck-intensity then follows as the quotient of luminance and speck-density. Admittedly, a higher speck-intensity would be meaningless at the onset of the Weber-regime, but this seems to be a rather arbitrary condition to start from.

The indifference with respect to the critical intensity is fostered by the development of cascade image-intensifier tubes. Three stage tubes provide speck-intensities above the most conservative estimates of a possible critical level, even for photopic observation. This, however, is attended by a loss in image quality. It thus remains interesting to know the critical speck-intensity, if existing. We now return to the question whether visual performance indeed levels off at higher speck-intensities.

Tol (1953) reports quantitative conclusions of an experiment with two different high speck-intensities. Of 5 observers 2 found no difference, 2 only a small difference, whereas for 1 observer contrast detectability was definitely lower at the lower speck-intensity.

Beurle (1969) predicted maximum contrast sensitivity for medium speck-intensity. At lower speck-intensities contrast sensitivity is reduced since not all specks are counted, whereas at higher speck-intensities contrast sensitivity will be reduced by shrinking of the summation area. In Beurle's opinion the effect of speck-noise and photon-noise is essentially the same, and contrast sensitivity is controlled by the retinal signal-to-noise ratio, but it should be recognized, that spatial and temporal processing are controlled by the retinal illuminance, *i.e.*, by the product of speck-density and speck-intensity. Whether this leads to a distinct maximum in the contrast sensitivity vs. speck-intensity relation may depend upon circumstances. The effect was experimentally demonstrated by Hodgson (1971) for large disks at a rather low speck-density as far as can be derived from the text.

Kühl, Geurts and Overhagen (1969) asked a group of observers to optimize the subjective quality of speck-images by adjusting the speck-intensity. Surprisingly, lower intensifications were preferred as the speck-density was raised.

Cuelenaere and Mulder (1972) studied the effect of different intensification factors in intensifier telescopes. They found a continuous amelioration of contrast sensitivity when the intensification was increased, at least in the investigated range.

Taylor (1972) demonstrated that high speck-intensities enable foveal vision with its inherent advantages. He compared two intensifier telescopes with a single-stage tube in one, and a three-stage tube in the other, resulting in low and high speck-intensity respectively. When the observer was allowed to use peripheral fixation the performance with the single stage tube was almost as good as with the three-stage tube. When peripheral fixation was excluded the three-stage tube was clearly superior.

Finally, a possible interaction of speck-intensity and optical blur must be mentioned. If a speck-image is blurred the contrast of the test object is reduced. This does not necessarily imply a lower signal to noise ratio, since the noise may be smoothed also, as Albrecht and Proper

(1965) and Mulder (1971) remarked. This will happen in general when signal and noise are both divisible such as in a beam current. It does not apply to the imaging of photon-noise, since photon are indivisible. It may apply to speck-noise, however, when the specks contain sufficient photons to be considered as divisible.

Summarizing the above literature on the effect of speck-intensity it is plausible that Ricco's summation area changes when the speck-intensity is varied over large ranges. What happens apart from that is not clear. The experiences of Kühl *et.al.* (1969) and of Cuelenaere and Mulder (1972) seem to be in conflict with the concept of a critical speck-intensity beyond which visual performance levels off.

§3.3. SIMULATION OF SPECK-IMAGES

To study the fundamental limits of vision with image intensification experimentally, speck-images were simulated on a kinescope-screen. Fig. 2 is a snapshot of such a speck-image.

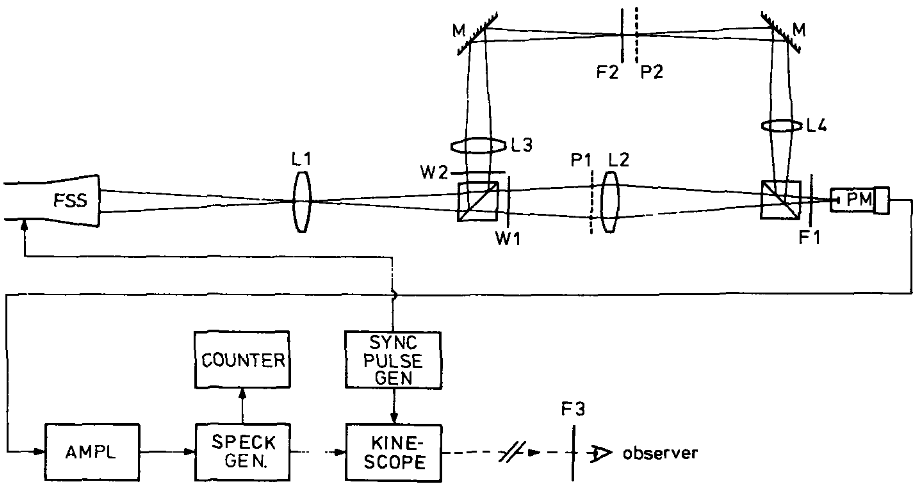

Fig. 7. The simulation set-up. A flying spot scans transmittant sine wave gratings at W1. A uniform field is superimposed via W2. The contrast of the sine wave grating is controlled by adjusting the polaroid systems P1 and P2. Neutral density filters F1 reduce the photon flux, detected by the photo-multiplier PM to such a degree, that the photons are converted into separate specks on the kinescope-screen. The apparent intensity of the specks is controlled with neutral density filters F3.

The proposed experiments can hardly be done with actual image intensifiers (Van Meeteren *et.al.*, 1971), in which the spatial frequency range is limited by the image quality of objective lens and image tube and contrasts are reduced by straylight. Further, speck-density and speck-intensity are not constant over the field of view and not accurately known. These difficulties were for the greater part evaded by the simulation set-up, rendered in Fig. 7.

The set-up was a modified version of the flying spot scanner system used by Rose (1948). Slides, inserted in the holder W1, were scanned by a flying spot, running synchronously with the line raster of a kinescope screen. The photon-flux, modulated by the image on the slide, was detected with a photomultiplier, converted into an electric signal, amplified and fed into the kinescope. With the aid of neutral density filters (F1) the incoming photon-flux was reduced to such a degree, that the detected photons resulted in separate pulses. These pulses passed a pulse-heigth discriminator, were converted into standard pulses and finally displayed as unit specks on the kinescope-screen. The halfwidth of the standard pulses was 0.8×10^{-7} sec corresponding to a visual angle of 0.5 min of arc on the kinescope-screen when observed from a distance of 3 m. The intensity of the specks on the kinescope-screen decreased to 1% in 10 msec.

A drawback of this simulation set up was that the specks could not coincide within time intervals of 0.04 sec and spatial intervals of about 1 min of arc along the raster lines, whereas the line distance was 0.4 min of arc, when observed from a distance of 3 m. As a consequence the speck-density should be restricted to about 50 specks per sec per min^2 of arc. The highest speck-density in the experiments was 18.2 specks per sec per min^2 of arc. In order to check whether the photon-noise was correctly simulated by this set-up, repeated countings of the speck-density were made. The standard deviation proved to be equal to the square root of the mean, as required. Fig. 8 shows a histogram of speck countings at a speck-density of 16 specks per sec per min^2 of arc. These countings refer to a basic interval of 4×10^{-7} sec in the video-signal, corresponding to a visual angle of 2.5 min of arc on a distance of 3 m. To obtain about 6 specks on the average 10 independent intervals were taken together from successive frames in each counting. The histogram shows good agreement with the Poisson distribution within an angular area a-

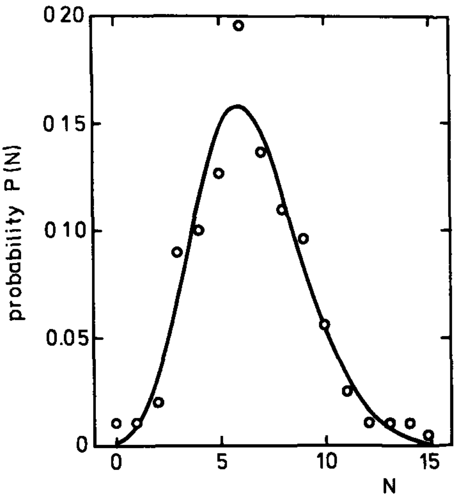

Fig. 8. Probability P(N) of N specks, after 200 countings over a small interval of the video-signal, compared with Poisson-distribution (see text).

bout as wide as the spread function of the human eye.

Via beam-splitting prisms and mirrors a second light path was created such that two images could be superimposed. In the present experiments transmittant sine wave gratings were inserted in the holder W1 and a uniform field in W2. The final contrast of the sine wave gratings could be controlled without changing luminance, by adjusting the polaroid systems P1 and P2. A small contrast reduction, caused by the set-up, had to be taken into account at the highest spatial frequencies. Because of the use of unit specks the non-linear relation between beam current and luminance of the kinescope-screen gave no cause for concern, as was confirmed by measurements of the screen-luminance as a function of speck-density.

The luminance of the kinescope-screen was calibrated with a luxmeter at a high speck-density. The speck-density was counted electronically. Thus the luminous intensity of the specks could be derived. Most experiments were made when looking at the kinescope-screen from a distance of 3 m through an artificial pupil of 3 mm. Taking into account the spectral composition of the light from the phosphor screen, it was calculated that in these conditions an average of 490 photons per speck entered the observer's eye. This speck-intensity could be reduced by inserting neutral density filters in front of the artificial pupil.

It should be realized that a strong reduction of the speck-intensity leads to the confusing concept of specks containing less than one photon. In fact, this means, that only some specks contain a photon and that others are "empty".One should not speak of specks then, but we will nevertheless do so for the sake of continuity. At such low speck-intensities the signal-to-noise ratio is determined by the fluctuations in the photon-flux. At higher speck-intensities the signal-to-noise ratio is determined by the fluctuations in the speck-density. Of course there is a transitional state in between. Thus, by varying the speck-intensity one can study the gradual transition from the photon-noise limited state to the speck-noise limited state.

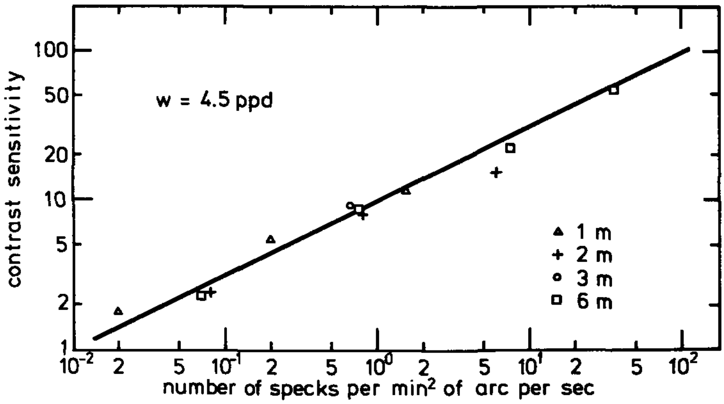

Fig. 9. Effect of observation distance in vision at speck-images.

§3.4. EFFECT OF OBSERVATION DISTANCE

When the attendant changes in spatial frequency and speck-density on the retina are compensated, contrast sensitivity will be independent of the observation distance. Coltman and Anderson (1960) confirmed this plausible statement experimentally. In the present case, however, the retinal size of the specks also changes from 0.25 min of arc at an observation distance of 6 m to 1.5 min of arc at 1 m. The possible effect of this was examined in a pilot experiment. The speck-intensity was made as high as possible in this experiment. No distance effect was found in the range of 1 to 6 m, as is shown in Fig. 9 for the contrast sensitivity at 4.5 ppd. This means that the size of the specks play no role if smaller than 1.5 min of arc. The subsequent experiments were made at an observation distance of 3 m, with specks of 0.5 min of arc, if not mentioned differently.

§3.5. EFFECT OF SPECK-INTENSITY

The effect of speck-intensity was studied with a sine wave grating of 4.5 ppd extending over a field of $3^{o} \times 3^{o}$. Considering that image intensification as a rule will enable foveal vision, this field was foveally fixated in most of the experiments. Some additional experiments on peripheral vision at speck-images will be described in §3.9.

The observations were made monocularly by two subjects through an artificial pupil of 3 mm. The results are presented in Fig. 10. The measur-

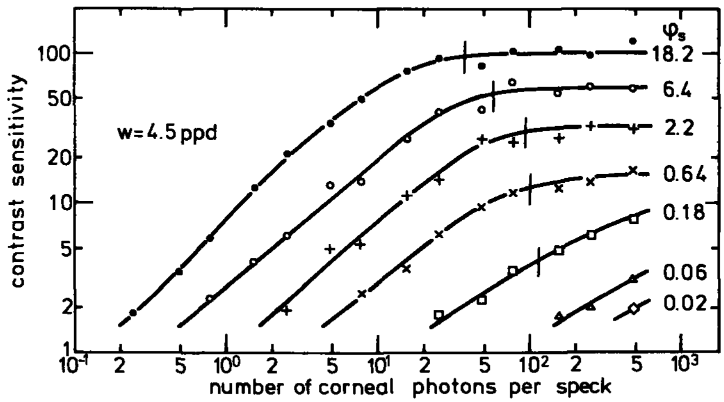

Fig. 10. Contrast sensitivity as a function of speck-intensity, with speck-density as parameter. The speck-intensity is expressed in the number of photons per speck entering the observer's eye. The speck-density is expressed in the number of specks per sec per min^2 of arc. The speck-intensity at which speck-images can just be distinguished from normal images is indicated by vertical bars.

ing points represent the averages over the two subjects and the two orientations of the sine wave grating. Contrast sensitivity at first increases when the number of photons per speck entering the artificial pupil is raised, and finally levels off. In the first stage the average number of photons per speck is too low to ascertain the detection of each speck. As the intensity of the specks is raised, more of them can be detected and contrast sensitivity increases. Finally, all specks are detected. Further intensification does not yield more specks. Thus, the signal-to-noise ratio, and, as a consequence, the contrast sensitivity level off. This at least is the most simple explanation of the experimental data and is further supported by the square root relation of contrast sensitivity and speck-density at the final level, which is illustrated in Fig. 11.

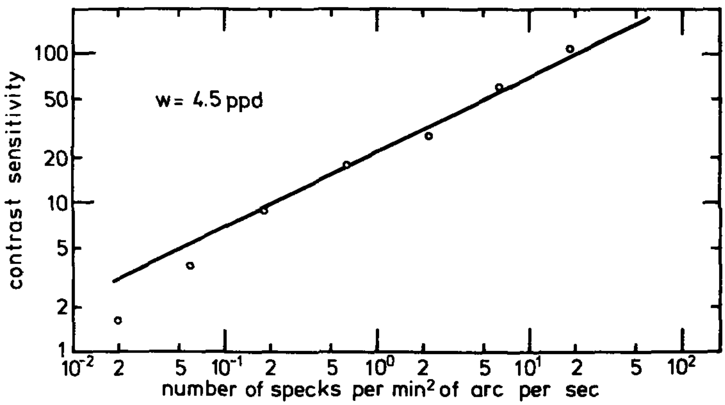

Fig. 11. Contrast sensitivity as a function of speck-density at high speck-intensity. Apart from a deviation at low speck-densities contrast sensitivity is proportional to the square root of speck-density.

Remarkably the minimum number of photons to obtain the final level appears to depend upon the speck-density. This effect is similar to the experience of Kühl *et.al.* (1969) who noted that more intensification is preferred subjectively at lower speck-density. As a consequence the square root relation between contrast sensitivity and speck-density is complicated and holds over a larger range as the intensification is increased. This may explain why Cuelenaere and Mulder (1971) found deviations from the De Vries-Rose law in vision through actual intensifier telescopes with variable intensification.

As a consequence of the effect just mentioned one cannot simply indicate one value for the required intensification. At the lowest realistic speck-densities about 500 photons per speck should enter the pupil of the observer's eye. Such a high intensification is not necessary at high speck-densities, but neither is it harmful to contrast sensitivity as follows from Fig. 10.

Contrary to Beurle's (1969) prediction we find no reduction of contrast sensitivity at higher speck-intensity. Based as it would be upon the degradation of spatial integration such an effect indeed should not be substantial in the fovea, as we will see in §3.6.

At high speck-intensity the visibility of the noise is considered as inconvenient by most observers, witness the experiments of Kühl *et. al.* (1969). The speck-intensity at which the noise becomes visible was determined in an additional experiment. A uniform speck-image was compared with an adjacent normal uniform field at the same luminance. The observers were asked to adjust a neutral density wedge in front of their eye in such a way that there was no difference in apparent noisiness of both fields. These wedge-settings were made with an accuracy of 20%. The results are indicated in Fig. 10 by vertical bars. The noise apparently becomes visible at about the same speck-intensity as is required to achieve the final contrast sensitivity level. Thus the intensification of image intensifiers preferably should be adjustable to avoid hindrance of visible noise at higher speck-densities.

§3.6. CONTRAST SENSITIVITY FUNCTIONS FOR UNAIDED FOVEAL VISION

The spatial processing of speck-images can be investigated by measuring contrast sensitivity functions. For comparison, a set of contrast sensitivity functions for *unaided* foveal vision with luminance as parameter, was measured first in exactly the same conditions. The observations were made monocularly through a 3 mm pupil and with a small foveally fixated sine wave field of $3^o \times 3^o$. The experimental set up used for these experiments is described elsewhere (Van Meeteren *et.al.* 1971). The results are presented in Fig. 12.

The contrast sensitivity functions for vision at a small foveally fixated field differ markedly from those for free vision at large fields as described in §2.3. Apparently contrast sensitivity drops drastically at low luminances when peripheral vision is excluded. Second, the form of the curves is nearly independent of luminance. Spatial bandwidth decreases but little at lower luminances. The strategy of the visual system to summate over larger areas in favour of contrast sensitivity apparently involves the use of the periphery. We will return to this in chapter 7.

The curves of Fig. 12 do not show a peaked maximum in the luminance range investigated. This is in agreement with measurements of Patel (1966) who found low frequency suppression but at higher retinal illu-

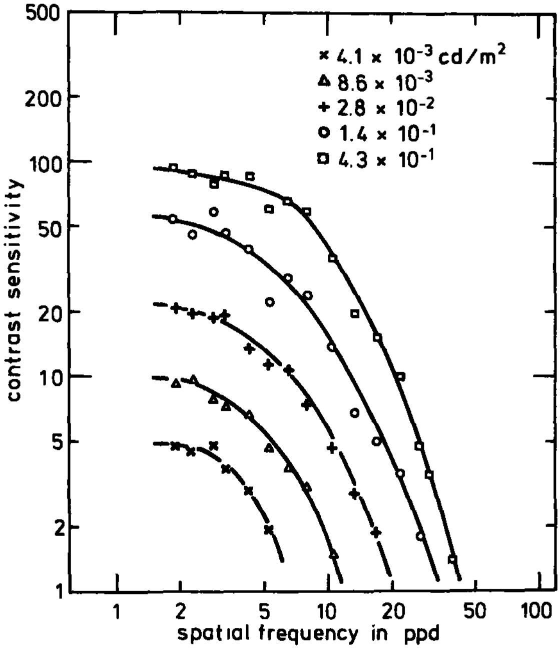

Fig. 12. Contrast sensitivity functions. Spatial frequency is plotted in periods per degree. These measurements refer to a foveally fixated field of 2.8° x 2.8° and a 3-mm artificial pupil.

minances only, in a small foveally fixated field.

§3.7. CONTRAST SENSITIVITY FUNCTIONS FOR VISION AT SPECK-IMAGES

Next, contrast sensitivity functions were determined in the same conditions for vision at speck-images. In all evaluations discussed in §3.2 it was assumed, that the spatial processing of speck-images is the same as in normal vision. The form of the contrast sensitivity functions for vision of speck-images thus should be the same as for normal vision. It is conceivable, however, that speck-images are processed on a more central stage of the visual system in a different, perhaps more ideal, way. Fig. 13 illustrates contrast sensitivity functions for 2.2 specks per min^2 of arc per sec at three different speck-intensities. The curves are taken from the measurements on normal vision in the same conditions described in the previous section. The measuring points follow the curves. This is trivial at the lower speck-intensities, where the speck-image

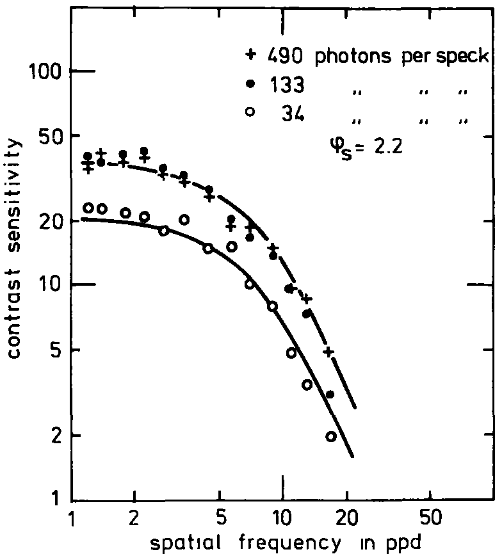

Fig. 13. Effect of speck-intensity upon contrast sensitivity functions. The form of the curves is derived from the measurements on normal unaided foveal vision (Fig. 12).

cannot be distinguished from the normal image and spatial processing has to be the same. However, spatial processing seems to be the same also at high speck-intensities where the specks are visible as such. Here also a good agreement of curves and measuring points is obtained after suitable shifts of the curves along the vertical axis. It should not be expected here, that the absolute values of contrast sensitivity for vision at speck-images and for normal vision at the same luminance coincide. The form of the contrast sensitivity functions for both kinds of vision, however, is apparently the same. This conclusion is confirmed at other speck-densities as illustrated in Fig. 14. The contrast sensitivity functions of Fig. 14 apply to a high speck-intensity of 490 corneal photons. Here again the curves are taken from the previous measurements on unaided vision in the same conditions and represent the form of the contrast sensitivity functions for normal foveal vision at the same retinal illuminance. Each curve again was shifted along the contrast sensitivity axis to obtain the best fit. At all speck-densities the fit is satisfactory. The form of the contrast sensitivity functions for vision at speck-images apparently is the same as in unaided vision and is controlled by the retinal illuminance. The spatial processing of speck-images by the visual system thus does not seem to be different from normal in the investigated ranges of speck-intensities and speck-densities.

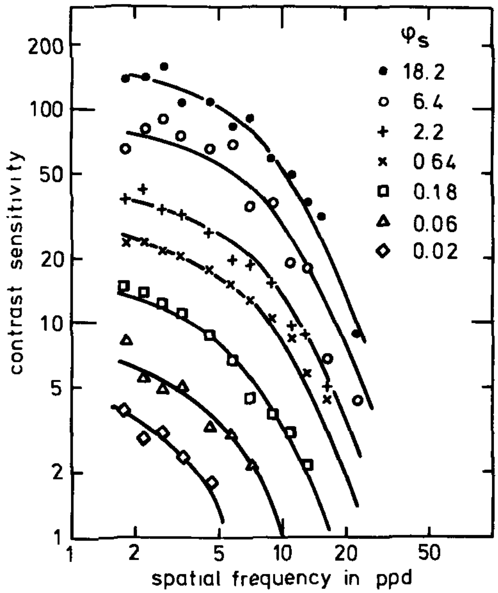

Fig. 14. Contrast sensitivity functions at high speck-intensity with the number of speck per min^2 of arc per sec as parameter. The curves are derived from the measurements on normal unaided foveal vision (Fig. 12).

§3.8. DISCUSSION

The present experiments in general confirm that the visual system does not differentiate between speck-noise and photon-noise. At higher speck-densities the intensity of the specks can be reduced from 500 to about 30 corneal photons without causing a change in contrast sensitivity. The most simple explanation of this is that neither the number of detected specks nor the threshold criterion is changed. From specks of 30 photons at best about one photon will be detected. This means that speck-images with specks of 30 photons cannot be discriminated from normal images, as was experimentally verified moreover. Yet, the same threshold criterion holds as for speck-images with specks of 500 photons. It was further found that spatial processing of normal images and speck-images is the same. It seems reasonable to conclude, that vision is limited by retinal noise, independent of its photon- or speck-origin.

For further discussion the data of Fig. 10 are replotted in Fig. 15 *vs.* screen luminance, *i.e.* the product of speck-intensity and speck-density. In this way they can be compared with the corresponding curve for normal foveal vision. The luminances of the speck-images and the normal field, used in the experiments, were calibrated in exactly the same way,

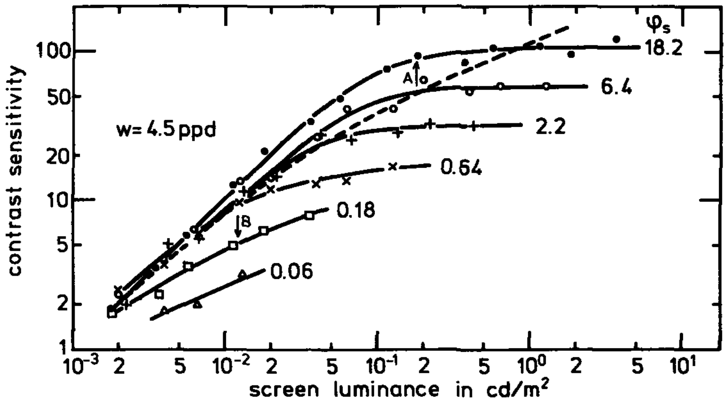

Fig. 15. Data of Fig. 10 replotted *vs.* luminance (*i.e.* the product of speck-intensity and speck-density) to be compared with the corresponding contrast sensitivity for normal unaided foveal vision (interrupted curve).

so that possible calibration errors cannot disturb the comparison. The curves for the different speck-densities now tend to coincide, with the normal "mother-curve" at low luminance. This was to be expected since at low speck-intensities speck-images cannot be distinguished from normal images. When the intensity of the specks is sufficiently high, all specks are detected by the retina of the observer and the curves for the different speck-densities branch off to their own final level. Thus, vision at speck-images is roughly equal to normal unaided vision as long as the intensity of the specks is low, and is limited by the fluctuations in the number of specks when the intensity of the specks is high.

Two deviations complicate this simple representation of the facts. First, at high speck-density the speck-intensity can be reduced to 30 corneal photons, and yet, all specks seem to be counted. In this case contrast sensitivity can be higher for speck-images than for normal vision at the same luminance, as arrow A in Fig. 15 indicates. It seems as if the quantum efficiency of the retina is higher when the light is clustered in specks. This type of non-linearity might point to coincidence-mechanisms as hypothesized by Bouman (Bouman and Koenderink, 1972). Such mechanisms are triggered when two or more absorbed photons coincide in a smaller area and time interval. Clustering of light in specks might enhance the probability of coinciding absorptions.

Second, at low speck-density the contrast sensitivity decreases immediately when the speck-intensity is reduced below 500 corneal photons, as indicated by arrow B in Fig. 16. This in itself is compatible with the foveal threshold for single specks (§4.2.2). It is difficult to reconcile the second effect with the first. When a coincidence-mechanism responds to specks of 30 corneal photons at A it should also respond to 150 corneal photons at B. One might hypothesize a second coincidence mechanism now: Two responses of the first are required within a certain area and time to pass the second one. This implies that the first mechanism is a sub-unit of the second, which reminds of Bouman's "human ommatidia" (Bouman and Koenderink, 1972). Zacks (1970) and Sakitt (1971) recently reported evidence also for sub-units within Bloch's time and Ricco's area respectively. An alternative explanation might be found in Barlow's (1958) internal-noise hypothesis; it is conceivable that the speck-noise is dominated here by internal-noise, unless the specks are sufficiently bright to overcome this barrier.

§3.9. ADDITIONAL MEASUREMENTS IN THE PERIPHERY

Considering that image intensification in general enables photopic vision the above experiments were made with small foveally fixated fields. Peripheral vision, however, may be involved also, for instance in the use of intensifier telescopes for search tasks. One might wonder moreover, whether simple devices with low intensification used in peripheral vision might compete with high intensification devices in foveal use.

Some additional measurements on peripheral vision at speck-images may be mentioned therefore. A sine wave grating of 2.2 ppd, extending over $3^o \times 3^o$ was presented 7^o nasally. The observation distance was reduced to 1 m to obtain higher speck-intensities. As a consequence the available range of speck-densities is limited to about 1 speck per min^2 of arc per sec. These measurements were made by the observers VG and AvM (instead of JB and AvM). VG has normal corrected vision. His contrast sensitivity proved to be slightly higher for vertical than for horizontal gratings. Contrast sensitivity was roughly the same for both observers. The average results are plotted in Fig. 16. It should be realized that peripheral threshold measurements in which one has to look beside the test object are far more difficult than foveal measurements. It is a

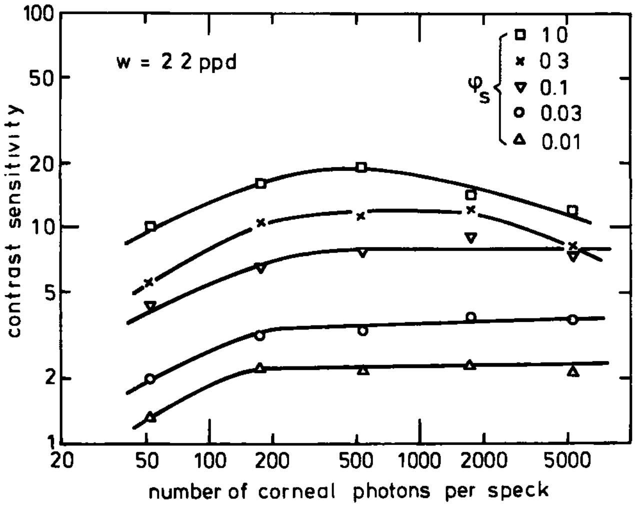

Fig. 16. Contrast sensitivity as a function of speck-intensity for peripheral fixation, 7^o nasally. Parameter is the speck-density expressed in numbers of specks per min^2 of arc per sec. Observers VG and AvM.

pity, in retrospect, that no measurements were made in between 50 and 200 corneal photons per speck (see Fig. 16: the experiment was done originally to determine the speck-noise level only).

The results are less complicated than in foveal vision. Contrast sensitivity obtains its highest value in between, say 150 and 200 corneal photons per speck, independent of the speck-density. This value is compatible with the threshold for single specks in scotopic vision.

It should be remarked that the above conclusion is restricted, of course, to the investigated range of speck-densities. However, at the higher speck-densities vision will be photopic in practice.

Finally, it may be noted that contrast sensitivity tends to decrease again when the speck-intensity is made very high, as was predicted by Beurle (1969) and demonstrated also by Hodgson (1971).

§3.10. CONCLUSIONS

Vision at images produced by image intensifiers, which convert the photons detected by the cathode of an image tube into bright specks on a display, is in general not different from normal unaided vision. Spatial processing is the same and controlled by the screen-luminance. Contrast sensitivity is similarly controlled by the retinal signal to noise ratio in both cases no matter the origin of the noise. Thus, all data on unaided vision are available for the evaluation of vision with image intensification by a simple transformation.

The minimum intensification to make sure that all specks are counted by the retina of the observer's eye surprisingly depends upon the speck-density. As far as photopic observation is concerned, about 500 photons per speck must enter the pupil of the observer's eye when the speck-density is low. For peripheral observation about 150-200 corneal photons per speck are sufficient, independent of the speck-density. Above these minimum speck-intensity levels vision is basically speck-noise limited. Contrast sensitivity obeys a square root law in that case.

Possible design consequences of the present results are mentioned in §5.7.

CHAPTER 4

THE QUANTUM EFFICIENCY OF THE EYE

§4.1. INTRODUCTION

The main conclusion of the preceding chapter was that vision with image intensification can be predicted from unaided vision by substituting speck-density for detected photon flux. This requires the quantum efficiency of the eye to be known first of all. One finds values between 0.5 and 10% in the literature, leading to different opinions on the potential gain of image intensifier tubes, of which the quantum efficiency is about 10%.

The measurements on vision at speck-images, described in chapter three, provide a new method to determine the quantum efficiency, operationally fitted to the present purpose. Before describing this method the literature on the quantum efficiency is briefly surveyed.

§4.2. LITERATURE ON THE QUANTUM EFFICIENCY

Three different measurements can be distinguished in which the quantum efficiency is defined differently:

1. Measurements of ocular transmission and pigment absorption lead to an estimation of the fraction of corneal photons that is absorbed by the receptors.
2. Measurements of absolute thresholds lead to the minimum number of corneal photons required for a visual perception.
3. Measurements of differential thresholds (contrast sensitivity) lead

to detected photon fluxes in the sense of the fluctuation theory (Eq. (2.2)).

These three methods need not to result in the same quantum efficiency. Not all absorbed photons may be effective; more than one effectively absorbed photon may be required to exceed the absolute threshold; and the effectiveness of absorbed photons may depend on the stimulus conditions.

4.2.1. Ocular transmission and pigment absorption

The ocular media transmit about 50% of the light at 510 nm and 60% at 550 nm, as was measured by Ludvigh and MacCarthy (1938).

The pigment absorption has been estimated in various ways with different results. Crescitelli and Dartnall (1953) measured the density of a solution of rhodopsin and derived an *in situ* pigment absorption of 3.4%. Rushton (1956) compared the amount of light reflected by the fundus in complete dark-adaptation and after full bleaching respectively. He concluded that maximum pigment absorption is 20% in rods. One may consider the result of Crescitelli and Dartnall as a lower limit: the pigment absorption may be higher *in vivo* thanks to the wave guide construction of the receptor. Rushton's value on the other hand might be too high, since it only applies to the light that passes the pigment, and consequently, does not account for light passing in between the receptors.

The pigment absorption seems to be higher in cones. Walraven and Bouman (1960) derived a value of about 80% from the wavelength-dependency of the Stiles-Crawford effect. Microspectrophotometric measurements of Dobelle, Marks and MacNichol (1969) support this high value. This pigment absorption again represents the light that enters the cones only, and the fraction of corneal photons that is absorbed might be lower.

Summarizing,the fraction of corneal photons that is absorbed in the retina is not well known. If it is assumed that most of the light inciding upon the retina traverses the receptors, this fraction may be as high as about 10% for rod areas and 50% for cone areas.

4.2.2. Absolute thresholds

Since Langley (1889) a number of authors determined the minimum energy to produce a visual effect in the most favourable conditions of dark-adapted peripheral vision. The older literature, surveyed by Hecht, Shlaer and Pirenne (1942) reports minimum energies of 17-90 corneal photons. The precise definition of the threshold is somewhat problematic. This is improved later, when Brumberg and Vavilow (1933), Hecht, Shlaer and Pirenne (1942) and Bouman and Van der Velden (1948) measure frequency of seeing curves by presenting small flashes of different energies repeatedly. Their results will be given here in the form of the number of corneal photons to obtain a probability of detection of 55%. One can roughly state, that this number N_{55} reflects the possible threshold number. Brumberg and Vavilow (1953) found N_{55} to be about 49. Hecht *et.al.* (1942) found N_{55} values in the range 51-113 for 7 subjects. Bouman and Van der Velden (1948) found N_{55} to be about 20. A weakness of the above measurements is that the observers knew that a flash was presented; this may have affected their decision. Baumgardt (1960) included catch-trials in the presentations and found N_{55} to be 80, 81, 95 and 97 respectively for four observers. Thus, N_{55} values all together are found in between 17 and 113. It is not likely that this wide spread is caused completely by individual subject differences. Part of it may result from different threshold criteria. Considering this, one might weigh Baumgardt's (1960) results heavier and estimate N_{55} in between 50 and 110.

There is less spread in the experimental absolute thresholds for foveal vision. Bouman and Van der Velden found thresholds of 800 corneal photons for small flashes at 560 nm. Marriott (1963) found the absolute foveal threshold to be 494-879 corneal photons at 550 nm for a group of 9 subjects, with an average of 606 and a standard deviation of 1[illegible]8. Older measurements, reviewed by Marriott, agree well with these results. Thus the foveal threshold is much higher than the peripheral threshold and is found in between 450 and 900 corneal photons.

The above absolute thresholds lead to quantum efficiencies of 1-2% in the periphery and 0.1-0.2% in the fovea, when it is assumed that one absorbed photon evokes a visual perception. The occurrence of spatial and temporal interactions, however, indicate that at least two absorbed photons are involved in the absolute threshold. This led Van der Velden (1944) to the two-quanta explanation of Piper's and Piëron's law. From this point of view the absolute threshold data lead to quantum efficiencies of 2-4% in the periphery and 0.2-0.4% in the fovea.

As a matter of fact one might assume also that more than two quanta must be absorbed near the absolute threshold. This accordingly leads to higher quantum efficiencies.

4.2.3. Fluctuation theoretical approach

By practicing the fluctuation theory in the form of Eq. (2.2) the quantum efficiency can be derived from contrast threshold measurements. The problem is that Eq. (2.2) contains four unknowns, namely k, τ, α and η. Rose (1948) determined $k = 5$ and $\tau = 0.2$ sec separately, as discussed in §3.2.1 and substituted the area of the test object for α^2. Starting from a number of experimental data derived from literature, Rose came to a quantum efficiency of 5% at lower luminances and 0.5% at higher luminances, not claiming high accuracy. On reflection,Rose's detection model is a curious mixture of idealism and realism: spatial integration is ideal, but temporal integration as well as the factor k are not ideal.

Clark Jones (1959) defined the "detective" quantum efficiency as the ratio of the number of corneal photons needed by an ideal detector and the corresponding number needed by the eye for the same task. This detective quantum efficiency, as derived from literature data obtained a highest value of nearly 1% in foveal vision for medium durations of 0.1-0.2 sec and for medium sizes of 4-10 min of arc, whereas it was lower for shorter and longer presentation times and for smaller and larger objects. This result agrees with the concept of limited summation times and areas; the visual system functions as an ideal detector only, when the stimulus just fits to its integration area and time.

Barlow (1958) presented a fluctuation theoretical interpretation of Stiles' (1953) measurements of photopic contrast thresholds. He took a k-value of 3.3 and substituted the duration (0.2 sec) and the size (0.79 deg^2) of Stiles' test objects for τ and α^2 in Eq. (2.2). He thus arrived at quantum efficiencies of about 0.4% for Stiles' red and green mechanisms. According to Barlow a k-value of 3.3 "corresponds to a degree of reliability which allows the subject to give 0.1% false responses to zero stimuli". Stiles' criterion, however, was a probability of detection of 50% and it is not clear how the k-value could be derived from an unmentioned false response rate. It further is doubtful whether the size of such a large test object can be substituted for α^2 in Eq. (2.2). Direct summation of photon fluxes over such a large area seem to be unlikely.

According to Barlow (1958) the absolute threshold is basically a differential threshold and described by Eq. (2.2) also, when it is assumed that there is a certain amount of internal noise or "dark light". Hallett (1969) recently interpreted absolute threshold measurements in this way. He found the absolute peripheral threshold intensity to be about 100 corneal photons for a small flash of short duration presented 18^{o} nasally. The internal noise would be characterized by about 30 corneal photons. The quantum efficiency then necessarily must be high, namely 10%, to explain the threshold. However, the threshold can be explained otherwise by the two-quanta hypothesis and the existence of dark noise is not demonstrated, neither by Barlow nor by Hallett.

Summarizing, the most reliable determination of the quantum efficiency within the frame work of the fluctuation theory was made by Clark Jones (1959). He derived a foveal quantum efficiency of nearly 1% from appropriate contrast sensitivity data. The quantum efficiency might be higher in the periphery, but lower than Rose's value of 5%, when it is considered that Rose's k-value is probably too high.

§4.3. NEW METHOD: COMPARISON WITH SPECK-NOISE LIMITED VISION

After the experiments of chapter 3 the quantum efficiency of the eye can be straightforwardly determined by comparison of unaided vision and speck-noise limited vision. One simply measures contrast sensitivity for a certain spatial frequency as a function of the corneal photon flux, and in a second experiment as a function of speck-density. The results of such measurements, made with a foveally fixated sine wave grating of 4.5 ppd extending over a $3^{o} \times 3^{o}$ field, are plotted in Fig. 17. The measurements of both curves were made by the same observers with the same method and in the same conditions. As argued in chapter 3 spatial and temporal processing as well as the threshold criterion are the same with respect to both curves. Combining Eq. (2.2) and Eq. (3.1) at a certain contrast sensitivity than gives:

$$\eta = \frac{\phi_s}{\phi_p} \tag{4.1}$$

It will be evident that k, τ and α^2 need not to be known at all. The

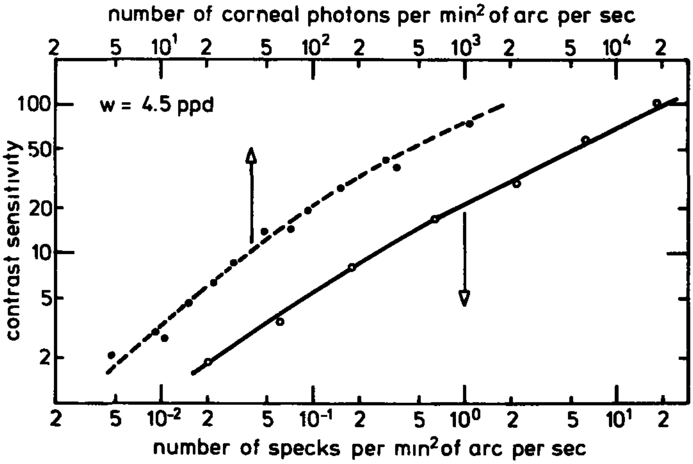

Fig. 17. Contrast sensitivity for unaided vision in foveal fixation as a function of the corneal photon flux (upper curve, upper scale) and for vision to speck-images as a function of speck-density (lower curve, lower scale). Observers JB and AvM. The comparison yields the quantum efficiency of the eye.

quantum efficiency can be read from Fig. 17 in this manner. Similar results are plotted in Fig. 18 for peripheral fixation, 7^{0} nasally. These measurements were made by VG and AvM (see also §3.9). Finally in Fig. 19 the quantum efficiencies derived from Figs. 17 and 18 are plotted vs. retinal illuminance. In both cases the quantum efficiency is about 1%, in

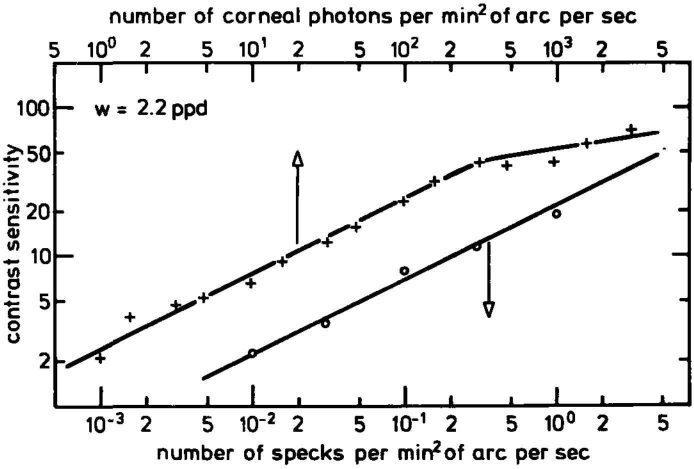

Fig. 18. Same as Fig. 17, for periperal fixation, 7^{o} nasal. Observers VG and AvM.

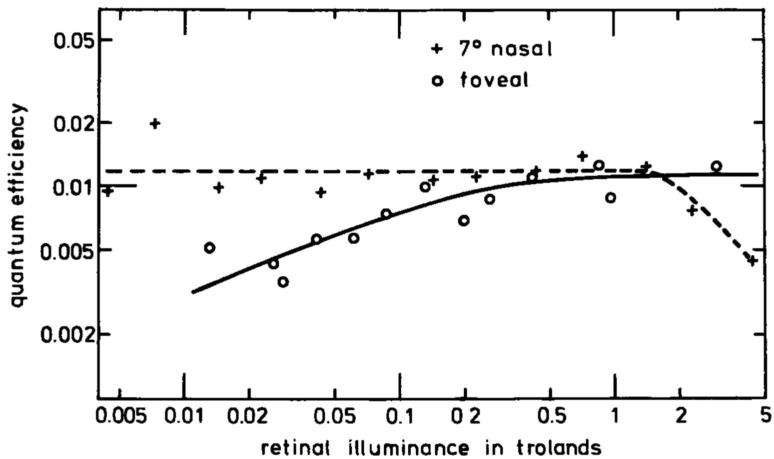

Fig. 19. Quantum efficiency of the human eye as derived from Figs 17 and 18 plotted *vs.* retinal illuminance.

good agreement with the result of Clark Jones (1959), mentioned in §4.2.3.

The foveal quantum efficiency, however, drops rapidly below 0.3 troland. This effect is compatible with the high absolute threshold for foveal observation of small flashes and might have the same origin (§3.8).

At higher retinal illuminance contrast sensitivity obtains the Weber-level in the periphery. This results in Fig. 19 in a decreasing quantum efficiency, as defined here. The same will happen in the fovea also at a higher retinal illuminance beyond the measuring range. The foveal quantum efficiency in fact is constant over a small luminance range only.

The fovea with its direct environment and the periphery are apparently equally sensitive in their typical working ranges. This is confirmed also by the uninterrupted square root relation between integrated contrast sensitivity and retinal illuminance (Van Meeteren and Vos, 1972).

The accuracy of the method can be judged from the spread in the "measuring" points of Fig. 19 as far as the underlying threshold measurements are concerned. Of course a calibration error in ϕ_p may have been made. The luminance of the field was measured with a brightness spot meter within ± 10% and the corresponding photopic and scotopic corneal photon fluxes were calculated from Eq. (5.5). The speck-density ϕ_s was counted electronically and we can imagine no other errors than in the geometrical dimensions, say up to 5%. It finally may be remarked that the simplicity of the method favours accuracy and interpretation: all unknowns but the one we are interested in are eliminated.

§4.4. DISCUSSION

Table I presents a survey of quantum-efficiency values according to the various methods. Is it possible to reconcile the differences?

Table I. Quantum efficiency according to different methods

Method	Periphery	Fovea
1. Pigment absorption	2-10%	50%
2. Absolute threshold (2-quanta explanation)	2- 4%	0.2-0.4%
3. Contrast threshold (fluctuation theory)	1%	1%

The psychophysical methods yield lower quantum efficiencies than would follow from the fraction of light that is absorbed by the visual pigments. This is acceptable to a certain degree. First, part of the light leaks in between the receptors probably, and second, not all absorbed photons may activate a receptor. According to Rushton (1972) only 60% of the photons caught lead to bleaching. These factors may explain the difference between the pigment absorption and the absolute threshold in the periphery, not in the fovea.

The difference between the peripheral quantum efficiencies derived from absolute threshold and contrast threshold measurements respectively suggest that the quantum efficiency depends upon the stimulus conditions. One might conclude that the quantum efficiency is "normally" about 1%, both in the fovea and in the periphery, but assumes a higher value in special cases. The same suggestion arose in §3.8 from the fact that 50 photons may evoke a foveal event when clustered in specks.

The low quantum efficiency emerging from the absolute foveal threshold is compatible with the decreasing foveal quantum efficiency following from contrast threshold measurements (Fig. 19). Both effects may have the same origin: either more severe coincidence conditions or a higher internal noise level in the fovea relative to the periphery.

As for the present purpose, the comparison of vision with image intensifiers and unaided vision, one may rely upon an operationally measured quantum efficiency of 1%.

CHAPTER 5

VISION THROUGH INTENSIFIER TELESCOPES

§5.1. THE PREDICTION OF VISUAL PERFORMANCE WITH IMAGE INTENSIFIER DEVICES

Continuing the line of the preceding chapters it should be possible now to predict contrast sensitivity functions for vision through image intensifier devices. This prediction is described here for vision through intensifier telescopes (Fig. 20) and experimentally verified for some actual devices. The prediction of visual performance in other applications of image intensification such as X-ray fluoroscopy and low light level television, is not basically different. Also the speck-noise experiments can be used to evaluate the effect upon contrast sensitivity of video-noise in general, *i.e.* not necessarily originating from fluctuations in the detected photon flux.

The prediction contains two stages. First, the physical image as presented on the final display to the observer must be described in terms of contrast (MTF), speck-density (photon-catch) and speck-intensity (intensification). More general one might specify a display signal-to-noise ratio in stead of speck-density. Second, the visual contrast sensitivity for vision at the display concerned follows either directly from the speck-image experiments of chapter 3, or from an appropriate comparison with the unaided eye.

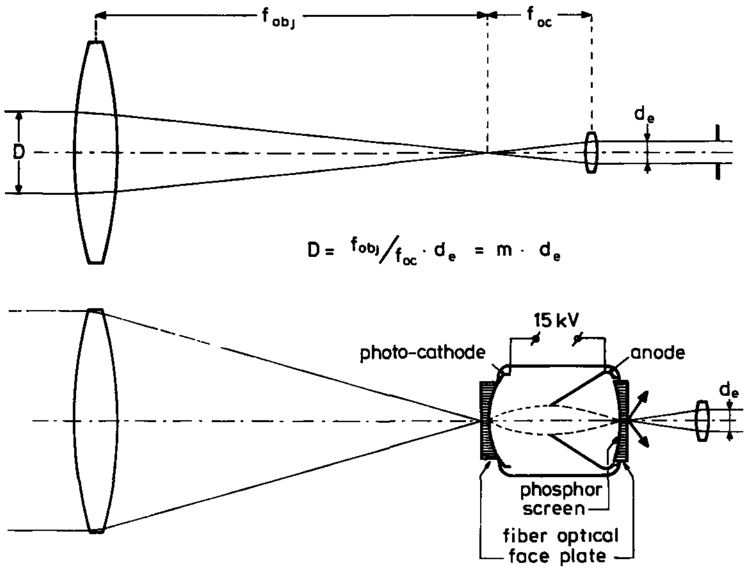

Fig. 20. Schematic diagram of a telescope with and without an image intensifier tube. Note that the effective diameter D of the entrance pupil is at best equal to $m.d_e$, in the absence of the intensifier tube, where m is the angular magnification and d_e is the diameter of the pupil of the observer's eye. The intensifier tube breaks through this relation of entrance pupil and angular magnification. Note also the light losses by diffuse scattering of the phosphor screen, which have to be compensated for by the intensification of the tube.

§5.2. VISION WITH NIGHT-GLASSES

Vision with night-glasses is shortly treated of first, as it is reasonable to compare intensifier telescopes first of all with them. Fig. 20 illustrates how the objective lense of a telescope, if sufficiently large, collects a factor m^2 more light than the unaided eye. This compensates exactly for the rarification of light over the image plane, as caused by the angular magnification m. Thus the function of perfect night-glasses is angular magnification at constant retinal illuminance. As a consequence the contrast sensitivity functions of the unaided eye are simply shifted by ideal night-glasses towards higher spatial frequencies in object space conformably to the angular magnification. Fig. 21 shows the experimental verification of this simple precept for vision through a pair of 7 x 50 night-glasses. The sine wave gratings were projected in this experiment on a white screen and observed from a distance of 4 m with the naked eyes and from a distance of 28 m through the binocular night-glasses. As follows from Fig. 21 the contrast sensitivity function for vision through the night-glasses remains slightly behind the prediction for ideal night-glasses, mainly due to contrast rendition by straylight and imperfect imaging.

Fig. 22 illustrates the MTF of the night-glasses used. Though far from perfect the imaging quality may be considered as representative, even for professional instruments (Van Schie and Risselada, 1973). There is a difficulty in the use of MTF's for direct viewing optical aids. One cannot simply multiply the contrast sensitivity function of the eye with the MTF of a telescope. Instrument and eye have to be dealt with as one optical unit, of which the MTF depends upon the algebraic sum of their separate wave aberrations. Strictly spoken one should specify the wave aberrations of telescopes in stead of their MTF's, and evaluate the possible interactions with the wave aberrations of the human eye. This is

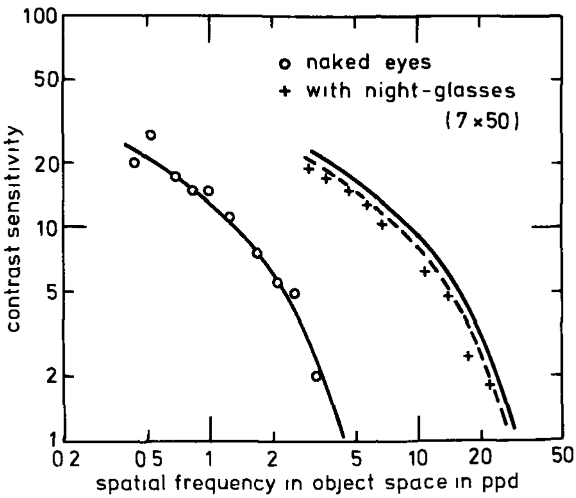

Fig. 21. Contrast sensitivity functions for unaided vision and vision through 7 x 50 night-glasses to sine wave fields of 15° diameter (in image space) at 3.5 x 10^{-4} cd/m^2 (in image space). The rightmost uninterrupted curve is obtained by shifting the contrast sensitivity function of the unaided eyes over a factor 7 corresponding to the angular magnification. After correction for imaging errors and straylight the interrupted curve predicts the contrast sensitivity function for vision through the night-glasses.

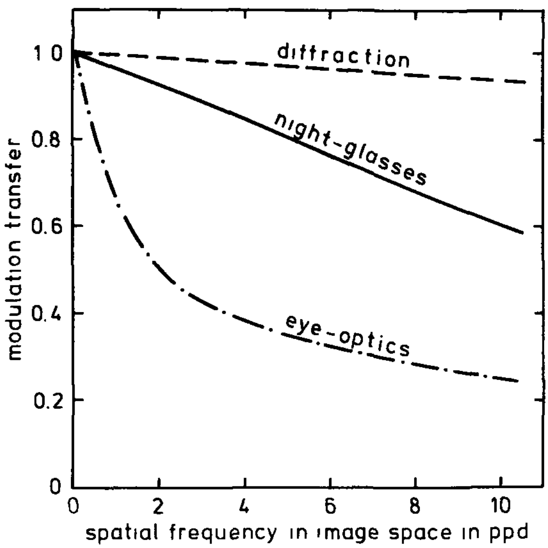

Fig. 22. Modulation transfer functions of a diffraction-limited telescope, a pair of 7 x 50 binoculars (night-glasses) and the eye-optics, all for a pupil of 7 mm in image space.

a cumbersome way. It seems to be more realistic to characterize direct viewing instruments by an *effective MTF*, defined as the ratio of the contrast sensitivities for aided and unaided vision. In practice a satisfactory estimation of the effective MTF may be obtained from the nominal MTF, when the latter is divided by the diffraction limited MTF (Van Meeteren, 1969). A second source of contrast rendition is instrumental straylight. As this factor depends upon the light distribution in object space it does not make sense to include it in the MTF. In the conditions of the experiment described above straylight reduced contrast by a factor 0.96. The interrupted curve in Fig. 20 is derived from the "perfect" curve after multiplication with the effective MTF and accounting for the straylight.

About 20% of the light is lost in coated binoculars. This was anticipated in the experiment by increasing the luminance in object space accordingly. In practice it implies a reduction of contrast sensitivity with a factor $(0.80)^{\frac{1}{2}} = 0.9$ according to the square root law, discussed in §2.4. Taking all losses together one comes to a total reduction of contrast sensitivity with a factor 0.70 roughly. Summarizing, night-glasses shift contrast sensitivity functions toward higher spatial frequencies according to the angular magnification. Due to straylight, imperfect imaging and light losses the contrast sensitivity functions fall downward also along the contrast sensitivity axis with about a factor 0.70.

Night-glasses cannot intensify the retinal illuminance. Their gain is provided exclusively in the form of angular magnification. This nevertheless enables a visual performance that normally belongs to a higher luminance level as Fig. 23 illustrates. Thus, night-glasses bring about a

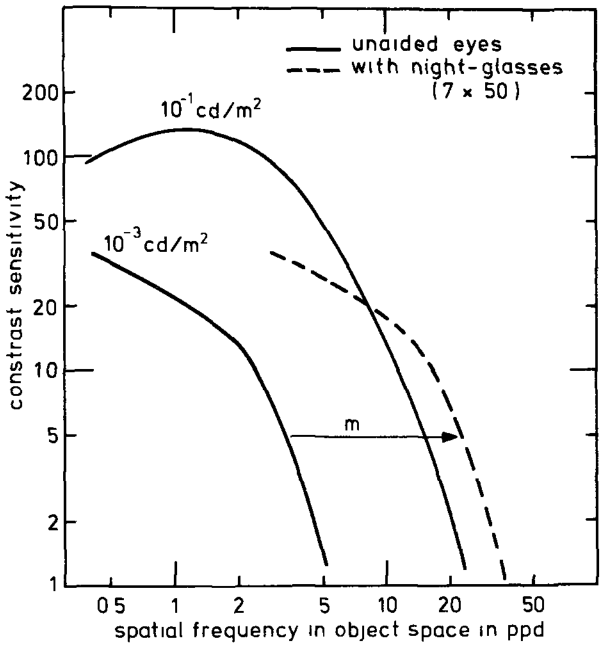

Fig. 23. The function of night-glasses. The contrast sensitivity function of the unaided eyes at 10^{-3} cd/m^2 is shifted towards higher spatial frequency in object space, so that the performance approximates the level of 10^{-1} cd/m^2.

functional gain in the luminance required for a certain visual performance. This especially applies to the detection of point sources. Pointsources are small relative to Ricco's area by definition. They are characterized by their intensity BdO, where B is their luminance and dO is their area. Imaged with luminance B and area m^2dO their intensity is m^2BdO when observed through night-glasses. Thus, they are brighter and can be detected more easily, though their luminance is essentially unaltered.

It has been assumed so far, that the exit pupil of the night-glasses just fills the pupil of the observer's eye. Only then the retinal illuminance will be the same as in unaided vision. Otherwise it will be reduced by a factor $D^2/(d_e^2.m^2)$, where D is the diameter of the entrance pupil of the night-glasses, m is the angular magnification and d_e is the diameter of the pupil of the eye. Thus chosing a larger magnification this simultaneously results in a lower retinal illuminance. The best tradeoff between more angular magnification and lower retinal illuminance has been discussed extensively in the German literature. According to Kühl (1927) visual acuity is roughly proportional to $E^{\frac{1}{4}}$ at low luminances, where E indicates the retinal illuminance (see also §2.3). Thus the gain G_r in resolving power is:

$$G_r = m \cdot \left[\frac{D^2}{d_e^2 \cdot m^2} \right]^{\frac{1}{4}} = f \cdot \sqrt{mD} \qquad (5.1)$$

The term $\sqrt{mD}$ became known as Dämmerungszahl or Twilightnumber. Eq. (5.1) is supported experimentally (Köhler and Leinhos, 1957). For the gain G_s in contrast sensitivity on the other hand one finds according to the fluctuation theory:

$$G_s = m \cdot \left[\frac{D^2}{d_e^2 \cdot m^2} \right]^{\frac{1}{2}} = \frac{D}{d_e} \qquad (5.2)$$

Thus it depends on the visual task whether, for instance, a 10 x 50 telescope is better than a 7 x 50 or not. Quantitatively the discussion is hardly relevant, however.

§5.3. THE USE OF IMAGE INTENSIFIER TUBES IN TELESCOPES

The compelling connection of photon-catch and angular magnification in common night-glasses might be broken by a diffuse transmitting screen in the focal plane of the telescope. The diffuse scattering, however, would imply that only a fraction of the light would enter the observer's eye, so that the original gain in photon-catch would be lost. The development of image intensifier tubes has changed all this. The telescope is cut, as it were, in the focal plane and an image intensifier tube is inserted, as Fig. 20 illustrates. The image intensifier tube functions like a diffuse transmitting screen with built-in electronic light intensification.

Various types of image intensifier tubes have been developed. An elementary form is illustrated in Fig. 20. The object space is imaged upon a photocathode. Once detected by the photocathode photons are converted into free electrons, which are accelerated by a high voltage electric field and hit a phosphor screen with sufficient energy to evoke a light flash of about 1000 photons. The image is preserved by electrostatic focusing. Admittedly the photocathode detects only 10% of the incident light and the final intensification is a factor 100 only, but that is sufficient to overcome the above mentioned scattering loss. Thus, with the aid of a rather simple image intensifier tube one might construct telescopes in which the gain in photon-catch is not necessarily attended by a high angular magnification. There is a second profit moreover: the photocathode is more sensitive than the retina. The final effective photon-catch can be two orders of magnitude higher, if sufficient intensification is applied to insure that each photon detected by the photocathode is also detected by the observer's eye.

A more detailed description of image intensifier tubes, including other types is presented by Schnitzler (1971).

§5.4. THE GAIN IN PHOTON-CATCH

When the luminance in object space is L cd/m^2, the light-flux E that enters a pupil of A m^2 will be:

$$E = 8.47 \times 10^{-8} AL \, \frac{\text{lumen}}{\text{min}^2 \text{ of arc}} \qquad (5.3)$$

The number of photons per sec per lumen, weighed after the spectral distribution $F(\lambda)$ of the light source and the relative spectral sensitivity $S(\lambda)$ of the detector, which will be called the photon-yield p, is:

$$p = \frac{\int F(\lambda)S(\lambda)\frac{\lambda}{hc}\,d\lambda}{680\int F(\lambda)V(\lambda)d\lambda} \, \frac{\text{photons}}{\text{sec. lumen}}, \qquad (5.4)$$

where $V(\lambda)$ is the photopic relative spectral sensitivity. Fig. 24 compares the spectral sensitivity of photopic vision, scotopic vision and the S-25 photocathode that is mostly used in image intensifier tubes.

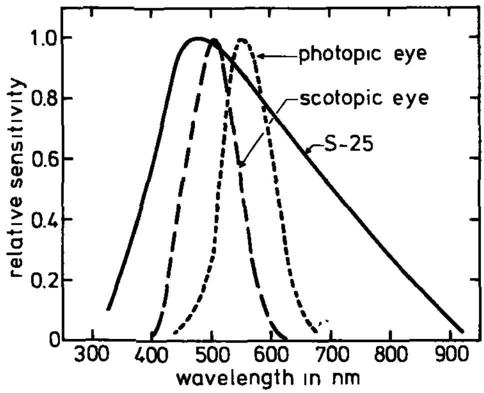

Fig. 24. Relative spectral sensitivity of the human eye in photopic and in scotopic vision, and of the S-25 photocathode (taken from Schnitzler, 1971).

Fig. 25 shows the spectral distribution of some relevant light sources. The corresponding photon-yields are given in Table II. Combining Eq. (5.3) and Eq. (5.4) the weighed photon flux is found:

$$\phi = 8.47 \times 10^{-8} \text{ p.A.L.} \frac{\text{photons}}{\text{sec. min}^2 \text{ of arc}} \tag{5.5}$$

In the photon-yield p, only the relative spectral sensitivity normalized to unity at the maximum is accounted for. The absolute sensitivity at the maximum is expressed separately in the quantum efficiency η. The de-

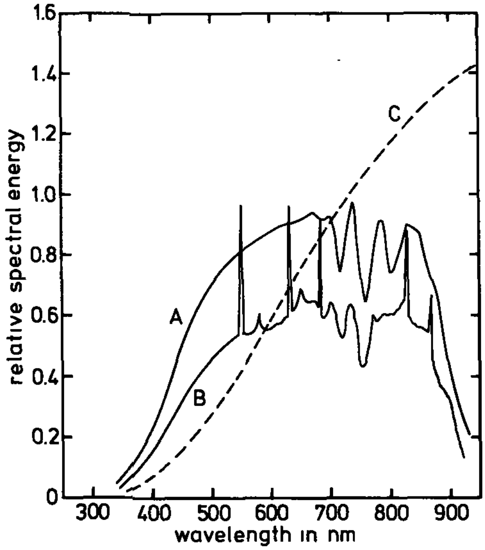

Fig. 25. Relative spectral distribution of some light sources. Curves A and B represent the irradiances from full moonlight plus airglow and 0.03 full moonlight plus airglow respectively on a clear night through 2 air masses, and are taken from Biberman (1971). Curve C represents standard light source A.

Table II. Photon-yield p according to Eq. (5.4)

	Standard light source A	Moonlight	Nightlight
photopic vision	4.27×10^{15}	4.19×10^{15}	4.09×10^{15}
scotopic vision	2.22×10^{15}	2.98×10^{15}	2.95×10^{15}
S-25 photocathode	16.2×10^{15}	11.93×10^{15}	11.82×10^{15}

tected photon flux ϕ_d now becomes:

$$\phi_d = 8.47 \times 10^{-8}\ \eta\tau pAL\ \frac{\text{photons}}{\text{sec. min}^2\text{ of arc}} \tag{5.6}$$

where τ is the transmission factor of the optical media. The ocular transmission of the human eye is usually included in the quantum efficiency. Thus as far as the human eye is concerned $\tau = 1.0$ formally in Eq. (5.6).

The gain P in photon-catch, provided by any aiding instrument with respect to the human scotopic eye follows immediately from Eq. (5.6):

$$P = \frac{[\tau\eta pA]_{\text{aid}}}{[\eta pA]_{\text{sc. eye}}} \tag{5.7}$$

P is the gain in detected photon flux with respect to the object-space and can be distinguished from the gain H in detected photon flux with respect to the image space:

$$H = \frac{P}{m^2} \tag{5.8}$$

where m is the angular magnification of the aiding instrument. The factor H was introduced by Dirksen and Van Schie (1963).

According to the experiments of chapter 3 one and the same fluctuation theory applies to vision with and without image intensification. From this point of view the contrast sensitivity functions of the unaided eye are shifted in general along the contrast sensitivity axis with a factor $\sqrt{H}$ by the use of the aiding instrument. Next to this they are shifted along the spatial frequency axis in object space with a factor m. The gain G_I in integrated contrast sensitivity thus will be:

$$G_I = m\sqrt{H} = \sqrt{P} \qquad (5.9)$$

Note that $P = \tau m^2$ and $H = \tau$ for common night-glasses, which states once more that the gain in photon-catch can only be used in the form of angular magnification in that case. The designer of intensifier telescopes on the other hand is essentially free to distribute the gain over m and H.

Table III presents a quantitative survey of the various pertinent data and the resulting gain factors P and H for unaided scotopic vision, 7 x 50 night-glasses, and two intensifier telescopes, which will be indicated as it-1 and it-2. It-2 has a catadioptric objective with central obscuration, which is included in the low transmission. The photon-yields in Table III refer to standard light source A and are taken from Table II (page 59). The quantum efficiency of the human eye is discussed extensively in chapter 4. The sensitivity of S-25 photocathodes is specified as 0.21 mA per lumen (standard light source A), by the manufacturer (Schnitzler, 1971), which corresponds to a quantum efficiency of 0.08 at the maximum of the spectral sensitivity curve.

It is silently assumed sofar that the gain in photon-catch is fully exploited. The specks on the phosphor screen must be sufficiently bright thereto. This condition is met by both intensifier telescopes mentioned in Table III, as a rough estimation of the corneal speck-intensity shows. Both instruments are equipped with three-stage-cascaded intensifier tubes,

Table III. Relevant data and gain factors of some aiding instruments

Quality	Symbol	Scot. eye	Night-glasses	Intensifier telescopes it-1	Intensifier telescopes it-2
Entrance pupil (m^2)	A	3.85×10^{-5}	1.89×10^{-3}	4.55×10^{-3}	4.64×10^{-3}
Transmission	τ	1.00	0.80	0.88	0.50
Photon-yield	p	2.22×10^{15}	2.22×10^{15}	16.2×10^{15}	16.2×10^{15}
Quantum efficiency	η	0.01	0.01	0.08	0.08
Gain in photon-catch	P	1.0	39.2	6080	3200
Angular magnification	m	1.0	7.0	3.5	4.0
Gain in photon flux in image space	H	1.0	0.80	496	200

which generate specks of about 60000 photons on the third and final phosphor screen. The it-1 scatters 0.6% or 360 of these into the pupil of the observer, when the latter has a diameter of 5 mm. The it-2 provides even a higher corneal speck-intensity. As can be read from Figs 10 and 16 a speck-intensity of 360 corneal photons will be sufficient in general.

§5.5. EXPERIMENTS WITH ACTUAL INTENSIFIER TELESCOPES

Fig. 26 illustrates measured contrast sensitivity functions for vision with the two intensifier telescopes mentioned above.

The parameter is luminance in object space. The difficulty arises here, that light units refer to the spectral sensitivity of the human eye by definition, and thus are no good measure for radiances weighed *by the spectral sensitivity of photocathodes. Biberman (1971) therefore* proscribes light units in connection with opto-electronic devices. With-

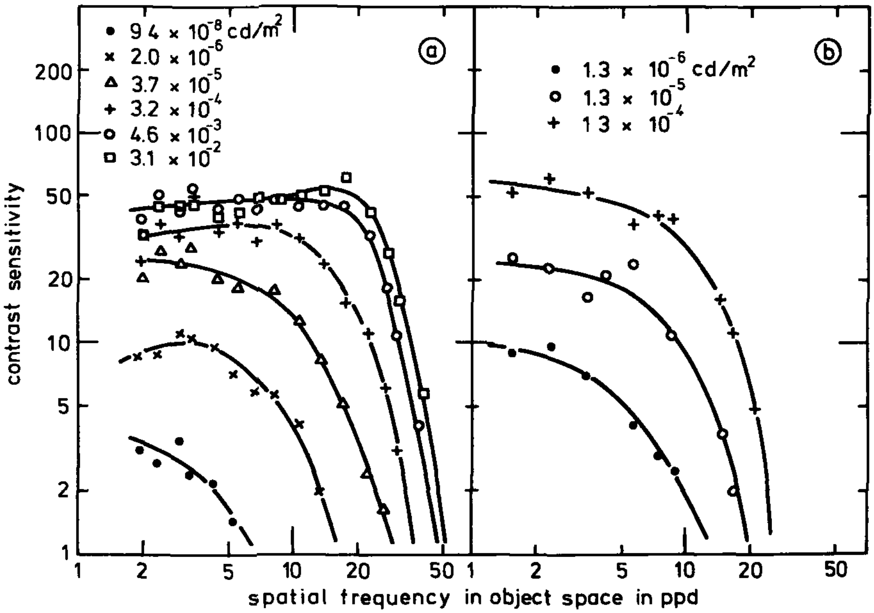

Fig. 26. Contrast sensitivity functions for vision through two actual image intensifier telescopes. Fig. 26a refers to vision with the it-1 to a sine wave field of 11° x 11° in image space (no artificial pupil). Fig. 26b refers to vision with the it-2 to a sine wave field of 15° in diameter in image space with an artificial pupil of 3 mm in front of the observer's eye. Luminances are expressed in equivalent levels of standard light source A (see §5.5).

in the framework of the present comparison of aided and unaided vision we nevertheless prefer to use light units. To avoid the problem we will express light levels in the object space of intensifier telescopes always in equivalent luminances L_A of standard light source A:

$$L_A = \left[\frac{p}{p_A}\right]_{S-25} \cdot L \qquad (5.10)$$

It will be evident from Eq. (5.4) that this procedure leads to correct photon fluxes, notwithstanding the use of different light sources. One may read from Table II how one lumen of moonlight or nightlight yields a little less S-25 photons than one lumen of standard light source A. Light source A is chosen here as a standard, since cathode sensitivities are usually specified also with respect to light source A. The light units used here can be converted into radiance units, if required, considering that the luminous efficiency of light source A is about 20 lumen per Watt.

Studying the contrast sensitivity functions for vision with both intensifier telescopes (Fig. 26) the gain relative to unaided vision (Fig. 3) is striking indeed: the curves refer to much lower luminances. Paying attention for instance to the curve for vision with it-2 at 1.3 x 10^{-4} cd/m^2 one notes considerable shifts toward higher spatial frequency and higher contrast sensitivity. On reflection, however, it is somewhat misleading to speak of simple shifts. The contrast sensitivity functions are cut off already at about 35 ppd in object space, or about 10 ppd in image space. This must be ascribed to imperfect imaging in the devices.

Fig. 27 illustrates the MTF's of the two intensifier telescopes as well as the eye optics for a 5 mm pupil (see chapter 6). The image quality of the intensifier telescopes clearly is the limiting factor. As to this the image quality of the objective lens and the image tube of it-1 are equally bad (Van Meeteren, Vos and Boogaard, 1971). The catadioptric objective of it-2 is practically perfect (Becker, 1970) and thus the MTF is controlled here by the image tube. Note that there is but little difference between the final MTF's of the two devices, when plotted *vs* spatial frequency in image space.

Considerable amounts of straylight may occur in intensifier telescopes, partly arising in the intensifier tube. In the center of a small black test object upon a uniform illuminated background, covering the

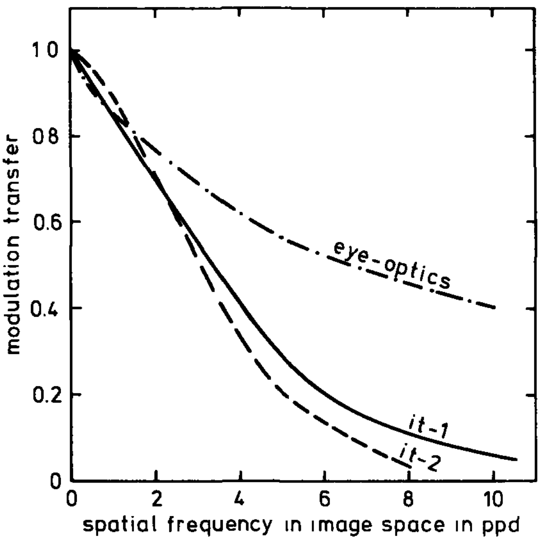

Fig. 27. Modulation transfer functions of two actual image intensifying telescopes. For comparison the modulation transfer of the eye optics is plotted here also for a pupil of 5 mm in diameter.

whole field of view of it-1, the veiling proved to be 20% of the background luminance. A veiling of 6% was found when only a field of 3^0 (in object space) was illuminated as in the above experiments. In it-2 4% straylight was measured in the center of a 3.8^0 field (in object space).

Accounting for the MTF's of the devices and for the contrast losses caused by straylight the quality of the image on the final phosphor screen can be reconstructed. Considering further the photon-catch and the corresponding speck-density the measured contrast sensitivity functions can be compared with the results of the speck-image experiments of chapter 3. If the agreement is satisfactory, this settles the prediction of contrast sensitivity for vision through actual intensifier telescopes.

For a fair comparison the measurements with it-1 were repeated in the same conditions as the speck-image experiments of chapter 3: using an artificial pupil of 3 mm and foveally fixated sine wave fields of 3^0 x 3^0 in image space. The results, plotted in Fig. 28a, differ barely from those of Fig. 26a, referring to larger sine wave fields and natural pupil. The data are replotted in Fig. 28b after correction for the MTF of it-1 and for straylight. Thus they can be compared with the predicted curves taken from Fig. 14 by interpolation at the appropriate speck-densities ϕ_d/m^2, where m is the angular magnification and ϕ_d follows from Eq. (5.6).

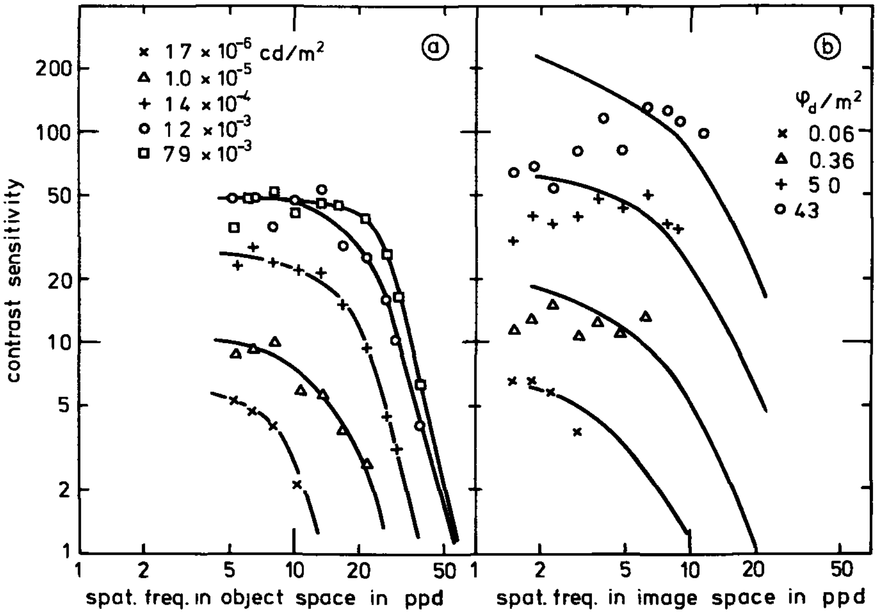

Fig. 28a. Contrast sensitivity functions for vision with the it-1 to a sine wave field of 3° x 3° in image space, using a 3 mm artificial pupil. The data are replotted in Fig. 28b after correction for the MTF of the it-1 and compared with predicted curves. The latter are derived from the speck-image experiments of chapter 3 (Fig. 14) and refer to the same experimental conditions as Fig. 26a. Parameter is here the detected photon flux ϕ_d/m^2 in image space calculated from the light levels of Fig. 26a according to Eq. (5.6).

Fig. 29 shows the same comparison for it-2. Here the data of Fig. 26b are replotted after correction for MTF and straylight, and compared with predicted curves.

For it-1 contrast sensitivity remains markedly behind the prediction at low spatial frequencies and higher luminances. Contrast sensitivity is limited to about 50 in vision through this device. This might quite well be due to the inhomogeneous structure of the fiber-optical face- and coupling plates in this older instrument. Contrasts lower then 2% apparently get lost in interference with the visible chicken-wire structure. In it-2 no such inhomogenities were visible and contrast sensitivity is not restricted in this way in the range investigated. Apart from this the actual and predicted contrast sensitivity levels agree statisfactorily for vision through it-1 and it-2. Dark current as well as additional noise (variable speck-intensity) of the intensifier tubes apparently have no measurable effect.

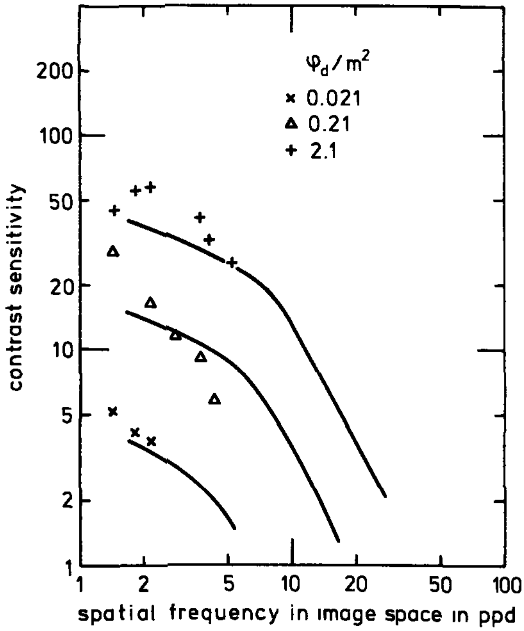

Fig. 29. Same as Fig. 28b. Here the contrast sensitivity data for vision with the it-2 are replotted after correction for the MTF of the device, and compared with their prediction.

§5.6. THE GAIN IN INTEGRATED CONTRAST SENSITIVITY

The net proceeds of intensifier telescopes may be characterized by the gain in integrated contrast sensitivity. The simple shifts of contrast sensitivity functions brought about by ideal devices are complicated by losses in actual devices. A simple and yet detailed description of the final gain thus cannot be given. Abandoning detail, however, the gain in integrated contrast sensitivity, introduced as a summary measure for visual performance in §2.5, may be discussed.

In Fig. 30 the integrated contrast sensitivity I is plotted *vs.* log luminance in object space for natural unaided vision, vision with 7 x 50 night-glasses, and for vision through the two intensifier telescopes. The net gain provided by the devices can be characterized now by a simple shift along the log luminance axis. One might speak of an effective luminance gain to be compared with the calculated gain in photon catch (Table III, page 60). This effective luminance gain amounts to a factor 1000 roughly for both intensifier telescopes, whereas the gain in photon catch according to Table III is 6080 for it-1 and 3200 for it-2. It should be realized first that monocular devices are compared here

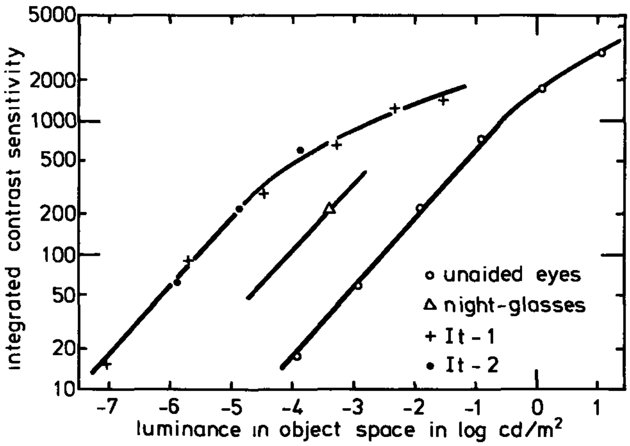

Fig. 30. Integrated contrast sensitivity (defined in Eq. (2.4)) for vision with unaided eyes, 7 x 50 night-glasses and two image intensifying telescopes, plotted *vs.* log luminance in object space (equivalent levels of standard light source A). Note the shift toward lower luminance provided by the aiding instruments. This shift might be interpreted as the effective luminance gain and can be compared as such with the original gain in photon-catch (§5.6).

with binocular unaided vision. Considering this the effective luminance gain ideally could have been 3040 and 1600 respectively as follows from §2.6. Thus the effective luminance gain differs from the ideal values by factors 3 and 1.6 for it-1 and it-2 respectively. These factors represent the losses arising from imperfect imaging in the devices. As such they indicate possible improvements of the gain by better technology.

§5.7. DESIGN CONSEQUENCES AND TEST PROCEDURES

One might wonder whether new design consequences for intensifier telescopes emanate from the present study, and whether it suggests new test procedures. In answering this question it should be realized that the present experiments first of all remove certain doubts on the fluctuation theory of vision with image intensifiers. As such they justify current design principles.

Next to that the experiments on the minimum required intensification to obtain the speck-noise limited contrast sensitivity levels (§3.5 and §3.9) may be helpfull to the design of image intensifiers. Schagen's

(1963) opinion, that 10 corneal photons per speck would be sufficient in scotopic observation of the phosphor screen is refuted. About 150 corneal photons per speck are required in peripheral observation (§3.9). Surprisingly, however, the speck-intensity does not need to be higher for photopic observation, when the retinal speck-density is not lower than 1 speck per sec per min^2 of arc (§3.5). And when the retinal speck-density is about 10 specks per sec per min^2 of arc it seems that even 30 corneal photons per speck suffice. Such a corneal speck-intensity may be realized with a single-stage image intensifier tube, resulting in specks of about 1000 photons on their phosphor screen, when the pupil of the observer's eye is about 6 mm in diameter and the focal length of the ocular lens is 17 mm.

To evaluate the practical significance of the retinal speck-densities just mentioned we may relate them to the luminance L in object space, taking for instance an entrance pupil of 2.8×10^{-3} m^2 (diameter 60 mm) and a transmission $\tau = 0.8$. It follows then from Eq. (5.6) that the detected photon flux in object space amounts to 2.5×10^5 L photons per sec per min^2 of arc, if L is expressed in cd/m^2 and refers to standard light source A. The retinal speck-density thus will be 2.5×10^5 L/m^2 in this example, where m is the angular magnification. With $L = 10^{-4}$ cd/m^2 a minimum retinal speck-density of 10 specks per sec per min^2 of arc can be obtained, but only if the angular magnification is smaller than 1.6. In general it seems to be possible to design intensifier telescopes equipped with a single-stage intensifier tube, and yet to obtain the speck-noise limited contrast sensitivity level, even in photopic observation, if the angular magnification is kept small. The loss in image quality resulting from cascading image intensifier tubes would be evaded in this way.

It has been emphasized that the angular magnification of intensifier telescopes can be chosen independently of the photon-catch, which is a large advantage over common night-glasses. However, the focal length f_{ob} of the objective lens cannot be too small relative to the diameter of the entrance pupil, and the focal length f_{oc} of the ocular lens cannot be too large relative to the pupil of the user's eye. As a consequence f_{ob}/f_{oc} will be about 4 in practice which leads to a corresponding angular magnification. Fortunately, demagnifying image tubes are available to reduce the total angular magnification, if required so. Thus the gain in photon catch can be used for a great part to obtain higher contrast sensitivity. The designer then should keep Weber's law in mind: beyond a certain level contrast sensitivity cannot be improved. In that case the gain in photon-catch can be better exploited in the form of angular magnification, which indeed is the principle of daylight optical aids.

Finally, it may be remarked that the further development of "second generation" microchannel-plate image intensifiers and transmission secondary-electron multipliers may render the problem of sufficient intensification and yet good image quality out of date in the future.

As to test procedures the present study connects to the measurement of cathode sensitivity, intensification and MTF. The speck-noise could be evaluated from photon-catch calculations, but it is preferable, of course, to measure the display signal-to-noise ratio and the dark current also.

Apart from this, it is proposed to measure contrast sensitivity functions for vision through new types of intensifier telescopes as a check on prediction. Especially when the speck-intensity is high there may be an interaction between MTF and signal-to-noise ratio, as discussed at the end of §3.2, which is difficult to predict.

§5.8. RECAPITULATION

Vision through intensifier telescopes, as an example of applied image intensification, can be understood and predicted from unaided vision by considering the gain in photon-catch, the angular magnification and the image quality of the devices.

CHAPTER 6

MODULATION TRANSFER FUNCTIONS OF THE EYE-OPTICS

§6.1. INTRODUCTION

The contrast sensitivity functions found by threshold measurements with sine wave gratings characterize the visual system as a whole. They are the joint product of optical and neural modulation transfer. Their interpretation implies the separation of these two components. One might question, for instance, whether the high frequency decay is caused completely by optical imperfections. In chapter 2 the gradual changes in the width of contrast sensitivity functions with luminance have been attributed to neural processing mainly, which has to be argued as yet. There are two alternative ways to separate the optical and the neural components of contrast sensitivity functions. One can either determine the optical MTF first and consider the residue as the neural contribution, or in the reverse, measure the neural contrast sensitivity function separetely and solve the optical MTF. Both ways have been explored in the literature. In this chapter the calculation of MTF's for the eye-optics will be described, starting from experimental data on the various geometrical aberrations taken from literature. These calculations provide a welcome supplement to recent measurements, and moreover reveal the relation of the MTF's to the underlying aberrations.

Though the eye undoubtedly is the most used optical instrument, its image quality is still subject to debate. The retinal image was not accessible to measurements in living eyes until Flamant (1955) managed to record the weak fundal reflection of a line source. Several authors since have improved the recording technique (Krauskopf, 1962; Röhler, 1962; Westheimer and Campbell, 1962), and removed certain doubts on the origin and nature of the fundus reflection (Campbell and Gubish, 1966; Röhler, Miller and Aberl, 1969). These measurements, however, reflect the combined effect of optical imaging and retinal scattering and it remains questionable in how far the latter is represented correctly. A second method to evaluate the quality of the retinal image was applied by Arnulf and Dupuy (1960), Westheimer (1960) and Campbell and Green (1965). They measured contrast thresholds for sine wave gratings imaged on the retina by the optics of the eye in the normal way and compared the results with contrast thresholds for sinusoidal interference fringes generated on the retina by coherent illumination of two narrow slits placed in front of the pupil (Le Grand, 1937). The modulation of the interference fringes is not affected by the imaging errors of the eye-optics, and thus, the optical MTF can be reconstructed. However, the role of retinal scattering is not clear in this method too, especially with respect to the interference gratings. Unfortunately, the results of the interference grating method cannot be compared with the results of the fundus reflection measurements since the latter were made in whitish light only and the first in monochromatic light only. Summarizing, the interpretation of both experimental methods is subject to uncertainty and an independent calculation of the optical quality of the human eye, preferably in terms of modulation transfer is needed.

A number of calculations on the image quality of the human eye are described in literature. The diffraction-limited cut-off frequency was calculated by Rayleigh (1903). The effect of chromatic aberration upon the edge-spread function was evaluated by Von Helmholtz (1866). Lapicque (1937) calculated the combined effect of diffraction, spherical aberration and chromatic aberration upon the point-spread function for a 5 mm pupil. He found only a small difference when the spherical aberration was neglected completely and concluded that the chromatic difference of focus is the most dominant aberration in white light. This encourages further calculations, because there is little variation in this aberration between different human eyes, so that the white light optical performance should be fairly constant, and its calculated value can be generalized. Apart from some incidental estimates of the effect of chromatic aberration upon modulation transfer (Campbell and Gubisch, 1966) no systematic calculations of modulation transfer functions of the human eye optics are known to us.

An important question concerns the effect of focus errors upon the modulation transfer functions. The image is judged ~~subjectively~~ as sharp within a rather large range of focus settings (Campbell,1957). According to Kasai,Kondo,Sekiguchi and Fujii (1971) the accomodation probably fluctuates around the hypermetropic border of this range. If so,the eye would normally be out of focus. MTF's for just noticeable focus errors may give an impression of the subjective tolerance as to visual image quality.

Visual acuity is reduced at low luminance, mainly because of the decreasing signal-to-noise ratio of the incoming photon flux. In addition to this, optical modulation transfer might also be worse for scotopic vision, due to different factors. First,the chromatic aberration is more pronounced in the scotopic spectral sensitivity range. Second, rods have no Stiles-Crawford effect (which diaphragms the pupil in photopic vision). Third, more peripheral parts of the retina are used in scotopic vision leading to more oblique aberrations. The total effect upon the modulation transfer functions for vision at low luminances will be calculated and discussed.

The present calculations have been made for white light (equal energy distribution) weighed either by the photopic or the scotopic spectral sensitivity. Some complementary calculations for light of standard source A have shown no significant differences, so that it can be stated that the results apply to whitish light in general. No results are presented here for monochromatic lights. The use of MTF-calculations for monochromatic light is doubtful with respect to the human eye. First, monochromatic aberrations are subject to individual variations, and second, the accomodation-mechanism seems not to be able to fully exploit the better monochromatic image (Fincham, 1953).

§6.2. GEOMETRICAL ABERRATION DATA

In §6.3 the calculation of MTF's from geometrical aberration data will be outlined in short. Introductory, the experimental data may be surveyed first.

Data on the chromatic difference of focus, spherical aberration and astigmatism are available in the literature. The amount of chromatic aberration is solidly based. The dispersion of the eye media is practically the same as that of water and there is little variation in the results of different eyes and from different authors. Fig. 31 shows the chromatic difference of focus D expressed in diopters as a function of wavelength according to the extensive measurements of Wald and Griffin (1947).

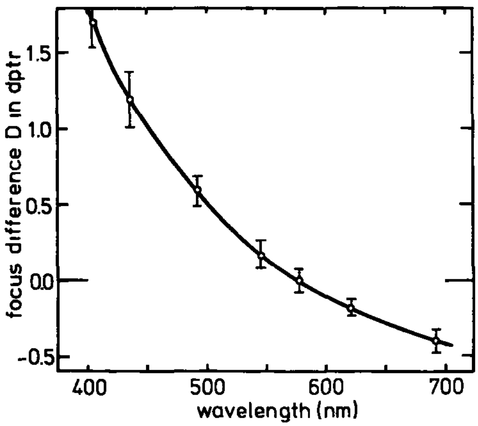

Fig. 31. Chromatic difference of focus, according to Wald and Griffin (1947). Average results and standard deviations of 14 subjects.

The spherical aberration may be characterized by the difference S in refractive power between marginal and central rays, expressed in diopters. Unlike chromatic aberration the data on spherical aberration show rather large differences between subjects. A sample of experimental data taken from literature is plotted in Fig. 32 and compared with the spherical aberration of the well-known Gullstrand eye model. In real eyes the spherical aberration is apparently smaller, thanks to the flattening of the cornea and the decreasing refractive index of the crystalline lens as the distance to the axis increases. When the crystalline lens is modified in the Gullstrand model with a quadratically decreasing refractive index $n = 1.3939 - 710\ r^2$, r being the distance to the axis in m, the interrupted curve in Fig. 32 is obtained. This curve is used as an estimation of actual spherical aberration in the following calculations.

Astigmatism is characterized by Sturm's interval I, expressing the difference in diopters between the sagittal and the tangential focus. Rempt, Hoogerheide and Hoogenboom (1971) recently measured astigmatism by sciascopy of almost 900 eyes, all satisfying minimum visual standards

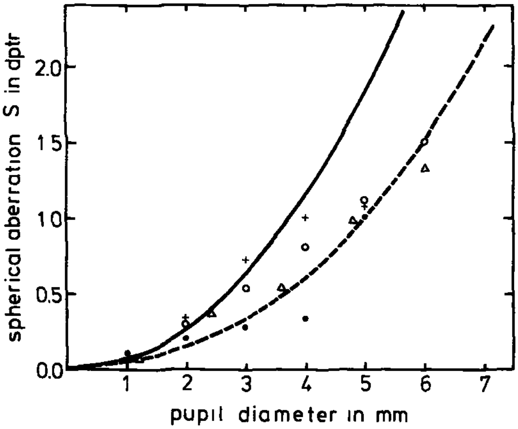

Fig. 32. Longitudinal spherical aberration in diopters. Experimental data of some authors are indicated. The upper curve refers to the Gullstrand eye, the lower curve refers to a modified Gullstrand eye.
Legend: o, Koomen *et.al.* (1949);
+, Francon (1951);
•, Ivanoff (1956);
Δ, Schober *et.al.* (1968).

required for aircrew licensing. Like Ferree, Rand and Hardy (1931) they found different patterns of astigmatism. About half the number of eyes, however, forms the largest class with "normal" astigmatism, *i.e.* with the retina in the middle of Sturm's interval, although with considerable variability in magnitude. The average Sturm's interval of a sample of 100 eyes with such normal astigmatism, taken from Rempt *et.al.*, is plotted in Fig. 33. An interpolation curve is drawn through the data points in order to estimate oblique astigmatism at small visual angles, where no measurements were made. Admittedly, marked individual deviations may occur, but it seems reasonable to conclude that oblique astigmatism is small in foveal vision and not really problematic in the peripheral areas used in scotopic vision.

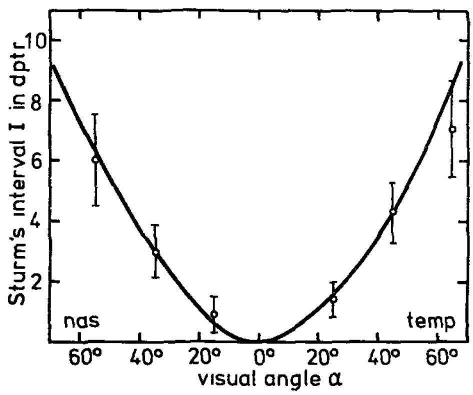

Fig. 33. Sturm's interval according to the measurements of Rempt *et.al.* (1971). Average results and standard deviations of 100 eyes with normal astigmatism. The interpolation curve is given by $I = 0.007\alpha^{1.7}$.

No experimental data on the amounts of coma and chromatic magnification error are available, but they can be derived from the spherical aberration and the chromatic difference of focus respectively. As to the chromatic magnification error this has been shown in studies on the colour stereoscopic effect (Vos, 1960). The point is, as Guidarelli (1972) remarked, that the human eye is practically homocentric: the center of curvature of the dominant corneal surface coincides roughly with the nodal points and with the center of curvature of the retina. Thus the eye would be free of oblique aberrations, if the pupil was also in that same position. That is why Ivanoff (1953) found the foveal viewing axis to be practically achromatic also. It implies that the only contributions to coma and chromatic magnification emerge from the position of the pupil with respect to the viewing axis. Due to the fact that the pupil is about 3.7 mm in front of the nodal points its position is eccentric with respect to the viewing axis, when the latter makes an angle with the optical axis. It will be explained in §6.3 how spherical aberration leads to coma in that case, and how the chromatic difference of focus leads to a chromatic magnification error.

Finally, it must be remarked that irregular aberrations may occur in the human eye and cause an additional blur. When a point source is observed out of focus the blur circle does not look uniform but like a "star". Since aphakes do not see such stars the effect is ascribed to the radial sutures of the crystalline lens (Lapicque, 1937). Van den Brink (1962) found irregular patterns of dioptric power by scanning of the eye optics with a small artificial pupil. His results are difficult to interpret, however, since differences in local dioptric-power are not good measures for aberrations (Schober, Müncker and Zolleis, 1968). Smirnov (1961) measured the wave aberration function $W(x,y)$ with monochromatic light in 12 different eyes and found irregularities superimposed over regular aberrations. His conclusion, however, is that monochromatic aberrations are small in general and practically without effect upon image quality. Possible irregularities in them thus seem to be of minor importance.

Epitomizing the above survey, Gullstrand's paraxial standard eye may be completed with "standard" third order geometrical aberrations. Chromatic difference of focus, spherical aberration and astigmatism could be taken from literature, whereas chromatic magnification error and coma follow from them. It must be remarked in this respect that the aberrations of Gullstrand's eye model itself are incorrect: the model should not be used otherwise than paraxially.

§6.3. WAVE ABERRATIONS AND THE MTF

The calculations of MTF's will be described here briefly: the reader is referred to textbooks for an account of the mathematics involved. The starting point is the wavefront in the exit pupil:

$$\begin{aligned} F(x,y) &= |F(x,y)|\cdot\exp\left\{\frac{2\pi i}{\lambda} W(x,y)\right\}, && \text{if } x^2+y^2 \leq 1 \\ F(x,y) &= 0, && \text{if } x^2+y^2 > 1, \end{aligned} \tag{6.1}$$

where x and y are coordinates in the pupil plane, normalized to unity at the border of the pupil. The phase of the wave front is expressed in the optical path-difference $W(x,y)$ with respect to the ideal spherical wavefront converging in the image point. The amplitude $F(x,y)$ will be mostly uniform except in the case of special apodization filters. In the human eye the socalled Stiles-Crawford effect finds expression in a non-uniform $|F(x,y)|$.

The complex optical transfer function $O(w)$ can be calculated by convolution of the pupil function:

$$O(w) = \frac{\iint F(x,y)\cdot F^*(x-2\frac{w}{w_d}\ ,\ y)dxdy}{\iint F(x,y)\cdot F^*(x,y)dxdy}\ , \tag{6.2}$$

where w is the spatial frequency and w_d is the diffraction limited cut-off frequency (O'Neill, 1963). Eq. (6.2) refers to sine wave gratings oriented in the direction of the y-axis. For other orientations of the sine wave gratings the pupil function must be convoluted analogously in a direction perpendicular to the orientation.

The modulus of the optical transfer function represents the ratio of the sine wave modulation in the image to the original modulation and is called *modulation transfer function* (MTF).

The diffraction limited cut-off frequency w_d can be written as:

$$w_d = \frac{2\pi}{360}\cdot\frac{n}{\lambda}\cdot\frac{2a}{f}\cdot b \quad \text{periods per degree} \tag{6.3}$$

Here $n = 1.336$ is the refractive index in image space; λ is the wavelength of the light; a is the variable radius of the exit pupil; $f = 0.022785$ m is the focal length and $b = 0.017055$ m is the distance from the second nodal point to the image plane. These data were taken from Gullstrand's model eye (Le Grand, 1952).

The various aberrations deform the ideal spherical wavefront and make the phase function $W(x,y)$ different from zero. Taking only third order aberrations and focusing errors into account one can write for $W(x,y)$:

$$W(x,y) = C_f(x^2+y^2) + C_s(x^2+y^2)^2 + C_m x + C_c(x^2+y^2)x + C_a x^2, \tag{6.4}$$

where C_f represents focusing errors, C_s spherical aberration, C_m distortion or magnification error, C_c coma and C_a astigmatism. This form of Eq. (6.4) implies that the meredian plane is defined by the optical axis and the x-axis.

The coefficients C_f, C_s and C_a are related to the corresponding geometrical aberrations D, S and I (see §6.2):

$$C_f = \frac{-a^2D}{2}$$

$$C_s = \frac{-a^2S}{4} \tag{6.5a}$$

$$C_a = \frac{-a^2I}{2}$$

The derivation of these relations can be found in the textbooks of Longhurst (1957) and O'Neill (1963), among others. As discussed in §6.2 distortion (chromatic magnification) and coma are due mainly to the eccentricity of the pupil with respect to the main ray. This eccentricity can be introduced in the focusing error term and the spherical aberration term of Eq. (6.4) by substitution of $x^1 = x-e/a$, where e/a is the eccentricity relative to the radius of the pupil. In this way a magnification error term and a coma term come out and one finds:

$$C_m = -2\frac{e}{a} C_f = eaD$$

$$C_c = -4 \frac{e}{a} C_s = eaS \tag{6.5b}$$

The Stiles-Crawford effect, if applying, is introduced in the form of the amplitude $|F(x,y)|$:

$$|F(x,y)| = \exp\{-\frac{\alpha^2}{2}(x^2+y^2)\}, \qquad (6.6)$$

where $\alpha = 0.108$ as derived from Crawford (1937). It is generally assumed that the Stiles-Crawford effect is related to the antenna-like construction of the cones. From this point of view the interaction of the optical image with the receptor-layer might be more complex and also change the phase-function $W(x,y)$. Such a possible effect is not introduced in the present calculations. In first order approximation it might add a pseudo focus-term to $W(x,y)$ and change the effective power of the eye optics rather than image quality.

The numerical evaluation of the convolution integrals (Eq. (6.2)) was made with a digital computer according to Hopkin's method (1957). The computer program was tested by calculating transfer functions for focusing errors that can also be derived analytically.

The optical transfer function for white light was calculated as a weighed superposition of monochromatic transfer functions:

$$O(w) = \frac{\sum i \; O(\lambda_i, w) V(\lambda_i)}{\sum i \; V(\lambda_i)}, \qquad (6.7)$$

where λ_i was taken in steps of 8 nm from 440 - 680 nm in the calculations for photopic vision and from 400 - 640 nm in the calculations for scotopic vision. $O(\lambda_i, w)$ is the complex optical transfer function at λ_i, taking into account the chromatic difference of focus and the lateral shift caused by the chromatic magnification error. $V(\lambda_i)$ is the photopic or the scotopic spectral sensitivity function.

§6.4. MTF's FOR FOVEAL VISION

The fovea is about 5^0 off-axis (Le Grand, 1952). The amount of coma, astigmatism and chromatic magnification error were chosen accordingly.

The Stiles-Crawford apodization proved to reduce the effect of aberrations markedly at larger pupil sizes (Van Meeteren, 1973) and was taken into account.

The MTF's depend first of all upon the state of focusing. Optimum focusing is probably an exception rather than a rule in normal vision. The range of focus settings within which the image is judged as sharp and within which the stimulus for better focusing probably is weak, proves to be rather large (Campbell, 1957). No wonder that accommodation shows microfluctuations of about 0.2 D (Campbell, Robson and Westheimer, 1958). It nevertheless makes sense to calculate modulation transfer functions for optimum focusing. First, they describe the upper-limit of image quality. Second, optimum focusing is often imposed experimentally with correction lenses after paralysis of accommodation. Third, in threshold experiments with long or unlimited presentation time the responses may be representative for the best focus setting. To find the optimum focus the modulation transfer was calculated as a function of focusing. Fig. 38 illustrates examples of such focusing curves. The optimum focus depends upon the spatial frequency. The lower the spatial frequency the more myopic the focus setting will be (Green and Campbell, 1965). There is but little change, however, in the optimum focus for spatial frequencies of 20 ppd and higher and the following MTF's for foveal vision refer to optimum focusing for 20 ppd, *i.e.* to optimum focusing for higher spatial frequencies in general.

Fig. 34 presents an analysis of the effects of the various aberrations as a function of pupil size. The human eye is practically diffraction limited at pupils smaller than 1 mm. Chromatic difference of focus is the most important aberration and reduces modulation transfer considerably when the pupil is larger than 2 mm. The total effect of spherical aber-

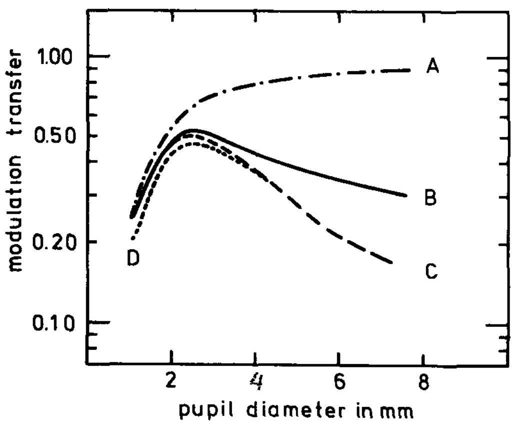

Fig. 34. Cumulative effect of the various aberrations upon the modulation transfer of vertical gratings at 20 ppd as a function of pupil size. Curve A refers to the diffraction limit, curve B to on-axis imaging with chromatic aberration, curve C to on-axis imaging with chromatic and spherical aberration and curve D to the foveal image with chromatic, spherical and oblique aberrations.

ration, coma and astimatism is negligible for pupils smaller than 3 mm and always moderate when compared with chromatic aberration. The chromatic magnification error reduces the transfer of vertically oriented sine wave gratings noticeably when the pupil is small.

As has been emphasized already, the predominant chromatic aberration is practically the same in different eyes. Thus the white light MTF of individual eyes will not drastically deviate from the calculated ones. Spherical aberration may be different in different eyes, but considering that its average effect is moderate, its variation probably will not lead to measurable differences in individual modulation transfer functions. This was confirmed by the fundus reflection measurements of Campbell and Gubisch (1966), who found practically the same MTF's in three different eyes.

The calculated modulation transfer functions for foveal vision in optimum focus are plotted in Fig. 35 with pupil size as the parameter. Different curves are presented for horizontal and vertical sine wave gratings.

Note in the first place the diffraction limited cut-off of the curves for small pupils. The best tradeoff between diffraction and chromatic

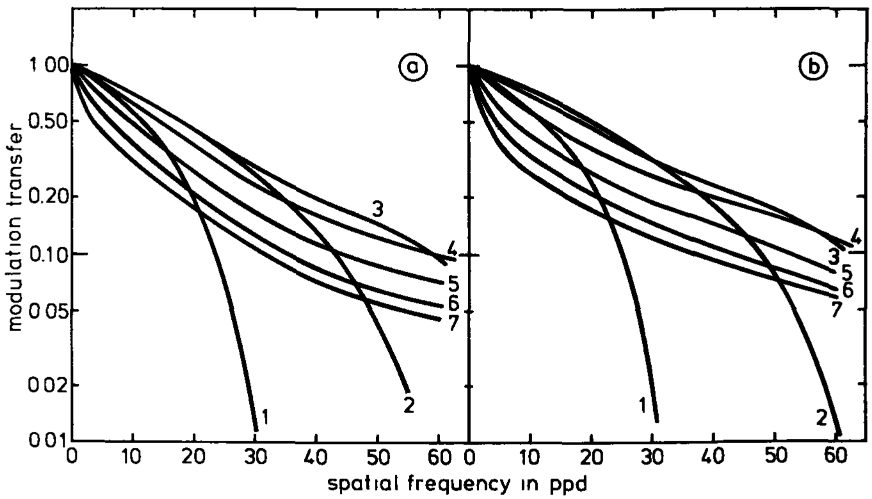

Fig. 35. Foveal modulation transfer functions for different pupil sizes. Fig. 35a refers to vertical sine wave gratings, Fig. 35b to horizontal sine wave gratings. The latter are not affected by the foveal chromatic magnification error.

aberration is found between 2 and 3 mm pupils.

The modulation transfer functions for pupils of 3 mm and larger are remarkably similar. The high-frequency decay is practically the same: the curves run parallel. In principle this phenomenon was already explained by Von Helmholtz (1866). Chromatic aberration causes a more or less wide skirt of light, due to wavelengths that are not in focus, upon which a relatively sharp image is superimposed. The skirt functions as a veiling luminance, reducing the modulation at all spatial frequencies by roughly the same factor.

The most important difference between horizontal and vertical sine wave gratings is that the first are not affected by the off-axis position of the fovea. The modulation transfer of horizontal gratings therefore is slightly better at higher spatial frequencies than the modulation transfer of vertical gratings.

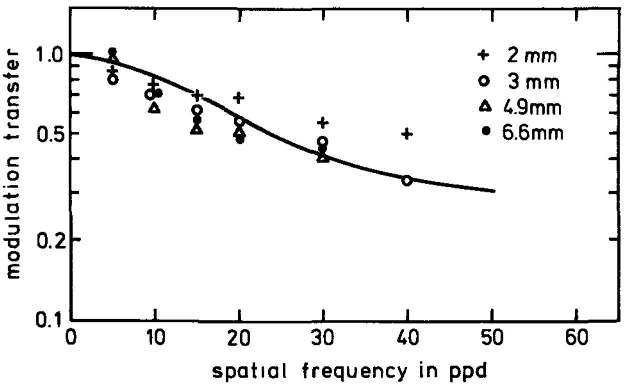

Fig. 36. Ratios of the modulation transfer functions, measured by Campbell and Gubisch (1966) and the presently calculated ones. The curve represents the modulation transfer function for retinal scattering, measured by Ohzu and Enoch (1972).

When the modulation transfer functions derived by Campbell and Gubisch (1966) from the weak fundus reflection of a narrow slit (fixated by the subject) are plotted in the way of Fig. 35, they look quite similar, apart from their steeper high-frequency decay. The curves for the various pupil sizes also run parallel and the effect of pupil size is the same. It seems as if the modulation transfer functions measured by Campbell and Gubisch (1966) are the product of the modulation transfer functions of the dioptrics of the eye and some other modulation transfer function.

This is illustrated in Fig. 36, where the quotients of the Campbell and Gubisch data and the presently calculated MTF's are plotted. Recently, Ohzu and Enoch (1972) managed to directly determine the MTF's of freshly isolated human foveas. This MTF is also plotted in Fig. 36. It seems that the difference between the MTF's measured by Campbell and Gubisch (1966) and the calculated MTF's for the dioptrics of the eye is equal to the MTF of the retina. Thus, two independent experiments and the present calculations confirm each other. This encourages further calculations in conditions where no measured MTF's are available.

§6.5. THE SUBJECTIVE TOLERANCE TO IMAGE QUALITY

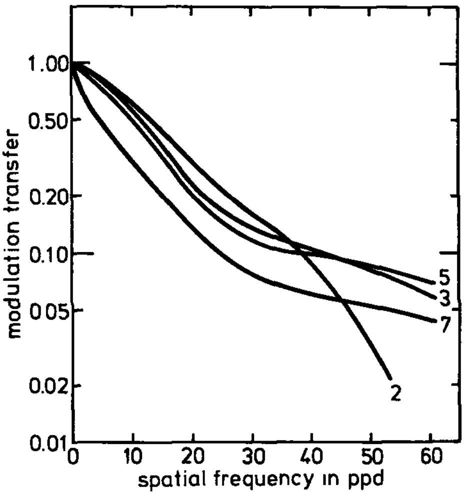

Fig. 37. Foveal modulation transfer functions for just noticeable focusing errors with pupil size as parameter. Focusing errors:
2 mm: -0.42 D 5 mm: -0.24 D;
3 mm: -0.35 D; 7 mm: -0.17 D.

Fig. 37 illustrates MTF's for focusing with just noticeable hypermetropic focus errors. The latter are taken from Campbell (1957). Such MTF's indicate the subjective tolerance to image quality. Although modulation transfer for pupils of 2 and 3 mm is reduced to half of its optimum value in the high frequency range the image is still judged subjectively as sharp. This can be understood when the modulation transfer function of the eye optics is multiplied with the contrast sensitivity function of the retina-brain system. It follows then, from the steepness of the overall contrast sensitivity functions, that visual acuity, defined as the highest spatial frequency that can be resolved, is reduced by 20% only.

It is remarkable that these MTF's practically coincide for different pupil sizes at high spatial frequencies. This might indicate that the tolerance limit is an absolute rather than a relative one: a certain image quality, characterized by the coinciding curves in Fig. 37, is considered to be satisfactory. According to Kasai *et.al.* (1971) the accommodation fluctuates around the just noticeable hypermetropic focus error in normal vision. If so, the coinciding curves in Fig. 37 are representative for image quality in practical vision.

In view of this tolerance, correction of the spherical aberration of the eye and even of the chromatic difference of focus is not likely to be of practical use. Several attempts to obtain better vision by such corrections have failed indeed (Von Helmholtz, 1866; Van Heel, 1946).

§6.6. MTF's AT LOW LUMINANCES

Three factors make the MTF for vision at low luminances worse than for daylight vision: larger chromatic difference of focus in the scotopic spectral sensitivity range, lack of Stiles-Crawford diaphragmation in rod vision, and the use of more peripheral parts of the retina involving larger oblique aberrations. As gratings of 20 periods per degree are below threshold at low luminances, there can be no optimum focusing at this spatial frequency. The relevant spatial frequency for optimum focusing decreases with luminance. In fact, this explains a considerable part of the well known night-myopia, since for lower spatial frequencies the optimum focus is more myopic, as is illustrated in Fig. 38 for a pupil of 7 mm. The optimum focus at 5 periods per degree is about

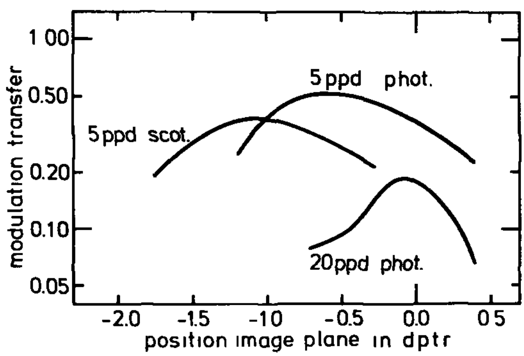

Fig. 38. Modulation transfer at 5 and 20 ppd as a function of focusing in photopic and scotopic vision through a 7 mm pupil. Note the two components of "night-myopia", *i.e.* the shift in the peak between 20 ppd and 5 ppd photopic (low-frequency myopia) and the shift between 5 ppd photopic and 5 ppd scotopic corresponding to the shift in spectral sensitivity.

0.5 D more myopic than at 20 periods per degree in this case. It was experimentally demonstrated also by Green and Campbell (1965) that part of the night-myopia is caused by the reduction of the relevant spatial frequency, and that low luminance is not necessarily a prerequisite. Larger amounts of myopia can be expected when the spatial frequency range is further reduced. However, the focusing curves grow flatter and finally no stimulus for better focusing remains. In this view the eye at rest, being about 2 D myopic (Schober, 1954), is focused as expected for nearly empty fields. In Fig. 38 the total amount of night myopia, caused by the low frequency effect together with 0.5 D corresponding to the Purkinje-shift is about 1 D.

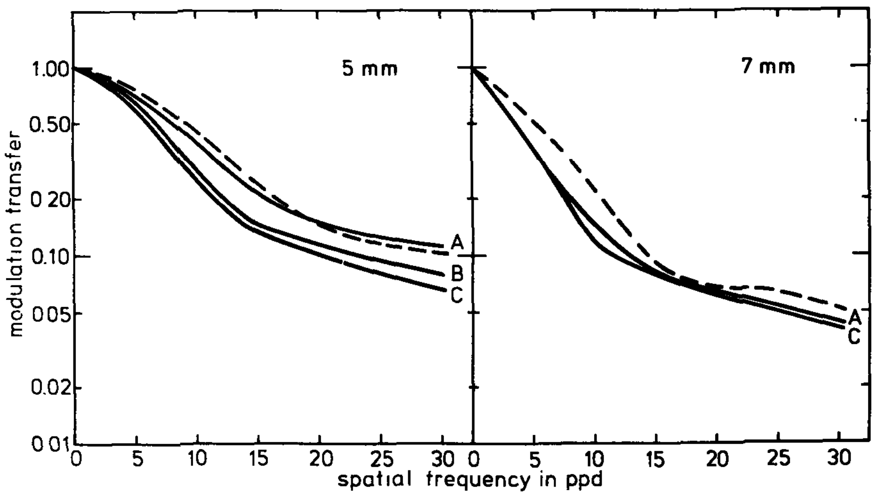

Fig. 39. Modulation transfer functions for scotopic vision through 5 and 7 mm pupils. Curve A: on-axis; curve B: 5° off-axis; curve C: 10° off-axis. For comparison the interrupted curve represents photopic vision 5° off-axis (fovea). These MTF's refer to optimum focusing at 5 ppd.

Some MTF's for scotopic vision of vertical sine wave gratings in optimum focus at 5 ppd are presented in Fig. 39 for pupils of 5 and 7 mm. For comparison the interrupted curve represents the MTF for photopic vision at 5° off-axis, also in optimum focus at 5 ppd. In general, image quality is worse in vision at low luminances, as was expected, but the difference is not really large in the spatial frequency range below 5 ppd. It would be incorrect, however, to assume that the quality of the optical image is nearly perfect in the low spatial frequency range of vision at low luminances. The MTF drops to 0.35 already at 5 ppd for a 7 mm pupil.

The effect of the larger chromatic difference of focus in scotopic vision can be judged from the comparison of curve B with the interrupted curves (curve B is omitted in Fig. 39 for the 7 mm pupil, but would run in between curves A and C). The effect of the chromatic magnification error, astigmatism and coma is shown by the curves A, B and C. This effect is comparable to the effect of the larger chromatic difference of focus for the 5 mm pupil, and it is almost negligible for the 7 mm pupil.

The MTF of the peripheral retina with a rather thick tissue layer in front of the receptors might be worse than in the fovea. Such a layer might just be absent in the fovea to avoid its inherent scattering. According to Ohzu and Enoch (1972), however, the major part of retinal blurring must be located in the outer segments of the receptors, not in the tissue layer just mentioned. They found the MTF of rat-retinas, which have no fovea, to be as good as the MTF of the human fovea. In this line the MTF of the peripheral retina will be roughly equal to the MTF of the fovea, and can be read from Fig. 36.

§6.7. RECAPITULATION

In whitish light the chromatic difference of focus is the predominating aberration of the human eye. As a consequence little individual differences are expected in the image quality of normal eyes. This justifies the calculation and general use of MTF's for the dioptrics of the human eye on the basis of "standard" geometrical aberrations. MTF's calculated in this manner are in agreement with experimental MTF's, as derived from fundus reflection measurements by Campbell and Gubisch (1966), after correction for the MTF of the retina, according to the measurements of Ohzu and Enoch (1972). Encouraged by this consistency the calculations have been extended to vision at low luminances.

CHAPTER 7

THE NEURAL COMPONENT

§7.1. CONTRAST SENSITIVITY FUNCTIONS OF THE RETINA-BRAIN SYSTEM

The overall contrast sensitivity functions are the product of optical imaging and neural processing. After the evaluation of the optical component in chapter five, the neural contribution obviouslv comes out as the residue. The ratios of overall contrast sensitivity functions and pertinent optical MTF's can be interpreted as contrast sensitivitv functions of the retina-brain system. Some examples derived from the overall contrast sensitivity functions for large sine wave fields (§2.3, Fig. 3) and for small foveally fixated sine wave fields (§3.6, Fig. 12) are rendered in Fig. 40. The corrections for the optical MTF's, inclusive retinal scattering, were made according to the size of the natural or the artificial pupil concerned, and, as to curve B, under the assumption of scotopic vision.

Similar contrast sensitivity functions of the retina-brain system have been determined in a completelv different manner by Arnulf and Dupuy (1960), Westheimer (1960), and Campbell and Green (1965). They evaded the optics of the eye by generating Young's interference gratings directly on the retina after a suggestion of Le Grand (1937). The curves of Fig. 40 agree with the results of these measurements in general aspects. The neural system contributes markedly to the high frequency decay of the visual system, and suppresses low spatial frequencies also at higher luminances. Considering the different conditions the present results cannot be compared in detail with those of the authors cited.

It was anticipated in chapter 2 that the changes in the overall contrast sensitivity functions with luminance level are of neural origin mainly. This is confirmed here in Fig. 40 after correction for the optical MTF. Fig. 40 further illustrates once more the functional difference of fovea and periphery, apart from the attending optical differences. The fovea is specialized for resolution at the cost of contrast sensitivity. The periphery sacrifices resolution in favour of contrast sensitivity. This can be understood from the fluctuation theory of vision when the form of the contrast sensitivity functions is related to the retinal summation areas, or more general to spatial interactions in the retina-brain system.

Different spatial interaction models will be discussed in the follow-

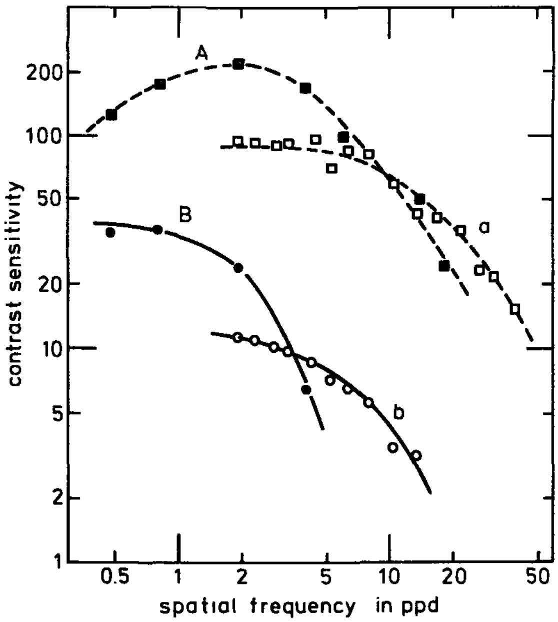

Fig. 40 Contrast sensitivity functions of the retina-brain system. Curves A and B are derived from Fig. 3 and refer to large sine wave fields in free fixation at 10^{-1} and 10^{-3} cd/m², observed through natural pupils of about 6.5 and 7 mm respectively. Curves a and b are derived from Fig. 12 and refer to small foveally fixated fields at 3.4×10^{-1} and 9.2×10^{3} cd/m², observed through an artificial pupil of 3 mm. These luminances are chosen in such a way, that the photon fluxes detected by the retina are about equal for curves a and A, and for curves b and B.

ing and it will be asked what model fits best with the sine wave contrast sensitivity functions.

§7.2. EFFECT OF FIELD SIZE

The high-frequency decay of the neural contrast sensitivity functions indicates spatial averaging over certain areas, such that smaller details are erased. The positive effect of increasing field size upon contrast sensitivity for sine wave gratings, mentioned in §2.1, reflects a second echelon of spatial integration. This kind of spatial integration extends over much larger areas, within which detail is apparently not erased. These two echelons have been distinguished first by Bouman and Van der Velden (1947) in their two-quanta-explanation of absolute thresholds. They hypothesized that two quanta must be absorbed within a small critical area and time interval in order to evoke a visual perception (first echelon). They further assumed, that the probability of detection accumulates when a test object is covered by more than one critical area (second echelon). One thus may speak of *probability summation* with respect to the second echelon. Bouman, Vos and Walraven (1963) distinguished summation of enery and summation of information. Schober and Hilz (1965) spoke of coherent and incoherent summation.

Fig. 41 illustrates the field-size effect for a foveally fixated sine wave grating of 26 ppd. The measurements were made by AvM for vertical gratings only. Contrast sensitivity levels off when the field is about 15 x 15 min^2 of arc, whereas the summation area of the first echelon (Ricco's area) is smaller than 3 x 3 min^2 of arc in this case. Morgan (1965) and Van Meeteren and Vos (1972) have shown, that the contrast sensitivity for sine wave gratings is about 5 - 10 times higher than would follow from the signal-to-noise ratio in a single summation unit. This may be explained now, when it is realized that on the second echelon the information of about 25 summation units is integrated. It should be remarked, however, that very little is known experimentally on probability summation in the detection of sine wave gratings. Fig. 41 illustrates the field size effect for one spectral frequency only. Further experiments are necessary to investigate the size and the form of the probability summation area as a function of spatial frequency and luminance among others.

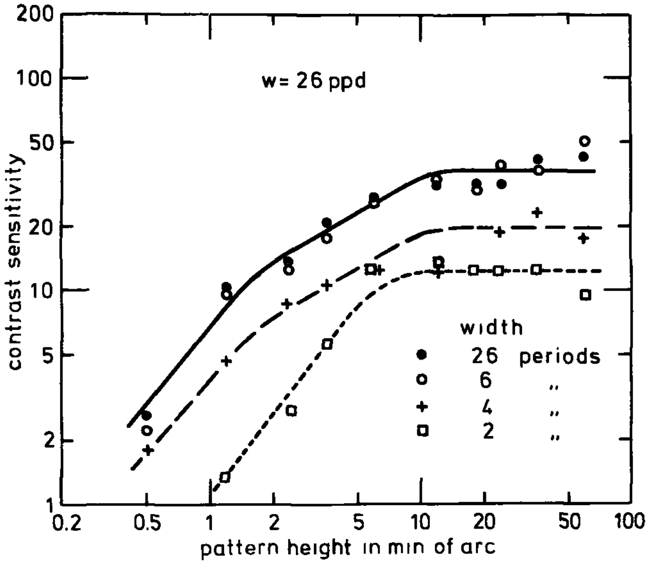

Fig. 41. The effect of field size (height and width) upon contrast sensitivity. Results of one observer (AvM) for a sine wave grating of 26 ppd in vertical orientation, observed in foveal fixation through an artificial pupil of 3 mm at a luminance of 30 cd/m². Note that the width of 1 period is 2.3 min of arc.

§7.3. SPATIAL WEIGHTING FUNCTIONS

Optical MTF's can be related to line spread functions by Fourier transformation. This elucidates their origin: the blurring of diffraction and aberration. Analogously one might compute the Fourier transforms of the neural contrast sensitivity functions and interpret the result as *weighting functions*, characterizing the neural spatial interactions (Ratliff, 1965). If this leads to an acceptable representation in agreement with common knowledge, one thus may consider the neural contrast sensitivity functions to be explained. However, at least four objections can be made:

1. More and more evidence has been gathered in recent years on the existence of special *sine wave channels* (Campbell, 1969). The question arisis then whether the contrast sensitivity functions of the retina-brain system should not be considered as the envelopes of the corresponding tuning curves rather than as a reflection of spatial interactions. This is highly improbable in my opinion. Even if sine wave

channels would exist, it is plausible that the form of the contrast sensitivity functions reflects spatial processing first of all. The input of possible sine wave channels will be subjected to retinal processing anyhow. There further is no reason to assign different sensitivity to the various possible, sine wave channels.

2. Probability summation might also be frequency dependent and introduce a component in the neural contrast sensitivity function (Hay and Chesters, 1972). This component according to Hav and Chesters would be absent in transfer functions measured in suprathreshold conditions, where probability summation is put out of order. Davidson (1968) and Campbell and Maffei (1970) compared transfer functions derived from threshold and suprathreshold measurements and found almost no difference in their form. This can only mean, that a probability summation component is absent in both. Harris (1964) formulated a mathematical theory of probability summation in the detection of images. According to this theory probabilitv summation over a certain area of a sine wave grating does not introduce a frequency-dependent term in the contrast sensitivity functions. This is plausible moreover when it is realized, that the probability of a sine wave signal is compared with the probability that the same signal is present in the white spatial spectrum of photon-noise. Thus contrast sensitivity functions do not contain a component coming from the signal-to-noise criterion itself, if probability summation extends over a fixed area.
3. The spatial interactions concerned may not be linear and linearity is a condition for meaningful Fourier transformation. However, spatial summation is apparently linear within Ricco-areas, although Sakitt (1971) recently found summation to be configuration-dependent within Ricco-areas in absolute threshold experiments. The linearity of lateral inhibition was investigated by Thomas (1968). Measurable nonlinear inhibition between two adjacent retinal areas was found, when the luminances of the latter differed more than a factor 2. Thus small signal linearitv practically applies to the threshold measurements we start from.
4. The weighting function of the retina is not invariant. Given the mosaic structure of the retina one cannot consider each retinal point as the center of continuously overlapping weighting functions. This follows also from the neural contrast sensitivity functions (Fig. 40).

For, if the retinal processing could be characterized bv an invariant weighting function, it would transfer the spatial spectra of signal and noise equally and the signal-to-noise ratio would not be altered. Thus the contrast sensitivity function of such a retina would be independent of spatial frequency. As far as this is not the case, it indicates the granularity of the sampling grid. Strictly spoken, Fourier-analysis is thus out of order. One nevertheless may relate the weighting functions of the non-overlapping receptive fields to the form of the neural contrast sensitivity functions by Fourier transformation. Let the receptive fields, centered at x = 0, be characterized by a weighting function g(x) in one-dimensional notation, where g(x) weights the contribution to the final output when the receptive field is stimulated at a distance x from the center. The maximum output of a receptive field in the presence of a sine wave grating is found when the receptive field is centered on a peak of the grating. The minimum output is found when the receptive field is centered on a trough of the grating. The modulation transfer can be defined as the ratio of the minimum difference between peak and trough in output and input signal. Though the output signal of the receptive field grid is by no means sinusoidal, one thus can compute its "amplitude" $a_o(w)$:

$$a_o(w) = \tfrac{1}{2}\, a_i(w) \int_{-\infty}^{\infty} |\cos(2\pi wx)-\cos(2\pi wx+\pi)|\, g(x)dx,$$

where $a_i(w)$ is the input amplitude of the sine wave grating. Or:

$$\frac{a_o(w)}{a_i(w)} = \int_{-\infty}^{\infty} \cos(2\pi wx)g(x)dx \qquad (7.1)$$

In other words the modulation transfer, defined in the above way as the ratio of the output "amplitude" $a_o(w)$ and the input amplitude $a_i(w)$, can be found by Fourier transformation of the weighting function. In the reverse one can find the weighting function by Fourier transformation of the neural contrast sensitivity function, when it is assumed that the threshold is determined indeed by the above output "amplitude" $a_o(w)$. However, the weighting functions are not invariant in one other aspect: they are not the same over the whole sine wave field. Thus the result of Fourier transformation will be an average weighting function.

Keeping the above objections in mind one may consider the weighting functions presented in Figs 42 and 43 as an attempt to relate the neural contrast sensitivity functions roughly to spatial interactions. The calculations have been described in more detail by Van Meeteren and Vos (1972).

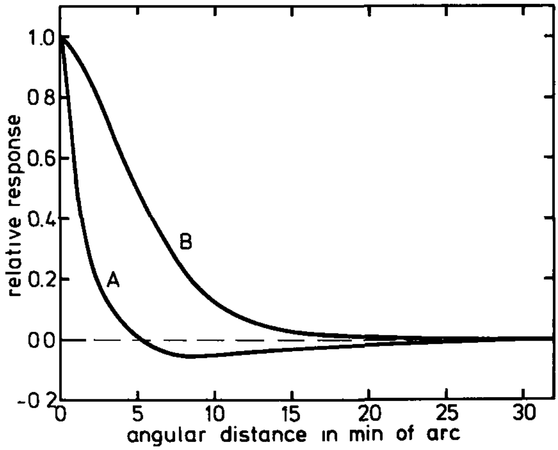

Fig. 42. Spatial weighting functions obtained by Fourrier-transformation of curves A and B in Fig. 40. These weighting functions characterize vision to large sine wave fields of $17^{\circ} \times 11^{\circ}$.

Curve B in Fig. 42 refers to a large field including the periphery and is typical for peripheral vision. At the higher luminance (curve A) the retinal position involved probably moves toward the fovea. The differences between curves A and B derived from the large field measurements represent the changes in practical vision when the luminance increases. Curves a and b in Fig. 43 are typical for the fovea and its direct environment. The halfwidth of the peripheral weighting function B is about 10 min of arc, whereas the foveal weighting function has a halfwidth of 1 - 2 min of arc. These halfwidths agree with the sizes of Ricco's complete summation areas as found by Bouman and Van der Velden (1948). They also agree with the results of Van den Brink and Bouman's (1954) study of integrative actions. They determined the degree of summation of two subliminal point-sources as a function of the mutual dis-

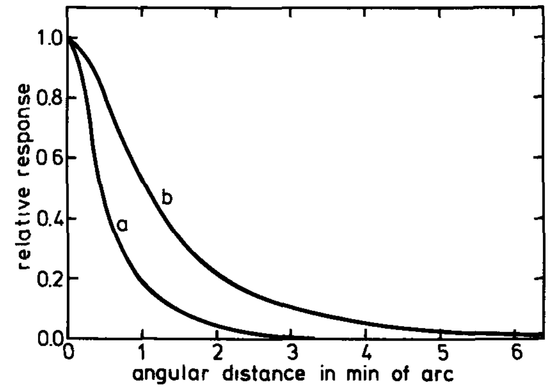

Fig. 43. Spatial weighting functions obtained by Fourrier-transformation of curves a and b in Fig. 40. These weighting functions characterize vision to small sine wave fields in foveal fixation.

tance. The above correspondence places the contrast sensitivity functions in line with older experiments on spatial summation using completely different methods.

Curve A shows lateral inhibition corresponding to the suppression of low spatial frequencies. Van Nes, Koenderink, Nas and Bouman (1967) remark that this suppression implies that the Weber-regime is obtained at a lower luminance as the spatial frequency is lower. This onset of the Weber-regime can be delayed here by moving the sine wave grating. A possible model that associates Weber-behaviour, suppression of low spatial frequencies and lateral inhibition with each other has been proposed by Koenderink, Van de Grind and Bouman (1971).

§7.4. EFFECTIVE SAMPLING AREA

In §2.4 the effective sampling area α_e of the retina was used in the context of the fluctuation theory. The derivation of Eq. (2.3) can be given now. The effective sampling size α_e of weighting function g(x) can be defined as:

$$\alpha_e = \int_{-\infty}^{\infty} g(x)dx \qquad (7.2)$$

It is assumed here, that lateral inhibition, if present, reduces the effectiveness of the receptive fields in collecting photons, rather than that surround photons would be instantaneously subtracted from central photons. In other words lateral inhibition reduces the effective size with an adaptational factor that is itself not subject to photon fluctuations. Eq. (2.3) can be derived from Eq.(7.2) as follows. According to Eq. (7.1) the normalized modulation transfer function T(w) can be written as:

$$T(w) = \frac{\int_{-\infty}^{\infty} \cos 2\pi w x g(x) dx}{\int_{-\infty}^{\infty} g(x) dx}$$

Thus:

$$\int_{o}^{\infty} T(w)dw = \frac{\int_{o}^{\infty}\int_{-\infty}^{\infty} \cos 2\pi w x g(x) dx dw}{\alpha_e} \tag{7.3}$$

The numerator of the right-hand part of Eq. (7.3) is equal to g(o)/2 (*cf.* Margenau and Murphy, 1943). One thus finds:

$$\alpha_e = \frac{1}{2\int_{o}^{\infty} T(w)dw}, \tag{7.4}$$

which is the expression of Eq. (2.3) in §2.4

§7.5. DISCUSSION

Striking a balance the contrast sensitivity functions for sine wave gratings can be interpreted in three components:

1. The optical MTF related to blurring of the retinal image.
2. The neural MTF related to retinal receptive fields (Ricco-areas).
3. Probability summation over larger areas, probably independent of spatial frequency.

Too little is known on probability summation to formulate a complete quantitative description of the detection of sine wave gratings. This is why I did not specify a k-factor for the detection of sine wave gratings in §2.4.

Two alternative approaches have been explored in the literature on vision with image intensification. First, there is Rose's model. Rose's (1948) assumption of complete summation over the whole test-object and comparison with the noise in an equal area of the background gained most adherence, witness the literature survey of §3.2. There are nevertheless serious objections:

a. The predicted relation of contrast threshold and object diameter does not come true. Experimental data indicate the existence of Ricco-areas.
b. The changes in Ricco-areas and the summation areas according to the method of Van der Brink and Bouman (1954) with luminance would be meaningless, if the visual system could adapt its area of complete summation at will to the size of the test object.
c. Rose's assumption implies that either the retina is equipped with simultaneously operating summation templates for the various sizes and forms of test objects, or builds up complete summation bv combining sub-units. The first seems to be a rather wastful construction. The second, however, implies a series of pre-threshold decisions within the sub-units concerned. The model does not explain such pre-threshold decisions. Apart from that, it is not clear why the final threshold, after a series of pre-thresholds, should be based once more upon a comparison of signal and noise in the whole test object.
d. With respect to sine wave gratings the Rose model most consistently implies summation over the whole sine wave field, although separately over the bright and the dark bars. Obviously, contrast sensitivity would be independent of spatial frequency in that case and the same conclusion holds when only a fraction of the sine wave field is used. According to the pure Rose model the signal-to-noise criterion thus would not introduce a frequency-dependent component in the contrast sensitivity functions of the retina brain system. Fig. 40 shows that the pure Rose model alone cannot account for the experimental results. Summation according to the Rose model may have added its frequency-independent component but is at least preceded by neural averaging within Ricco areas. Note that as a new element the separation of two different types of summation is brought in by the sine wave measurements. The high-frequency decay of the neural contrast sensitivity function is not due to the size of the whole test object

but to the smalness of its details. This immediately indicates, that summation according to the Rose model, if true, must be built up indeed by combining Ricco areas. Some authors suggest that summation of sine wave gratings extends over a fixed number of periods. It should be emphasized that this is an infringement of the concept of complete summation over the whole test object. Rosell's (1971) opinion that only one period is used is at least contradicted by Fig. 41. Coltman and Anderson (1960) came to about 7 periods, but they varied the length of the bars simultaneously and studied one spatial frequency only, so that their conclusion is somewhat incidental. According to the hypothesis of summation over a fixed number of periods the contrast sensitivity of the retina-brain system would be proportional to $1/\sqrt{w}$. This is not confirmed in Fig. 40. It is further conceivable that the summation area is symmetric and adapts to the period of sine wave gratings. This would lead to a contrast sensitivity proportional to $1/w$, which would not be too conflicting with the data of Fig. 40. However, as follows from Fig. 41 spatial integration extends over much larger areas than would correspond to the period of the grating in general.

Kincaid, Blackwell and Kristofferson (1960) derived what they called "element contribution functions" from contrast threshold measurements as a function of the diameter of circular test objects. The apperent contribution of each element of the test object was reconstructed from its effect upon the threshold. In this manner spatial integration inside and outside Ricco's areas is interpreted as complete and incomplete direct summation respectively. Algebraic approximations of such element contribution functions have been formulated earlier by Graham, Brown and Mote (1939) and Nolan (1957) and later by Fry (1965). Recently, the concept of element contribution functions has been introduced in the evaluation of vision with image intensifiers also by Beurle (1969) and by Legault (1971).

A serious objection to the element contribution functions is that direct summation and probability summation are intertwined in them. Thus they represent both in an unclear way and cannot serve an analytical purpose. Van den Brink and Bouman (1954) studied the interaction of two point sources in threshold measurements, so that they could separate direct summation and probability summation. This method as well as the Fourier transformation of contrast sensitivity functions leads to narrower weighting functions than the element contribution functions concerned.

The mere existence of probability summation complicates the prediction of visual performance. Optical imaging and with some care neural interactions also can be considered as linear processes. The final threshold decision involving probability summation, however, escapes from this simple procedure. It is not possible for instance to predict contrast thresholds for circular test objects from contrast thresholds measured with sine wave gratings (Blackwell, 1968) and the same holds in the reverse. That notwithstanding this complication the use of sine wave gratings as elementary test objects offers some advantages, has been argued in §1.2.

§7.6. RECAPITULATION

Two different echelons of spatial integration should be distinguished: direct summation within Ricco areas, followed by some form of probability summation over larger areas. It can be argued, that probability summation does not add a frequency-dependent component to contrast sensitivity functions for sine wave gratings. Fourier transformation of the neural contrast sensitivity functions results in spatial weighting functions for the first echelon. The halfwidths of these agree with the sizes of Ricco areas in corresponding conditions. The probability summation complicates the prediction of contrast sensitivity for other test objects from contrast sensitivity functions for sine wave gratings.

SUMMARY

The quality of optical instruments is characterized at present by the modulation transfer of sine wave gratings (Fig. 1) as a function of spatial frequency. Modulation transfer is defined as the ratio of contrast in image and object space. Considering that the human eye is the final link in most chains of optical instruments it is preferable to have its characteristics expressed in a similar way. In this thesis vision with and without image intensification is studied in terms of contrast sensitivity functions for sine wave gratings. The minimum contrast required for the discrimination of horizontal and vertical sine wave gratings is measured as a function of spatial frequency, and contrast sensitivity is defined as the reciprocal of this threshold. Such contrast sensitivity functions are directly comparable to modulation transfer functions. Apart from the transfer of contrast, however, they also reflect the sensitivity of the visual system. Typical contrast sensitivity functions for: unaided vision, foveal vision in particular, vision through nightglasses, and vision through some image intensifier telescopes, are illustrated in Figs 3, 12, 21 and 26.

Contrast sensitivity *gradually* decreases with luminance as the reader may know from own experience. The most likely explanation, known as the De Vries-Rose hypothesis, is that vision is photon-noise limited at low light levels. This is plausible when the pattern of photons detected by the retina is like the speck-pattern of Fig. 2. It is significant in this respect that the visual system summates the retinal photon-flux over larger areas at lower luminances and thus smoothes the photon-noise in favour of contrast sensitivity. At higher luminances on the other hand, the summation area is smaller in favour of resolution.The integral

$\int S(w)dw$ of contrast sensitivity $S(w)$ over spatial frequency w is proposed in chapter 2 as a new index of visual performance, doing justice to both strategies. This integral proves to be proportional to the square root of luminance over a range of five decades in agreement with the De Vries-Rose hypothesis.

Photoelectronic image intensifiers display a bright speck of light for each photon detected. Thus the photon-image detected by the photocathode of such a device is displayed as a speck-image and observed as such by the user. Fig. 2 is a snapshot of such a speck-image. It will be evident, that vision with image intensification is ultimately speck-noise limited. A series of experiments, described in chapter 3, supports the assumption that there is no difference between speck-noise limited vision and photon-noise limited vision. Contrast sensitivity proves to be proportional to the square root of speck-density (number of specks per sec per min^2 of arc upon the retina). By varying the intensity of the specks (number of photons per speck entering the pupil of the observer's eye) the gradual transition from "normal vision" to speck-noise limited vision was followed. No indication was found of a possibly different detection-criterion in these two cases. Also, the form of the contrast sensitivity functions demonstrates that the spatial processing is the same in both cases. The contrast sensitivity obtains the speck-noise limited value as soon as the intensification is sufficiently high. About 150-200 photons per speck must enter the observer's eye to that end in peripheral observation. In foveal observation 500 corneal photons per speck are required when the speck-density is low (low luminance in object space), whereas only 50 corneal photons per speck suffice when the speck-density is high. This remarkable difference is discussed in §3.8. The consequences of these results for the design of image intensifier telescopes are discussed in §5.7.

If vision with image intensifiers and unaided vision obey the same signal-to-noise criterion, then they are directly comparable on the basis of their photon-catch. How favourable this comparison is for the photocathodes of image intensifiers depends upon the quantum efficiency of the unaided human eye. A new method to determine the quantum efficiency of the eye is introduced in chapter 4. This method is based upon the quantitative comparison of contrast sensitivity in the same conditions. It follows then, that about 1% of the photon-flux that enters the eye is effectively absorbed. There are indications that the quantum efficiency is higher in special conditions, but for the comparison of vision through image intensifying devices with unaided vision the present operational value applies.

Vision through telescopes equipped with image intensifier tubes is evaluated in chapter 5. The gain in photon-catch provided by image intensifier telescopes with respect to unaided vision is in the order of thousands thanks to the higher sensitivity of the photocathode and the larger entrance pupil. Larger entrance pupils are also obtained by common night-glasses, but in that case the gain in photon-catch is necessarily attended by high angular magnification. The designer of image intensifier telescopes, however, is free to distribute the gain in photon-catch over speck-density in image space and angular magnification. Measured contrast sensitivity for vision through two actual image intensifier telescopes comes satisfactorily close to its prediction from photon-catch and MTF. Thus visual performance can be evaluated in the design-stage of a device.

The contrast sensitivity functions derived from threshold measurements, as defined above, reflect the visual system as a whole. They are the joint product of optical imaging and neural processing. The separation and interpretation of the corresponding components is attempted in chapters 6 and 7. In chapter 6 MTF's are calculated for the optics of the eye with pupil size as parameter starting from experimental data on the geometrical aberrations, as far as available in the literature. Such calculations make sense especially in whitish light, where the chromatic aberration is predominant and practically not different in individual eyes. The calculated MTF's agree with the fundus reflection measurements of Campbell and Gubisch (1966) when the latter are corrected for the MTF of the retina as measured by Ohzu and Enoch (1972). This consistency of the present calculations with two independent experimental determinations removes the uncertainty on the image quality of the human eye. The calculations have been extended to the special conditions of vision at low luminances: more astigmatism in peripheral observation, larger chromatic aberration and no Stiles-Crawford apodization.

Finally in chapter 7 the contrast sensitivity functions of the retina-brain system and with that the neural spatial interactions come up for discussion. These contrast sensitivity functions are derived from the overall contrast sensitivity functions after correction for the MTF of the eye-optics. Some existing models of spatial interactions are briefly discussed. The present contrast sensitivity functions of the retina-brain system support the models that involve two different kinds of spatial integration. Next to *direct summation* within so-called Ricco-areas a second kind of integration occurs. Though this integration extends over considerably larger areas, benifiting contrast sensitivity, it does not affect resolution. One speaks of *probability summation* in this respect, considering that the probability of detection might accumulate in one way or another. Sine wave gratings may be most appropriate to study both kinds of spatial integration since their detail is not necessarily interwoven with their extent. The prediction of contrast sensitivity for other test objects from contrast sensitivity functions for sine wave gratings is complicated by the probability summation process.

VISUELE ASPEKTEN VAN HELDERHEIDSVERSTERKING

SAMENVATTING

In dit proefschrift wordt onderzocht in hoeverre de grenzen van het zien door toepassing van elektron-optische helderheidsversterking kunnen worden verlegd. Voor de beschrijving van de visuele prestatie wordt daarbij aangesloten bij de thans algemeen gangbare *modulatieoverdrachtsfunkties* (MTF's). Deze geven voor spatiële sinuspatronen (Fig. 1) de verhouding van de modulatie in de afbeelding tot de modulatie in het voorwerpsvlak als funktie van de spatiële frekwentie. Overwegende, dat het menselijk oog als laatste schakel optreedt in vrijwel ieder afbeeldingsproces, ligt het voor de hand zijn eigenschappen op soortgelijke manier te beschrijven. Daartoe kan men kontrastdrempels voor het zien van spatiële sinuspatronen meten. De resultaten van deze metingen kunnen worden weergegeven in de vorm van *kontrastgevoeligheidsfunkties*, die direkt vergelijkbaar zijn met de genoemde MTF's. Naast de *overdracht* van kontrast vertegenwoordigen zij echter ook de *gevoeligheid* van kontrast. Typerende kontrastgevoeligheidsfunkties voor het blote oog en het met enkele helderheidsversterkende instrumenten gewapende oog worden geïllustreerd in de Figuren 3, 12 en 26.

Bij lagere lichtniveaus neemt de kontrastgevoeligheid *geleidelijk* af, zoals men uit eigen ervaring zal weten. De meest waarschijnlijke verklaring daarvoor biedt de De Vries-Rose hypothese, volgens welke het zien bepaald wordt door de fotonenruis. Dat is aannemelijk wanneer men bedenkt, dat het door het netvlies gedetekteerde fotonenpatroon er uit ziet als Fig. 2. Het is van betekenis in dit verband, dat het visuele systeem bij lagere lichtniveaus de fotonenruis uitmiddelt over grotere sommatiegebiedjes, ten gunste van de kontrastgevoeligheid. Bij hogere lichtniveaus daarentegen, wordt het sommatiegebiedje kleiner gekozen ten gunste van het oplossend vermogen. Wil men de visuele prestaties in één grootheid samenvatten, dan leent zich daartoe in het bijzonder de integraal $\int S(w)dw$ van de kontrastgevoeligheid $S(w)$ over de spatiële frekwentie w. Deze *geïntegreerde kontrastgevoeligheid* blijkt voor het blote oog evenredig te zijn aan de wortel uit de helderheid over bijna vijf dekaden, in overeenstemming met de De Vries-Rose hypothese.

Elektron-optische helderheidsversterkerbuizen zetten de door hun kathode gedetekteerde fotonen om in heldere lichtspikkeltjes op een fosforscherm. Zo wordt het door de kathode gedetekteerde fotonenbeeld als "spikkeltjesbeeld" zichtbaar gemaakt en als zodanig door de gebruiker van het instrument waargenomen. Fig. 2 is een moment-opname van zo'n spikkeltjesbeeld. Het zal duidelijk zijn, dat het zien door middel van helderheidsversterkers uiteindelijk weer begrensd wordt door de fluktuaties in de door de kathode gedetekteerde fotonenstroom, die zich nu als spikkeltjesruis manifesteren. In hoofdstuk 3 worden enkele experimenten beschreven, betreffende de kontrastgevoeligheid als funktie van de spikkeltjesdichtheid en de spikkeltjesintensiteit. Door de spikkeltjesintensiteit te variëren kon de geleidelijke overgang van het "gewone" zien naar het spikkeltjeszien worden onderzocht. Er werden daarbij geen aanwijzingen gevonden, dat het detektiekriterium voor deze twee gevallen verschillend zou zijn. Ook is de spatiële signaalbewerking in beide gevallen kennelijk hetzelfde. Blijkbaar is het zien met helderheidsversterkers eenvoudig vergelijkbaar met het ongewapende zien op basis van gelijke signaal-ruis verhoudingen. De kontrastgevoeligheid bereikt het door de spikkeltjesruis begrensde niveau pas bij voldoende lichtversterking. Circa 150-200 fotonen per spikkeltje dienen daartoe bij perifere waarneming in het oog van de waarnemer binnen te komen. Bij foveale waarneming moeten er dat 500 zijn als de spikkeltjesdichtheid laag is, en slechts 50 als de spikkeltjesdichtheid hoog is. Dit merkwaardige verschil wordt in §3.8 ter diskussie gesteld. Gevolgen voor het ontwerpen van helderheidsversterkende kijkers komen in §5.7 aan de orde.

Door vergelijking van de kontrastgevoeligheid van het ongewapende oog met de door spikkeltjesruis begrensde kontrastgevoeligheid wordt in hoofdstuk 4 de kwanten-efficiëntie van het oog bepaald. De door het ongewapende oog nuttig geabsorbeerde fotonendichtheid wordt daarbij gelijk gesteld aan de bij dezelfde kontrastgevoeligheid behorende spikkeltjesdichtheid. Op deze wijze volgt, dat circa 1% van de in het oog binnenkomende fotonenflux nuttig wordt gebruikt. Er zijn aanwijzingen, dat de kwanten-efficiëntie onder speciale voorwaarden hoger kan zijn, maar voor de vergelijking van beeldversterkerbuis en oog geldt de hier operationeel bepaalde waarde.

In hoofdstuk 5 wordt het zien met helderheidsversterkende kijkers geëvalueerd. De winst in fotonenvangst ten opzichte van het ongewapende zien kan meer dan een faktor 1000 bedragen, dankzij de grotere gevoeligheid van de fotokathode (vergeleken met het netvlies), en de veel grotere intree-pupil. Grotere intree-pupillen kan men ook realiseren met gewone nachtkijkers, maar dan gekoppeld aan grote hoekvergroting. De ontwerper van helderheidsversterkende kijkers heeft daarentegen de vrijheid om de winst in fotonenvangst te verdelen over de spikkeltjesdichtheid in de beeldruimte en de hoekvergroting. Gemeten kontrastgevoeligheden voor het zien met enkele bestaande helderheidsversterkende kijkers komen redelijk overeen met de voorspelling op grond van de fotonenvangst en de MTF van deze instrumenten. De visuele prestatie kan op deze wijze in het ontwerp-stadium worden beoordeeld.

In de hoofdstukken 6 en 7 tenslotte wordt nader ingegaan op de interpretatie van de kontrastgevoeligheidsfunkties van het menselijk oog. Zij vertegenwoordigen zowel de afbeelding door de oogoptiek als de spatiële integratie-processen in het netvlies-hersen systeem. In hoofdstuk 6 worden MTF's voor de oogoptiek berekend met als parameter de pupilgrootte, uitgaande van aan de literatuur ontleende experimentele gegevens over de geometrische aberraties. Deze berekeningen zijn vooral zinvol voor wit licht, waarbij de chromatische aberratie, die weinig spreiding vertoont van oog tot oog, het belangrijkst is. De berekende MTF's stemmen overeen met de door Campbell en Gubisch (1966) gemeten MTF's, indien wordt aangenomen, dat bij de laatsten een komponent voor retinale verstrooiing is inbegrepen gelijk aan de door Ohzu en Enoch (1972) gemeten MTF van het netvlies. Deze overeenkomst tussen de onderhavige berekeningen en de aangehaalde experimenten neemt de onzekerheid over de beeldkwaliteit van het oog weg. De berekeningen werden uitgebreid tot de speciale kondities die gelden bij lage helderheid: meer astigmatisme door perifere waarneming, grotere chromatische aberratie binnen het spektrale bereik van de staafjes en geen Stiles-Crawford effekt (dat bij gebruik van kegeltjes de pupil diafragmeert). Hoewel het zien bij lage helderheid beperkt blijft tot de lagere spatiële frekwenties, zou het toch onjuist zijn de afbeeldingsonscherpte van de oogoptiek te verwaarlozen.

In hoofdstuk 7 komen de kontrastgevoeligheidsfunkties van het netvlies-hersen systeem en daarmee de vraag naar de neurale spatiële interakties aan de orde. Deze kontrastgevoeligheidsfunkties worden hier uit die van het visuele systeem als geheel afgeleid na korrektie voor de MTF van de oogoptiek. Enkele bestaande modellen van spatiële interakties worden in het kort ter diskussie gesteld. De gevonden kontrastgevoeligheidsfunkties van het netvlies-hersen systeem ondersteunen die modellen, die onderscheid maken tussen twee verschillende soorten van spatiële interaktie. Naast *direkte sommatie* binnen zogenaamde Ricco-gebiedjes bestaat er een tweede soort integratie over aanzienlijk grotere gebieden, zeer ten gunste van de kontrastgevoeligheid, waarbij het oplossend vermogen echter niet wordt aangetast. Men spreekt in deze wel van *waarschijnlijkheidssommatie*, overwegende, dat de kans op detektie op één of andere wijze zou kumuleren. Spatiële sinuspatronen lijken erg geschikt om deze beide typen van spatiële interakties te onderzoeken, omdat hun detail niet noodzakelijk aan hun uitgestrektheid is gekoppeld. De voorspelling van de kontrastgevoeligheid voor andere testobjekten op grond van kontrastgevoeligheidsfunkties voor sinuspatronen wordt gekompliceerd door de waarschijnlijkheidssommatie.

REFERENCES

ALBRECHT, C., & PROPER, J., Detail rendition in X-ray images: theory and experiments. Medica Mundi *11*, 44-48 (1965).

ARNULF, A., La vision dans les instruments. Edition de la Revue d'Optique, Paris (1937).

ARNULF, A., & DUPUY, C., La transmission des contrastes par le système optique de l'oeil et les seuiles des contrastes rêtiniens. C.R. Acad. Sci., Paris *250*, 2757-2759 (1960).

BAKER, L.R., Status of OTF in 1970. Optica Acta *18*, 81-92 (1971).

BALASKOVIC, P., Les amplificateurs de luminance et l'observations aux faible niveaux lumineuse. Revue Technique CFTH No. 42, 71-90 (1965).

BARLOW, H.B., Intrinsic noise of cones. In: Nat. Phys. Lab. Symp. on visual problems of colour, 617-630. H.M. Stationary Office, London (1958).

BAUMGARDT, E., Mesure pyrométrique du seuil visuel absolu. Optica Acta *7*, 305-316 (1960).

BECKER, J., Optical systems for use at low light levels. Optica Acta *17*, 481-495 (1970).

BEURLE, R.L., Visual performance and the use of image intensifiers. Nato symposium on image evaluation, Munich 1969, 3-27 (1969).

BIBERMAN, L.M., Natural levels of illumination and irradiance. In: Photo-electronic imaging devices. Vol. 1, 39-67. Ed.: L.M. Biberman and S. Nudelman. Plenum-Press New York (1971).

BLACKWELL, H.R., Contrast thresholds of the human eye. J. Opt. Soc. Am. *36*, 624-643 (1946).

BLACKWELL, H.R., Visual factors related to the design and use of direct-view electro-optical devices. In: Current developments in optics and vision. Meeting of committee on vision, 1967, 93-108. Ac. Sc. Washington DC (1968).

BOUMAN, M.A., & VELDEN, H.A. van der, The two-quanta explanation of the dependence of the threshold values and visual acuity on the visual angle and the time of observation. J. Opt. Soc. Am. *37*, 908-919 (1947).

BOUMAN, M.A., & VELDEN, H.A. van der, The two-quanta hypothesis as a general explanation for the behavior of threshold values and visual acuity for the several receptors of the human eye. J. Opt. Soc. Am. *38*, 570-581 (1948).

BOUMAN, M.A., VOS, J.J., & WALRAVEN, P.L., Fluctuation theory of luminance and chromaticity discrimination. J. Opt. Soc. Am. *53*, 121-128 (1963).

BOUMAN, M.A., & KOENDERINK, J.J., Psychophysical basis of coincidence mechanisms in the human visual system. Reviews of Physiology *65*, 126-172 (1972).

BRINK, G. van den, & BOUMAN, M.A., Variation of integrative actions in the retinal system: an adaptional phenomenon. J. Opt. Soc. Am. *44*, 616-620 (1954).

BRINK, G. van den, Measurements of the geometrical aberrations of the eye. Vision Res. *2*, 233-244 (1962).

BRUMBERG, E., & VAVILOV, S., Visuelle Messungen der statistischen Photonenschwankungen. Bull. Acad. Sci. URSS, 919-941 (1933).

CAMPBELL, F.W., The depth of field of the human eye. Optica Acta *4*, 157-164 (1957).

CAMPBELL, F.W., ROBSON, J.G., & WESTHEIMER, G., Fluctuations of accommodation under steady viewing conditions. J. Physiol. *145*, 579-594 (1959).

CAMPBELL, F.W., & GREEN, D.G., Optical and retinal factors affecting visual resolution. J. Physiol. *181*, 576-593 (1965).

CAMPBELL, F.W., & GREEN, D.G., Monocular versus binocular visual acuity. Nature *208*, 191-192 (1965).

CAMPBELL, F.W., & GUBISCH, R.W., Optical quality of the human eye. J. Physiol. *186*, 558-578 (1966).

CAMPBELL, F.W., KULIKOWSKI, J.J., & LEVINSON, J., The effect of orientation on the visual resolution of gratings. J. Physiol. *187*, 427-436 (1966).

CAMPBELL, F.W., Trends in physiological optics. In: Proc. Int. School of Phys. Enrico Fermi, Course *43*, 137-143 (1969).

CAMPBELL, F.W., & MAFFEI, L., Electrophysiological evidence for the existence of orientation and size detectors in the human visual system. J. Physiol. London *207*, 635-652 (1970).

CLARK JONES, R., Quantum efficiency of human vision. J. Opt. Soc. Am. *49*, 645-653 (1959).

COLTMAN, J.W., Scintillation limitations to resolving power in imaging devices. J. Opt. Soc. Am. *44*, 234-237 (1954).

COLTMAN, J.W., & ANDERSON, A.E., Noise limitations to resolving power in electronic imaging. Proc. I.R.E. *48*, 858-865 (1960).

CRAWFORD, B.H., The luminous efficiency of light entering the eye pupil at different points and its relation to brightness threshold measurements. Proc. Roy. Soc. London *B 124*, 81-96 (1937).

CRESCITELLI, F., & DARTNALL, H.J.A., Human visual purple. Nature *172*, 195-200 (1953).

CUELENAERE, A.J., & MULDER, H., Performance of the eye-with-image intensifier. Optica Acta *19*, 413-415 (1972).

DAITCH, J.M., & GREEN, D.G., Contrast sensitivity of the human peripheral retina. Vision Res. *9*, 947-952 (1969).

DAVIDSON, M., Perturbation approach to spatial brightness interaction in human vision. J. Opt. Soc. Am. *58*, 1300-1308 (1968).

DENIER VAN DER GON, J.J., Gezichtsscherpte, een fysisch-fysiologische studie. Thesis, Amsterdam (1959).

DIRKSEN, H.J., & SCHIE, J. van, A characteristic of image intensifiers. Report Ph. L. 1963-41. Phys. Lab. TNO, The Hague (1963).

DOBELLE, W.H., MARKS, W.B., & MacNICHOL jr., E.F., Visual pigment density in single primate foveal cones. Science *166*, 1508-1510 (1969).

FERREE, C.E., RAND, G., & HARDY, C., Refraction for the peripheral field of vision. Archives of Opthalm. *5*, 717-731 (1931).

FINCHAM, E.F., Defects of the colour-sense mechanism as indicated by the accommodation reflex. J. Physiol. *121*, 570-580 (1953).

FINDLAY, J.M., A spatial integration effect in visual acuity. Vision Res. *9*, 157-166 (1969).

FLAMANT, F., Etude de la répartition de lumière dans l'image rétinienne d'une fente. Revue d'Optique *34*, 433-459 (1955).

FRANCON, M., Aberration sphérique, chromatisme et pouvoir séparateur de l'oeil. Revue d'Optique *30*, 71-80 (1951).

FRY, G.A., Physiological irradiation across the retina. J. Opt. Soc. Am. *55*, 108-111, (1965).

GRAHAM, C.H., BROWN, R.H., & MOTE, F.A., The relation of size of stimulus and intensity in the human eye: I. Intensity thresholds for white light. J. Exp. Psychol. *24*, 555-573, (1939).

GREEN, D.G., & CAMPBELL, F.W., Effect of focus on the visual response to a sinusoidally modulated spatial stimulus. J. Opt. Soc. Am. *55*, 1154-1157 (1965).

GREEN, D.G., The contrast sensitivity of the colour mechanisms of the human eye. J. Physiol. *196*, 415-429 (1968).

GUIDARELLI, S., Off-axis imaging in the human eye. Atti della Fondazione Giorgio Ronchi *27*, 449-460 (1972).

HALLETT, P.E., Quantum efficiency and false positive rate. J. Physiol. *202*, 421-436 (1969).

HARRIS, J.L., Resolving power and decision theory. J. Opt. Soc. Am. *54*, 606-611 (1964).

HAY, G.A., & CHESTERS, M.S., Signal-transfer functions in threshold and suprathreshold vision. J. Opt. Soc. Am. *62*, 990-998 (1972).

HECHT, S., SHLAER, S., & PIRENNE, M.H., Energy, quanta and vision. J. of. Gen. Physiol. *25*, 819-840 (1942).

HEEL, A.C.G. van, Correcting the spherical and the chromatic aberrations of the eye. J. Opt. Soc. Am. *36*, 237-239 (1946).

HELMHOLTZ, H. von, Handbuch der Physiologischen Optik, Dritte Auflage, Band I. Ed.: W. Nagel, Rostock (1909).

HODGSON, R.M., Visual perception with electronic imaging systems. Progress Report J. 11.71 University of Nottingham (1971).

HOPKINS, H.H., The numerical evaluation of the frequency response of optical systems. Proc. Phys. Soc. London *B 70*, 1002-1005 (1957).

IVANOFF, A., Les aberrations de l'oeil, leur role dans l'accommodation. Ed. de la Revue d'Optique, Paris (1953).

IVANOFF, A., About the spherical aberration of the eye. J. Opt. Soc. Am. *46*, 901-903 (1956).

KASAI, T., KONDO, K., SEKIGUCHI, M., & FUJII, K., Influence of the depth of focus on the human eye accommodation, Jap. J. Med. Electron. Biol. Eng. *9*, 28-36 (1971).

KELLY, D.H., Visual responses to time-dependent stimuli. I. Amplitude sensitivity measurements. J. Opt. Soc. Am. *51*, 422-429 (1961).

KELLY, D.H., Lateral inhibition in human colour mechanisms. J. Physiol. *228*, 55-72 (1973).

KINCAID, W.M., BLACKWELL, H.R., & KRISTOFFERSON, A.B., Neural formulation of the effects of target size and shape upon visual detection. J. Opt. Soc. Am. *50*, 143-148 (1960).

KOENDERINK,J.J., GRIND, W.A. van de, & BOUMAN, M.A., Foveal information processing at photopic luminances. Kybernetik *8*, 128-144 (1971).

KÖHLER, H., & LEINHOS, R., Untersuchungen zu den Gesetzen des Fernrohrsehens. Optica Acta *4*, 88-101 (1957).

KONIG, A., Die Abhängigkeit der Sehschärfe von der Beleuchtungsintensität. Sitz. Bev. Akad. Wissensch. Berlin, 13 Mai 1897, 559-575 (1897).

KOOMEN, M., TOUSEY, R., & SCOLNIK, R., The spherical aberration of the eye. J. Opt. Soc. Am. *39*, 370-376 (1949).

KRAUSKOPF, J., Light distribution in human retinal images. J. Opt. Soc. Am. *52*, 1046-1050 (1962).

KUHL, A., Die visuelle Leistung von Fernrohren. Zeitschrift für Instrumentenkunde *47*, 75-86 (1927).

KUHL, W., GEURTS, A., & OVERHAGEN, J. van, Information transfer with high-gain image intensifiers. In: Advances in electronics and electronphysics *28*, 615-627 (1969).

LANGLEY, S.P., Energy and vision. Phil. Mag. *27*, series 5, 1-23 (1889).

LAPICQUE, C., Les images rétiniennes régulières. Leurs déformations par irrégularités optiques de l'oeil. In: La formation des images rétiniennes, 12-38. Ed. Revue d'Optique, Paris (1937).

LEGAULT, R.R., Visual detection process for electrooptical images: Man-The final stage of an electro-optical imaging system. In: Photoelectronic imaging devices. Vol. 1, 69-86, Ed.: L.M. Biberman and S. Nudelman, Plenum Press New York (1971).

LE GRAND, Y., Sur un mode de vision éliminant les défauts optiques de l'oeil. In: La formation des images rétiniennes, 6-11. Ed. Revue d'Optiques, Paris (1937).

LE GRAND, Y., Optique Physiologique. I. La dioptrique de l'oeil et sa correction. Paris (1952).

LONGHURST, R.S., Geometrical and physical optics. Longmans (1957).

LUDVIGH, E., & McCARTHY, E.F., Absorption of visible light by the refractive media of the human eye. Arch. Opthal. *20*, 37-51 (1938).

MARGENAU, H., & MURPHY, G.H., The mathematics of physics and chemistry. New York (1943).

MARRIOTT, F.H.C., The foveal visual threshold for short flashes and small fields. J. Physiol. *169*, 416-423 (1963).

MEETEREN, A. van, Spatial sine wave response of the visual system: a critical literature survey. Report IZF 1966-7, Soesterberg, The Netherlands (1966).

MEETEREN, A. van, Modulation sensitivity in instrumental vision. In: Nato Symposium on image evaluation. München, 279-291 (1969).

MEETEREN, A. van, VOS, J.J. & BOOGAARD, J., Das Sehen mit den Small Starlight Scope, einem Dreistufen-Bildverstärker. Optik *32*, 456-467 (1971).

MEETEREN, A. van, & VOS, J.J., Resolution and contrast sensitivitv at low luminances.

Vision Res. *12*, 825-833 (1972).

MEETEREN, A. van & ZONNEVELD, F.W., A quantitative performance measure for night vision. Optica Acta *19*, 409-411 (1972).

MEETEREN, A. van, Calculations of the optical modulation transfer functions of the human eye for white light. To be published in Optica Acta (1973).

MORGAN, R.H., Quantum fluctuation and visual perception. In: Diagnostic Radiologic Instrumentation, Charles C. Thomas, Springfield, Ill., 61-91 (1965).

MULDER, H., Signal-Rausch-Verhältnis in bildübertragende Systemen. Optik *32*, 418-429 (1971).

NES, F.L. van & BOUMAN, M.A., Spatial modulation transfer in the human eye. J. Opt. Soc. Am. *57*, 401-406 (1967).

NES, F.L. van, KOENDERINK, J.J., NAS, H., & BOUMAN, M.A., Spatiotemporal modulation transfer in the human eye. J. Opt. Soc. Am. *57*, 1082-1088 (1967).

NES, F.L. van, Experimental studies in spatiotemporal contrast transfer by the human eye. Thesis, Utrecht (1968).

NOLAN, G.F., On the functional relation between luminous energy, target size and duration for foveal stimuli. J. Opt. Soc. Am. *47*, 394-397 (1957).

OHZU, H., & ENOCH, J.M., Optical modulation by the isolated fovea. Vision Res. *12*, 245-251 (1972).

O'NEILL, E.L., Introduction to statistical optics. Addison-Wesley Publ. Cy. Inc. (1963).

PALMA, J.J. de, & LOWRY, E.M., Sine wave response of the visual system, II. Sine wave and square wave contrast sensitivity. J. Opt. Soc. Am. *52*, 328-335 (1962).

PATEL, A.S., Spatial resolution by the human visual system. The effect of mean retinal illuminance. J. Opt. Soc. Am. *56*, 689-694 (1966).

PIRENNE, M.H., Physiological mechanisms of vision and the quantum nature of light. Biol. Rev. *31*, 194-241 (1956).

RATLIFF, F., Machbands: Quantitative studies on neural networks in the retina. Holden Day, San Francisco (1965).

RAYLEIGH, Lord, On the theory of optical images, with special reference to the microscope, J. Roy. Microscop. Soc. London Pt *1*, 474-482 (1903).

REMPT, F., HOOGERHEIDE, J., & HOOGENBOOM, W.P.H., Peripheral retinoscopy and the skiagram. Opthalmologica *162*, 1-10 (1971).

ROBSON, J.G., & CAMPBELL, F.W., A threshold contrast function for the visual system. In: The physiological basis of form discrimination. Symposium Brown University, Rhode

Island (1964).

RÖHLER, R., Die Abbildungseigenschaften der Augenmedien. Vision Res. *2*, 391-429 (1962).

RÖHLER, R., MILLER, U., & ABERL, M., Zur Messung der Modulationsübertragungsfunktion des lebenden menslichen Auges im reflektierten Licht. Vision Res. *9*, 407-428 (1969).

RONCHI, L., & NES, F.L. van, Contrast transfer in the eye as a function of spatial frequency: a literature survey. Atti Della Fond. Giorgio Ronchi *21*, 218-234 (1966).

ROSE, A., The sensitivity performance of the human eye on an absolute scale. J. Opt. Soc. Am. *38*, 196-208 (1948).

ROSELL, F.A., Television camera tube performance and data. In: Low-light-level devices: a designer's manual. IDA Report R 169, 175-464 (1971).

ROSENBRUCH, K.J., Die Kontrastempfindlichkeit des Auges als Beitrag zur Frage der Gütebewertung optischer Bilder. Optik *16*, 135-145 (1959).

RUSHTON, W.A.H., The rhodopsin density in the human rods. J. Physiol. *134*, 30-46 (1956).

RUSHTON, W.A.H., Visual pigments in man. Handbook of sensory physiology VII/I, 364-394. Ed.: H.J.A. Dartnall, New York (1972).

SAKITT, B., Configuration dependence of scotopic spatial summation. J. Physiol. *216*, 513-529 (1971).

SCHAGEN, P., Electronic aids to night vision. The Tel. Soc. J. *10*, 218-228 (1963).

SCHADE, O.H., Optical and photoelectric analog of the eye. J. Opt. Soc. Am. *46*, 721-739. (1956).

SCHIE, J. van, & RISSELADA, T.F., MTF-measurements on some binoculars. Report Ph.L. 3/73, Phys. Lab. TNO, The Hague. In Dutch (1973).

SCHNITZLER, A.D., Image-intensifier tube structures. In: Low-light-level devices: a designer's manual, 139-173. Ed.: IDA, Arlington (1971).

SCHOBER, H., Ueber die Akkommodationsruhelage. Optik *11*, 282-290 (1954).

SCHOBER, H.A.W., & HILZ, R., Contrast sensitivitv of the human eye for square-wave gratings. J. Opt. Soc. Am. *55*, 1086-1091 (1965).

SCHOBER, H., MÜNKER, H., & ZOLLEIS, F., Die Aberration des menslichen Auges und ihre Messung. Optica Acta *15*, 47-57 (1968).

SELWYN,F.W.H., The photographic and visual resolving power of lenses. Part I: Visual resolving power. Phot. J. *88B*, 6-12 (1948).

SMIRNOV, M.S., Measurement of wave aberration in the human eye. Biophysics *6*, 52-65 (1961).

SNYDER, H.L., A measure of image quality. In: Visual search, committee on Vision Symposium 1970, 93-106. Ed.: National Academy of Sciences, Washington DC (1973).

SOEST, J.L. van, Informatie- en Communicatietheorie. Delft (1952).

STILES, W.S., Further studies of visual mechanisms by the two-colour threshold method. In: Coloquio sobre problemas opticas de la vision, Madrid 1953, 65-103 (1953).

STURM, R.E., & MORGAN, R.H., Screen intensification systems and their liminations. Amer. J. Roentgenol. *62*, 617-634

TAYLOR, D.G., The minimum brightness gain in viewers using image intensifiers. Optica Acta *19*, 421-424 (1972).

THOMAS, J.P., Linearity of spatial integrations involving inhibitory interactions. Vision Res. *8*, 49-68 (1968).

TOL, T., Fluctuaties bij röntgenbeeldversterkers. Ned. Tijdschr. voor Natuurkunde *19*, 31-42 (1953).

VELDEN, H.A. van der, Over het aantal lichtquanta, dat nodig is voor een lichtprikkel bij het menselijk oog. Physica *4*, 179-189 (1944).

VOS, J.J., Some new aspects of color stereoscopy. J. Opt. Soc. Am. *50*, 785-790 (1960).

VOS, J.J. & WALRAVEN, P.L., An analytical description of the line element in the zone-fluctuation model of colour. Vision Res. *12*, 1327-1365 (1972).

VRIES, H. de, The quantum character of light and its bearing upon threshold of vision, the differential sensitivity and visual acuity of the eye. Physica *10*, 553-564 (1943).

WAARD, C. de, De uitvinding der verrekijkers. Den Haag (1906).

WALD, G., & GRIFFIN, D.R., The change in refractive power of the human eye in dim and bright light. J. Opt. Soc. Am. *37*, 321-326 (1947).

WALRAVEN, P.L. & BOUMAN, M.A., Relation between directional sensitivity and spectral response curves in human cone vision. J. Opt. Soc. Am. *50*, 780-784 (1960).

WALRAVEN, P.L., On the mechanisms of colour vision. Thesis, Utrecht (1962).

WESTHEIMER, G., Modulation thresholds for sinusoidal light distributions on the retina. J. Physiol. *152*, 67-74 (1960).

WESTHEIMER, G., & CAMPBELL, F.W., Light distribution in the image formed by the living human eye. J. Opt. Soc. Am. *52*, 1040-1045 (1962).

WESTHEIMER, G., Visual acuity. A. Rev. Psychol. *16*, 359-380 (1965).

ZACKS, J.H., Temporal summation phenomena at threshold and their relation to visual mechanisms. Science *170*, 197-199 (1970).